

Novel methods in Peroxide Bleaching

by

Daniel James Finnegan, B.App.Sc. , G.dip. P & P Tech.

Submitted in fulfilment of the requirements

for the degree of Master of Science

Department of Chemistry

University of Tasmania

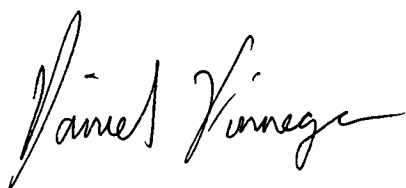
This thesis contains no material which has been accepted for the award of any other higher degree or graduate diploma in any other tertiary institution, and to the best of my knowledge and belief, contains no material previously published or written by another person, except where due reference is made in the text.

A handwritten signature in black ink, reading "Daniel Finnegan". The signature is written in a cursive style with a long horizontal flourish at the end.

Daniel Finnegan

Date: 7 / 7 / 98

This thesis may be made available for loan and limited copying in accordance with the *Copyright Act 1968*.

A handwritten signature in black ink, reading "Daniel Finnegan". The signature is written in a cursive style with a long horizontal stroke at the end.

Daniel Finnegan

Date: 7 / 7 / 98

ABSTRACT

Hydrogen peroxide has been used by manufacturers of high yield mechanical pulps as the preferred bleaching chemical. For example, Australian Newsprint Mills(ANM) Ltd operates a hydrogen peroxide refiner bleaching Pine TMP plant at its Albury mill and a peroxide tower bleaching plant at the Boyer mill processing Eucalypt CCS.

Hydrogen peroxide bleaching requires alkaline conditions to form the active bleaching species OOH^- . However, under these conditions hydrogen peroxide is very susceptible to transition metal ion catalysed decomposition. The metals manganese, iron, and copper promote the greatest rate of peroxide decomposition.

DTPA is added to chelate the transition metal ions in the process and prevent hydrogen peroxide decomposition. DTPA is a strong complexing agent and there are some concerns about its environmental impact. Alternatives to DTPA have been investigated. Recently a patent was published using Zeolite as an alternative chemical to DTPA.

In this project the affect of zeolite and sodium citrate on peroxide decomposition and bleaching of Pine TMP and Eucalypt CCS pulp has been investigated. Manganese, a known decomposition catalyst, has been used to produce conditions which induce peroxide decomposition. Various factors including pH, zeolite type, zeolite

concentration and sodium citrate concentrations were all found to affect the rate of peroxide decomposition and bleaching response.

Zeolite-A was found to reduce decomposition more than the other two zeolites, types X and Y. Zeolite-A has a lower Si/Al ratio which allows for greater cation exchange. The combined zeolite and citrate system had the greatest stabilising effect on decomposition of peroxide solutions in the presence of manganese under alkaline conditions.

Zeolite-A also had a better bleaching response than the other zeolites. Combined zeolite-A and citrate systems achieved brightness results slightly less than DTPA though the residual peroxide concentrations were significantly lower for peroxide bleaching of Pine TMP. The order of chemical addition is important. If the alkali is added prior to zeolite, and manganese is oxidised from Mn^{2+} state to higher states forming Mn-O-Mn type complexes, zeolite was found to be ineffective. Consequently zeolite-A had no effect on manganese induced peroxide decomposition leading to a poor peroxide bleaching response with Eucalypt CCS pulps.

Zeolite is believed to be acting as a chelating agent rather than as a catalyst for hydrogen peroxide oxidation reactions (bleaching). Zeolite is able to cation exchange Mn^{2+} ions but not Mn-O-Mn complexes. If Mn-O-Mn complexes are allowed to form, decomposition of peroxide occurs. Addition of citrate helps transfer Mn ions into the zeolite structure rather than providing an overall increase in chelating ability.

Addition of zeolite improves optical properties of handsheets by increasing opacity and light scattering co-efficient which is beneficial to newsprint grades. No significant losses in strength of handsheets occurred with the addition of zeolite.

ACKNOWLEDGEMENTS:

I would like to express my sincere thanks to my supervisors, Dr Karen Stack and Dr Laurie Dunn, for the interest, support and guidance they have provided for the completion of this research project. I would also like to thank Dr Bob Cox and Mr Paul Banham of Australian Newsprint Mills LTD for interest and technical guidance in this work.

Thanks must also be extended to the technical staff in the chemistry department, particularly Peter Dove, John Davis and Mike Brandon for their expert and prompt response for building and installation of equipment required in this project.

I would like to thank the my fellow students, Catherine, Damien, Madhu, Rhitu, Vicky and Yos for their friendship and provided an excellent atmosphere for work and social life.

Finally my thanks must go to the Pulp and Paper Research Group, Solvay Interlox PTY. LTD. and Australian Newsprint Mills LTD. for the generous financial support of this research project.

TABLE OF CONTENTS

Title	i
Declaration	ii
Authority of Access	iii
Abstract	iv
Acknowledgements	vi
Table of Contents	vii
Glossary	xiii
GENERAL INTRODUCTION	1
Research Proposal	2
Chapter 1: Introduction to Peroxide Bleaching	3
1.1 Why is hydrogen peroxide used as a bleaching chemical	3
1.2 Peroxide decomposition	4
1.3 Metal catalysed peroxide decomposition	5
1.4 Hydrogen peroxide stabilisation	7
1.5 Factors affecting peroxide bleaching of mechanical pulps	8
1.6 References	10
Chapter 2: Zeolites	15
2.1 Zeolite structures	15
2.2 Industrial Applications	18
2.2.1 Zeolites as absorption and separation agents	18

2.2.2 Zeolites in detergents	19
2.2.3 Zeolites in Pulp and Paper making	21
2.3 Zeolites and the Environment	21
2.4 References	22

RESULTS AND DISCUSSION

Part 1: Peroxide decomposition in the absence of pulp	24
Introduction	24
Experimental	24
 Chapter 3: Peroxide decomposition at 20°C	 28
3.1: Transition metal ions and peroxide decomposition	28
3.2: Zeolite types with manganese	31
3.3: Zeolite types and chemical addition order	40
3.4: Zeolite-A and peroxide decomposition	45
3.5: Peroxide decomposition with citrate	48
3.6: Peroxide decomposition with zeolite-A and sodium citrate	52
3.7: Peroxide decomposition with DTPA	54
3.8: Conclusion	55
 Chapter 4: Peroxide decomposition at 70°C	 57
4.1: Peroxide decomposition with manganese	57
4.2: Peroxide decomposition with zeolite type	59
4.3: Peroxide decomposition with zeolite-A charge	61

4.4: Peroxide decomposition with organic chelating agents	67
4.4.1: Peroxide decomposition with sodium citrate charge	67
4.4.2: Effect of chelating agent under acid and alkaline conditions on peroxide decomposition	69
4.5: Peroxide decomposition with a system of zeolite-A and citrate	71
4.6: Conclusion	72
References (Part 1)	74
 Part 2: Peroxide bleaching of Pine TMP and Eucalypt CCS	75
Introduction	75
Experimental	75
 Chapter 5: Brightness evaluations of peroxide bleaching with Pine TMP	82
5.1: Zeolite-A and peroxide bleaching	82
5.2: Sodium citrate and peroxide bleaching	85
5.3: Pretreatment time of zeolite-A systems with peroxide bleaching	88
5.4: DTPA and zeolite-A systems at various peroxide charges	90
5.5: Zeolite types and peroxide bleaching	91
5.6: Conclusions	94
 Chapter 6: Brightness evaluations of Eucalypt CCS bleached with peroxide	96
6.1: Peroxide charge and Eucalypt CCS bleaching	96
6.2: Manganese and peroxide bleaching of Eucalypt CCS	98
6.3: Sodium hydroxide and bleaching of Eucalypt CCS	100
6.4: Zeolite-A and peroxide bleaching of Eucalypt CCS	102

6.5: Sodium citrate and peroxide bleaching of Eucalypt CCS	104
6.6: DTPA and peroxide bleaching of Eucalypt CCS	106
6.7: Conclusion	107
 Chapter 7: Strength properties of Bleached Pine TMP	 108
7.1: Peroxide bleaching and Tear Index	108
7.2: Peroxide bleaching and Tensile Index	109
7.3: Peroxide bleaching and Roughness	110
7.4: Peroxide bleaching and Porosity	112
7.5: Peroxide bleaching and Optical properties	113
7.6: Conclusion	116
 Chapter 8: Strength properties of bleached Eucalypt CCS	 117
8.1: Peroxide bleaching and Tear Index	117
8.2: Peroxide bleaching and Tensile Index	119
8.3: Peroxide bleaching and Roughness	120
8.4: Peroxide bleaching and sheet Porosity	122
8.5: Peroxide bleaching and Optical properties	123
8.6: Conclusion	125
 References (Part 2)	 126
 CONCLUSION	 127
Mechanism of zeolite/citrate action	128
Future Work	132
 References (conclusion)	 132

APPENDIX:

Design, Construction and Use of a Pneumatic Laboratory scale Pulp Press

Introduction	A1
Design and Construction	A2
Results	A5
Conclusion	A6
Acknowledgements	A6
Engineering diagrams	A8

Glossary

Definition of Terms:

Zeolite; an aluminosilicate material with regular pore and crystal sizes.

Charge;

Part 1, decomposition studies: The applied amount of an additive as a weight percent of the total reaction mass. For example 1% zeolite-A is equal to 5 grams of zeolite-A in a total reaction mass of 500 grams.

Part 2, peroxide bleaching studies: The applied amount of an additive as a weight percent of the mass of oven dried pulp. For example 1% zeolite-A is equal to 0.2 grams of zeolite-A in a mixture containing 20 grams of oven dried pulp.

The change in definition occurs so that the ratio between additives can remain the same between the two studies, but not use excessive amounts of chemicals particularly in the bleaching studies.

Abbreviations:

TMP:	Thermo-mechanical Pulp
CCS:	Cold Caustic Soda; soaking of eucalypt chips before refining.
AAS:	Atomic Absorption Spectrometry
S/C:	Stock Consistency
DTPA:	Diethylenetriaminepentaacetic acid
Z- A,X,Y:	Zeolite type A, X or Y
Na- A,X,Y:	Sodium zeolite- A,X or Y
H- A,X,Y:	Acid zeolite- A,X or Y

INTRODUCTION

In recent years there have been concerns over the effects of chlorinated organics from bleach plant effluent on the environment. Consequently, there has been great interest in adopting more environmentally friendly bleaching chemicals such as oxygen, ozone and hydrogen peroxide(1).

Hydrogen peroxide in particular has been used by manufacturers of high yield mechanical pulps as the preferred bleaching chemical. For example, Australian Newsprint Mills(ANM) Ltd operates a hydrogen peroxide refiner bleaching Pine Thermomechanical pulp (TMP) plant at its Albury mill and a peroxide tower bleaching plant at the Boyer mill processing Eucalypt Cold Caustic Soda pulp (CCS).

Hydrogen peroxide bleaching requires alkaline conditions to form the active bleaching species OOH^- . However, under these conditions hydrogen peroxide is very susceptible to transition metal ion catalysed decomposition(2,3). The metals manganese, iron, and copper promote the greatest rate of peroxide decomposition(2,4,5).

Consequently, most peroxide bleaching stages involve either a chelation stage and/or addition of stabilisation chemicals to prevent or inhibit the effects of metal catalysed decomposition. In particular, DTPA (chelation) and sodium silicate (stabilisation) are used to limit the effects of metal induced decomposition(6). These two chemicals do have their own drawbacks. Sodium silicate is known to precipitate out of solution leading to clogging of wires and felts downstream of the bleach plant. There are environmental concerns about DTPA. DTPA itself is a known carcinogen, and handling needs to be controlled. The other concern is its ability to form strong metal complexes and the high stability constants of these complexes can be a liability in the environment, where DTPA can mobilise heavy metals in silt and soil, for example, back into the

food chain(7,8). Consequently, there has been some investigation into the use of alternative chemicals for the chelation of transition metal ions from pulp. Zeolites are one such example (9,10).

Research Proposal:

The aim of this research is to investigate the effect of using zeolites in peroxide bleaching of Pine thermo-mechanical pulp (TMP) and Eucalypt cold caustic soda (CCS) mechanical pulps.

One of the major drawbacks to peroxide bleaching is decomposition by transition metal ions. Therefore in the first part of this thesis, zeolite will be used in model systems containing transition metal ions in order to evaluate the effectiveness in preventing peroxide decomposition.

The second half of this thesis is devoted to the role of zeolite in pulp bleaching systems containing Pine TMP or Eucalypt CCS. Brightness, residual peroxide, pulp properties such as tear, tensile, roughness, porosity, and optical properties such as opacity and light scattering co-efficient will be used to evaluate zeolites against the conventional chelating agent DTPA and systems with no chelating agent.

CHAPTER 1: Introduction to Peroxide Bleaching

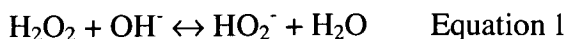
This chapter will cover the literature on hydrogen peroxide bleaching of wood pulp, in particular mechanical pulping processes. The effect of peroxide decomposition, metal ions, chelating agents, and bleaching parameters such as alkalinity, pH, bleaching temperature, stock consistency, and retention time on the efficiency of a hydrogen peroxide bleaching stage are also covered.

1.1 Why is hydrogen peroxide used as a bleaching chemical ?

Chlorine based chemicals particularly chlorine gas (Cl_2) and hypochlorite have been the bleaching chemicals of choice for most of this century because of their effectiveness as bleaching agents and low cost. Consequently, hydrogen peroxide, in the past, has been limited to use in chemical pulps due to its high cost (11-13). However since the early 1980's concerns about dioxin and other chlorinated organics in pulp mill effluent's have lead to an increase demand for ECF (Elemental Chlorine Free), and TCF (Total Chlorine Free) pulps (14,15). In ECF pulps, chlorine has been substituted with chlorine dioxide (ClO_2), whereas TCF pulps use a variety of oxygen based bleaching agents such as oxygen, ozone and hydrogen peroxide. In chemical pulps peroxide is used for delignification and brightening. The active species of peroxide bleaching are thought to be hydroxyl radicals, perhydroxyl radicals and molecular oxygen, which are formed from peroxide decomposition (11,12).

Mechanical pulps typically use hydrogen peroxide or dithionite (hydrosulphite) to brighten rather than delignify pulps (16). The reductive hydrosulphite bleaching is more cost effective than peroxide, but is used mainly for low to medium brightness gains (16,17). Traditionally peroxide bleaching occurs in towers at medium consistency, temperatures of 40°C to 70°C , alkaline conditions, and retention times of 1 to 2 hours (17,21). However hydrogen peroxide has also been used in refiner bleaching (high consistency, high temperature, and short reaction times) (18,20) and steep bleaching

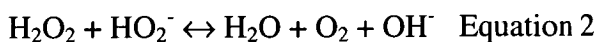
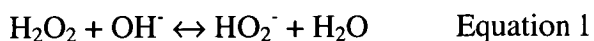
(medium/high consistency, low temperature, long reaction times) (19,20). In mechanical pulps the active bleaching species is thought to be the perhydroxyl anion (HO_2^-) which is formed with alkali according to equation 1 (21,22).



However one of the major drawbacks with hydrogen peroxide bleaching under alkaline conditions is peroxide decomposition. Peroxide decomposition reactions lower the available oxidising power and hence lead to lower bleaching efficiency (23-25). Consequently there have been a number of studies which have investigated decomposition reactions and as a result peroxide bleaching has become more cost effective (25-33).

1.2 Peroxide decomposition

There have been many studies (26, 34-40) investigating peroxide decomposition. High purity peroxide solutions at low pH have been found to be stable against peroxide decomposition (26). However as the pH of the solution is raised, the rate of decomposition increases to a maximum at pH of 11, and then decreases on addition of more alkali (34,36,40). These observations were thought to follow a homogenous base catalysed decomposition mechanism as shown by equations 1 and 2 (34).



However when improved purification techniques utilising complexing agents such as ethylenediaminetetraacetic acid (EDTA) (36,38) and diethylenetriaminepentaacetic acid (DTPA) (40), alkaline peroxide decomposition has been suppressed. Therefore the use of these metal ion chelants has cast doubt on the base catalysed decomposition

mechanism. The catalytic decomposition mechanism is due to impurities, particularly trace amount of transition metal ions. The transition metal ions are added through alkali sources, water or peroxide, and from reaction vessels (36,37). A number of studies which introduced transition metal ions have found that the rate of decomposition increases with pH. The pH conditions under which maximum decomposition occurs varies with the metal ion present (26,36,40). For instance the maximum decomposition rate occurs at pH 9.5 for manganese, 11.6 for iron and 12.0 for copper (36).

Alkaline solutions of hydrogen peroxide are commonly prepared as bleach liquor in the pulp and paper industry (26-32,40). The addition of the chelating agent DTPA to the bleach liquor has been found to stop peroxide decomposition and hence leading to the conclusion that metal induced decomposition occurs under these conditions (40).

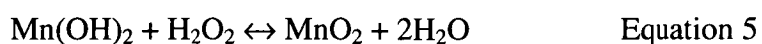
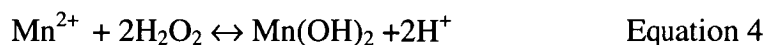
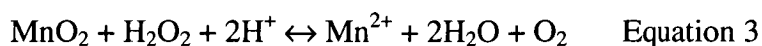
1.3 Metal catalysed peroxide decomposition

The ability to decompose peroxide by metal catalysts systems is linked to the electrochemical behaviour (41-44). Decomposition catalysts must have two oxidation states with a redox potential such that peroxide can oxidise and reduce the lower and higher oxidation states respectively (45), to actively participate in peroxide decomposition reactions. Other factors such as temperature and pH have a large impact on action of the catalytic system (23,26,36,40,62).

In relation to the pulp and paper industry the transition metal ions of manganese, iron and copper are considered the most significant as peroxide decomposition catalysts (23,24,31,40). These metals are introduced into the bleaching system through process water, equipment, and wood itself (23,24). The presence of these metals, under alkaline conditions typically used with peroxide bleaching, can lead to excessive decomposition if the metals are not effectively controlled (23,31). Of the three metals, manganese is the most significant in peroxide decomposition reactions (24,46).

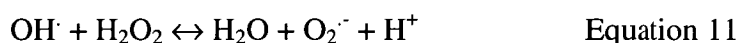
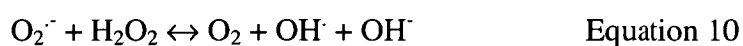
The manganese induced peroxide decomposition has been reported to be significantly affected by the manganese species present (13,23,29,40). Manganese has a complicated relationship between pH and catalytic activity. The maximum decomposition rate occurs at pH 9.5-10.5, followed by a decrease as the pH is raised to 10.5-11.0, with a further increases in pH resulting in a slightly increased rate of decomposition (13,36,40). This complicated system is based on manganese forming a number of species such as $\text{Mn}(\text{OH})_2$, MnO , Mn_3O_4 , MnOOH , Mn_2O_3 , and Mn-O-Mn complexes as well as soluble Mn^{2+} and Mn^{3+} in alkaline solutions (47-54).

It has been reported that addition of manganous salts to peroxide solutions gave no decomposition until the addition of sufficient alkali to produce a brown colloidal precipitate(55). Studies involving manganese at pH 9.8,10.8 and 11.8 concluded that manganese is insoluble and manganese dioxide (MnO_2) is the most likely decomposition species (40). However solid manganese species have also been reported to dissolve on addition of hydrogen peroxide (29,56). Further investigation into the decomposition of peroxide with manganese suggested that colloidal manganese dioxide is reduced to soluble manganese hydroxide followed by subsequent reoxidation with peroxide acting as both a reducing and oxidising agent as shown by equations 3 to 5 (55). Radioactively labelled manganese was found in even distribution between colloid and solution after the peroxide decomposition reaction (55).



More recent studies with manganese dioxide induced decomposition have shown there is an excess of surface oxygen indicating that the colloid contains Mn^{3+} centres (57,58).

Consequently it is believed that decomposition occurs through a $\text{Mn}^{4+}/\text{Mn}^{3+}$ couple (57,58). Other studies have also found the reaction between manganese dioxide and peroxide to be autocatalytic, although activation can also be achieved with addition of Mn^{3+} or Mn^{2+} (59). The mechanism occurs as shown by equations 6-11.



1.4 Hydrogen peroxide stabilization

The three most common agents used in preventing transition metal catalysed peroxide decomposition are chelating agents, sodium silicate and magnesium compounds (17,25-30, 60). Sodium silicate is thought to deactivate solid forms of the transition metal decomposition catalysts, in particular manganese and iron species(27). The sodium silicate is proposed to form Si-O-Mn structural units which reduce catalytic behaviour (29,60). Magnesium has been shown to form an insoluble magnesium hydroxide that absorbs iron and copper and consequently deactivates the catalytic species (61). The addition of magnesium to manganese containing solutions, however increases the rate of peroxide decomposition. Magnesium is thought to alter the redox potential of the metal catalysts and hence impacting on the catalytic ability of the metals (29,60). Magnesium and sodium silicate are often used together in bleaching liquors. A colloidal magnesium silicate is thought to occur, which adsorbs the metal ion catalysts forming a particularly effective stabilizing agent (18,28,31).

Chelating agents are used in the peroxide bleaching process to complex transition metal ions and subsequently remove them prior to addition of peroxide (63). Furthermore addition of chelating agents to alkaline peroxide solutions has been shown to modify catalytic activity towards peroxide decomposition (23,64). The modification of the catalyst depends on the metal and chelating agent, and can lead to either stabilization or acceleration of decomposition (23,43). For instance DTPA (diethylenetriaminepentaacetic acid) decreases catalytic activity for manganese and copper, but accelerates decomposition with iron (23). The addition of chelating agents is thought to reduce the activity of decomposition catalysts by saturation of the coordination sites of the metal ions, leading to a prevention or inaction between peroxide and the metal ion (31,64-69). In the pulp and paper industry EDTA (36), DTPA (40) or DTMPA (23) are commonly used to provide substantial stabilization of alkaline peroxide bleach liquors.

1.5 Factors affecting peroxide bleaching of mechanical pulps

There have been a number of factors which affect the peroxide bleaching, including : wood source, pulping technique, and pulp bleaching parameters (21,25).

The wood source can influence the brightness of a peroxide bleaching stage with various bleaching responses for different wood species (2,21,25). Brightness of bleached pulp from a certain species has been reported to vary from site to site, tree to tree, and with the age of the trees. Pulp from younger trees are easier to bleach than that from older trees (25).

The brightness of mechanical pulps have been reported to be affected by factors such as temperature, pretreatment, pretreatment time, refiner pressure and retention time in refining (25). The pulping processes also are a major source of transition metal ions, particularly iron and copper which can lead to peroxide decomposition and poor

bleaching responses (24). The temperature in refining and retention time can affect the form of the metals in particular iron, and the degree of colour formation by transition metal ions (70).

Increases in peroxide charges have been reported to increase brightness gains along with increased peroxide consumption (21,25). The increases in brightness become smaller as higher levels of peroxide are used (25). The high cost of peroxide has generally limited the level of peroxide used in the pulp and paper industry (21), although very high charges of peroxide may be used if the residual peroxide is recycled.

High pulp consistency is favourable for peroxide bleaching (21-25,71-73). It is thought that at high consistencies the peroxide concentration in the pulp is at a higher level for a given peroxide charge and consequently more peroxide is in the fibre wall and available for bleaching reactions (25,71,72). Also it is possible the decomposition reactions are not favoured at high consistency (74). The increased dewatering with high consistency pulps may also improve the bleaching process by removing transition metals and other dissolved substances (74).

Alkalinity is an important factor in peroxide bleaching with the alkali responsible for generating perhydroxyl anions from peroxide which are accepted to be the active bleaching species (25,71,75-77). High levels of alkali can however be detrimental to the bleaching process with chromophore production from lignin, “alkali darkening” reactions and conditions which favour peroxide decomposition (23,25,75-80).

Consequently there is an optimum level of alkali for a given peroxide charge which maximises bleaching reaction and minimises chromophore and peroxide decomposition reactions (72,75,76). The optimum pH is affected by the rate of pH decrease through the bleaching process with neutralising reactions with wood acids formed during bleaching, but also by the rate of peroxide decomposition which increases pH

(29,77,81,83). The decrease in alkali level throughout the bleaching process is beneficial to brightness as high initial charges favour peroxide activation, while low alkali levels at the end of the bleach stage with near peroxide exhaustion reduce the brightness reversion due to alkali darkening (77,83).

Temperature plays a significant role in the rate of peroxide bleaching, with higher temperatures reducing the reaction time required for a given brightness gain (21,82). In a study over 30°C to 95°C, brightness gains at higher temperatures were found to occur with higher residual peroxide concentrations, suggesting that the active bleaching species reacts rapidly with pulp before it is reduced by decomposition (82).

The bleaching or retention time for peroxide bleaching is affected by the other parameters already discussed in this section. Retention time can affect the brightness of a bleaching stage in a negative manner if the time is too short or too long. Retention times that are too short can lead to bleaching not reaching completion and therefore low brightness and waste of chemicals occur. If the retention time is too long alkali darkening reactions can significantly reduce the final pulp brightness (21,83).

1.6 References:

- (1) Dence, C.W., Reeve, D.W., 163-181 **Pulp Bleaching: Principles and Practice** : Tappi Press (1996)
- (2) Allison, R.W., *Appita*, **36**(5):362(1983)
- (3) Singh, R.P., 211-253 **The bleaching of Pulp** - 3rd edition: Tappi Press (1979)
- (4) Smith, P.K., McDonough, T.J., *Svensk Papperstidning*, **88**(12):106(1985)
- (5) Galbacs, Z.M., Csanyi, L.J., *J. Chem. Soc. Dalton Trans.*, :2353(1983)
- (6) Bambrick, D.R., *Tappi*, **68**(6):96(1985)
- (7) Egli, T., *Microbiological Sciences*, **5**(2):36(1988)

- (8) Means, J.L., Kucak, T., Crerar, D.A., *Environmental Pollution (Series B)* **1**:45 (1980)
- (9) Leonhardt, W., Suss, H.U., Glaum, H., German Patent DE 41 18 899 C1 : (1992)
- (10) Sain, M.M., Daneault, C., *Appita*, **50**(1):61(1997)
- (11) Lachenal, D., de Choudens, C., Monzie, P., *Tappi*, **63**(4):119 (1980)
- (12) Lachenal, D., de Choudens, C., Monzie, P., Soria, L., *Tappi Int. Pulp Bleach. Conf.*, :145 (1982)
- (13) Hartler, N., Lindhal, E., Moberg, C.G., Stockman, L., *Tappi*, **43**(10):806 (1960)
- (14) Pearson, J., *Pulp Paper Int.*, **34**(3):50 (1992)
- (15) Swann, C., *Papermaker*, :36 April (1996)
- (16) McDonough, T.J., *Pulp Paper Can.*, **93**(4):T108 (1992)
- (17) Andrews, D.H., *Pulp Paper Mag. Can.*, **69**(11):T273 (1968)
- (18) Sharpe, P.E., Rothenberg, S., *Tappi*, :109 May (1988)
- (19) Mulcahy, J.P., Neilson, M.J., Maddern, K.N., *Appita*, **42**(6):424 (1980)
- (20) Strunk, W.G., *Pulp Paper*, **54**(6):156 (1980)
- (21) Richert, J.S., Pete, R.H., *Tappi*, **32**(3):97 (1949)
- (22) Slove, M.L., *Tappi*, **48**(9):535 (1965)
- (23) Burton, J.T., Campbell, L.L., *Int. Symp. Wood Pulping Chem.*, :255 (1985)
- (24) Colodette, J.L., Dence, C.W., *J. Pulp Paper Sci.*, **15**(3):j79 (1989)
- (25) Dence, C.W., Omori, S., *Tappi*, **69**(10):120 (1986)
- (26) Nicoll, W.D., Smith, A.F., *Ind. Eng. Chem.*, **47**(12):2548 (1955)
- (27) Colodette, J.L., Rothenberg, S., Dence, C.W., *J. Pulp Paper Sci.*, **15**(1):J3 (1989)
- (28) Colodette, J.L., Rothenberg, S., Dence, C.W., *J. Pulp Paper Sci.*, **15**(2):J45 (1989)
- (29) Abbot, J., *J. Pulp Paper Sci.*, **17**(1):J10 (1991)
- (30) Burton, J.T., *J. Pulp Paper Sci.*, **12**(4):J95 (1986)
- (31) Bambrick, D.R., *Tappi*, **68**(6):96 (1985)

- (32) Kutney, G.W., *Pulp Paper Can.*, **86**(12):T402 (1985)
- (33) Burton, J.T., Campbell, L.L., Donnini, G.P., *Pulp Paper Can.*, **88**(6):T224 (1987)
- (34) Duke, F.R., Haas, T.W., *J. Phys. Chem.*, **65**:304 (1961)
- (35) Herbst, J.H.E., Barton, S.C., *Tappi*, **46**(8):486 (1963)
- (36) Galbacs, Z.M., Csanyi, L.J., *J. Chem. Soc., Dalton Trans.*, :2353 (1983)
- (37) Spalek, O., Balej, J., Paseka, I., *J. Chem. Soc., Faraday Trans. 1.*, **78**:2349 (1982)
- (38) Koubek, E., Haggett, M.L., Battaglia, C.J., Ibne-Rasa, K.M., Pyun, H. Y., Edwards, J.O., *J. Amer. Chem. Soc.*, **85**:2263 (1963)
- (39) Evans, D.F., Upton, M.W., *J. Chem. Soc., Dalton Trans.*, :2525 (1985)
- (40) Colodette, J.L., Rothenberg, S., Dence, C.W., *J. Pulp Paper Sci.*, **14**(6):J126 (1988)
- (41) Mochida, I., Yasutake, A., Fujitsu, H., Takeshita, K., *J. Phys. Chem.*, **86**:3468 (1982)
- (42) Sigel, H., Wyss, K., Fischer, B.E., Prijs, B., *Inorg. Chem.*, **18**(5):1354 (1979)
- (43) Sharma, V.S., Schubert, J., *Inorg. Chem.*, **10**(2):251 (1971)
- (44) Mochida, I., Takeshita, K., *J. Phys. Chem.*, **78**(16):1653 (1974)
- (45) Goldstein, J.R., Tseung, A.C.C., *J. Catal.*, **32**:452 (1974)
- (46) Kutney, G.W., Evans, T.D., *Svensk Papperstidn.*, **88**(9):R84 (1985)
- (47) Chouaib, F., Heubel, P.H., Sanson, M.D.C., Picard, G., Tremillon, B., *J. Electroanal. Chem.*, **127**:179 (1981)
- (48) Durrant D.J., Durrant B., **Introduction to advanced inorganic chemistry-** 2nd edition: Longman group Ltd (1970)
- (49) Cotton F.A., Wilkinson G., **Advanced Inorganic chemistry: a comprehensive text** 3rd edition : Interscience Publishers (1972)
- (50) Bodini, M.E., Willis, L.A., Riechel, T.L., Sawyer, T.D., *Inorg. Chem.*, **15**(7):1538 (1976)

- (51) Bodini, M.E., Sawyer, T.D., *J. Amer. Chem. Soc.*, **98**(26):8366 (1976)
- (52) Biedermann, B., Palombari, R., *Acta Chem. Scand. A*, **32**(5):381 (1978)
- (53) Yoshino, Y., Ouchi, A., Tsunoda, Y., Kojima, M., *Can. J. Chem.*, **40**:775 (1962)
- (54) Hem, J.D., Lind, C.J., *Geochim. et Cosmochim. Acta*, **58**(6):1601 (1994)
- (55) Broughton, D.B., Wentworth, R.L., *J. Amer. Chem. Soc.*, **69**:744 (1947)
- (56) Razouk, R.I., Habashy, G.M., Kelada, N.P., *J. Catal.*, **25**:183 (1972)
- (57) Kanungo, S.B., Parida, K.M., Sant, B.R., *Electrochim. Acta*, **26**:1157 (1981)
- (58) Kanungo, S.B., *J. Catal.*, **58**:419 (1979)
- (59) Baral, S., Lume-Pereira, C., Janata, E., Henglein, A., *J. Phys. Chem.*, **89**:5779 (1985)
- (60) Brown, D.M., **Affects of metal catalysed peroxide decomposition on the bleaching of mechanical pulp**: PhD Thesis, University of Tasmania (1993)
- (61) Gilbert, A.F., Pavlovova, E., Rapson, W.H., *Tappi*, **56**(6):95 (1973)
- (62) Liden, J., Ohman, L.O., *J. Pulp Paper Sci.*, **23**(5):J193 (1997)
- (63) Whiting, P., Pitcher, J.M., Manchester, D.F., *J. Pulp Paper Sci.*, **10**(5):J119 (1984)
- (64) Sigel, H., *Angew. Chem. Int. Eng. Edit.*, **8**(3):167 (1969)
- (65) Sigel, H., Muller, U., *Helv. Chim. Acta*, **49**(77):671 (1976)
- (66) Erlenmeyer, H., Sigel, H., Muller, U., *Helv. Chim. Acta*, **49**(78):681 (1976)
- (67) Brelid, H., Friberg, T., Simonson, R., *Nordic Pulp Paper Res. J.*, (2):105 (1996)
- (68) Bouchard, J., Nugent, H.M., Berry, R.M., *J. Pulp Paper Sci.*, **21**(6):J203 (1995)
- (69) Lapierre, L., Bouchard, J., Berry, R.M., Van Lierop, B., *J. Pulp Paper Sci.*, **21**(8):J268 (1995)
- (70) Rothenberg, S., Robinson, D.H., *Tappi*, **63**(9):117 (1980)
- (71) Meyrant, P., Dodson, M., *Tappi Pulping Conf.*, :669 (1989)
- (72) Moldenius, S., *Svensk Papperstidn.*, **85**(15):R116 (1982)
- (73) Hobbs, G.C., Abbot, J., *Appita*, **45**(5):344 (1992)
- (74) Hagglund, T., Lindstrom, L., *Int. Pulp Bleach. Conf.*, :163 (1985)

- (75) Lachenal, D., Dubreuil, M., Bourson, L., *Tappi*, **76**(10):195 (1990)
- (76) Martin, D.M., *Tappi*, **40**(2):65 (1957)
- (77) Colodette, J., Fairbank, M.G., Whiting, P., J. *Pulp Paper Sci.*, **16**(2):J53 (1990)
- (78) Kutney, G.W., Evans, T.D., *Svensk Papperstidn.*, **88**(6):R78 (1985)
- (79) Allison, R.W., Graham, K.L., *J. Pulp Paper Sci.*, **16**(1):J28 (1990)
- (80) Giust, W., McLellan, F., Whiting, P., *J. Pulp Paper Sci.*, **17**(3):J73 (1991)
- (81) Rapson, W.H., *Tappi*, **39**(5):284 (1956)
- (82) Liebergott, N., Van Lierop, B., Heitner, C., *Int. Mech. Pulp. Conf.*, :75
(1987)
- (83) Martin, D.M., *Tappi*, **40**(2):72 (1957)

CHAPTER 2: ZEOLITES

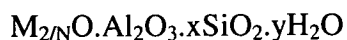
This chapter will cover the literature on zeolites, what they are, their structure, and their applications as molecular sieves/separation agents, absorption agents, catalysts and use in laundry detergents. Zeolites have also been used in by a small number of researchers in papermaking, particularly for pulp bleaching and deinking.

2.1 Zeolite Structures.

Zeolites are a class of porous inorganic solids. They are aluminosilicates in which SiO_4 and AlO_4 groups are linked to form ring structures. These ring structures further link together to form a 3 dimensional structure containing channels and cavities. It is these channels and cavities that give zeolites their unique properties and enable them to be used as molecular sieves, catalysts and cation exchangers (1-4).

Zeolite was coined in 1756 for natural minerals which gave out steam when heated. The word comes from two Greek words “zeo”, to boil, and “lithos”, stone (1). In more recent times with modern chemical techniques zeolites have been found to be hydrated crystalline aluminosilicates. The zeolite structure is based on polymeric framework tetrahedra of SiO_4 and AlO_4 . The silicon and aluminium are joined through a single oxygen atom, ie Si-O-Al-O-Si . Silicon has a valence of 4+ so the overall charge of SiO_4 is neutral ie O^{2-} shares one electron between two Si or Al atoms. Aluminium however only has a valence of 3+ so that the overall charge is AlO_4^- , consequently counter ions are needed usually alkali metal or alkaline earth cations such as Na^+ , Ca^{2+} , Mg^{2+} (1-3). These cations are readily exchanged (6). Loewenstein’s rule postulates that $\text{Al}^+-\text{O}-\text{Al}^+$ structures cannot occur as the conjugated negative charges are less stable than isolated charges $\text{Si-O-Al}^+-\text{O-Si}$. Therefore Si/Al ratios > 1 are allowed and this has been most commonly observed (1).

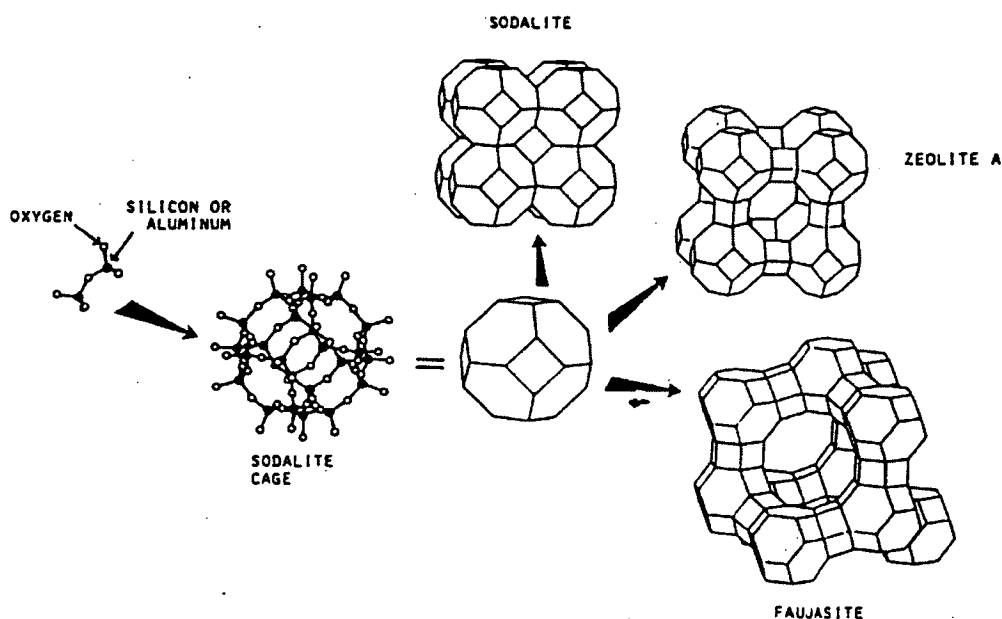
Chemically they can be represented by the empirical formula (4);



where N= cation charge, $x > 2$ (depending on Si/Al ratio), and y represents water in internal channels and cages.

The tetrahedral SiO_4 and AlO_4 link together in 4 and 6 member rings to form cage structures as shown in diagram 1. This type of cage is called a sodalite or β -cage. These cages link through the 4 membered rings with a quadric prism to form zeolite-A structures(9,10) and through the 6 membered rings with hexagonal prisms to form the faujasite (zeolite- X and zeolite-Y) structure as shown by diagram 1.

Diagram 1: Schematic of zeolite frameworks (1)



Other zeolite structures can also contain 8 membered rings which can lead to non symmetry of structural cages (like β -cage units) and consequently very complex pore and channel structures (2,4,6). Zeolite-A for instance has uniform pore and channel structures in 3 dimensions, however zeolite ZSM-5 has straight channels in the y direction, but “zig zag” channels in the x and z directions(5).

In general the largest known pore size for any zeolite is 13 Å (2,4), and a particle distribution from 2 to 10 µm. The uniform pore size distribution and consequently a narrow particle size range compared to amorphous silica make its use ideal in a number of applications(1,4). The crystalline particles are generally cubic as seen under scanning electron microscopy although spherical particles are also known for synthetic zeolites and there are some fibrous particles within the natural zeolite group(1,4,11).

There are approximately 150 zeolite structures known with 40 natural zeolite minerals and the rest are synthetic (3,4). Unique structures occur in both synthetic and natural zeolites while there are some structures such as faujasite (natural) that occur both as natural and synthetic (zeolite-X and zeolite-Y). Seven of the 40 known natural zeolites have commercial potential on the basis of purity and quantity. Some of the synthetic zeolites are not just aluminosilicate materials. New zeolite structures also include aluminophosphates, silicoaluminophosphates, other frameworks containing zirconium, titanium, chromium, gallium, germanium and even iron (4).

In this study the commercially available zeolites types A, X, and Y will be used, so further discussion will concentrate on these synthetic types. These zeolites are usually synthesised by using the hydrothermal method. Sodium silicate, sodium aluminate and sodium hydroxide are combined (concentrations depend on Si/Al ratio required). A sodium aluminosilicate gel forms which is seeded with the appropriate zeolite. The mixture is heated between 50°C and 200°C for a specific amount of time to allow crystallisation to occur. Filtration, spray drying, and calcining of crystals occur before packaging in most commercial processes (4,11,13). Synthetic zeolites can also be modified or designed by addition of alkylammonium compounds or lignosulphates as the seeding agents (4,12,13). Another method for production of zeolites is conversion of kaolin into metakaolin at 550-600°C followed by low temperature aging with sodium hydroxide. Zeolites with higher Si/Al ratios than 2 generally require extra SiO₂ to be

added with kaolin. The advantage of this method is that kaolin can be formed into pellets or other shapes and the zeolite can be created in situ (4). Otherwise clays or silica containing binders are required for pelletisation(3).

2.2 Industrial Applications.

Zeolites have many industrial applications because of their large internal volume, channels, pores and cation exchange capacity. In 1985, 495 million pounds of zeolite were used in the USA alone as detergents, catalysts, adsorbents and separation agents (14).

2.2.1 Zeolites as Absorption and Separation agents.

Zeolites are able to function as absorption and separation agents because they have channels and pores that are in the molecular size range of small compounds. They also have large void fractions (volumes) and are hydrophilic in nature (1-4). Absorption of molecules is a matter of pore filling rather than surface area effects (2). Zeolites are particularly good at absorption of water, CO₂ and sulphur compounds such as H₂S and mercaptans. Consequently zeolites have been used in purifying and drying air before liquidification and removal of the compounds listed above from various gas mixtures. Zeolites can also be used to separate mixtures of chemicals in both liquid and gas phase. For example linear alkanes can be separated from branched alkanes as only the linear chains can fit into the zeolite based on pore size(1-4). Other examples of separations involving zeolites include fructose/glucose mixtures, amino acids, antibiotics and ethanol from aqueous ethanol solution through a composite selective membrane (1). Conversely reaction products formed inside the zeolite structure can also be separated based on molecule shape as only certain ones can escape (1). Separations are governed by 1) framework structure which determines pore size and volume, 2) exchange cations which depending on charge, size and location contribute to electric field effects that may interact with absorbate molecules, and 3) the amount of dehydration which may distort

the framework or interact with cation movement throughout the structure (2). The Si/Al ratio can also have an impact on separation as high to very high ratios change the structure to more hydrophobic in nature. This can be achieved by dealuminating the zeolite with acid. The all silica molecular sieve silicalite can remove organic compounds from water (2,4).

2.2.2 Zeolites in detergents.

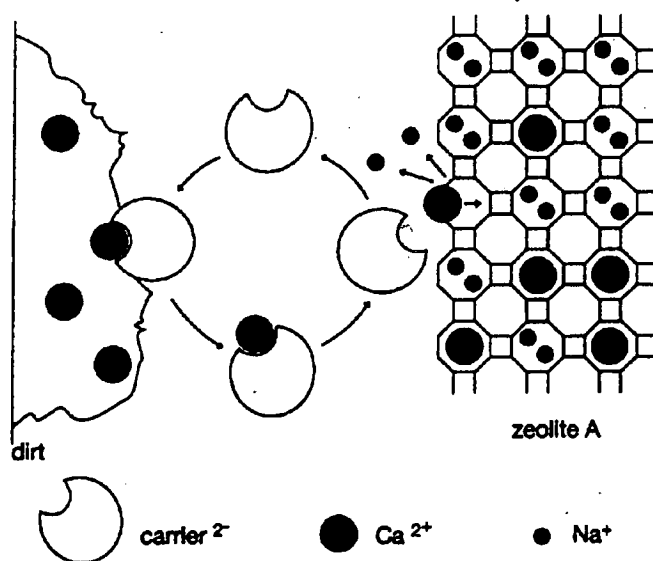
Zeolites have only had a role in detergents within the last 20 years, however now the application in detergents has the largest market share of the zeolite market. For instance the US market in 1975 of 58 million pounds, catalysts had 69% and adsorbents 31% of the market. In 1985 however detergents had 81%, catalysts 11% and adsorbents 8% of a 495 million pound US market (14). The use of zeolites in detergents has primarily been as a replacement for triphosphate chelating agents as these agents are by law in some countries banned because they can cause eutrophication of local water ways, in particular slow flowing rivers, creeks and rivulets (3,11). Eutrophication can lead to marine organism death followed by creation of hydrogen sulphide, methane and carbon dioxide as degradation products and in severe cases even siltation (11).

Triphosphate chelating was employed in detergents to remove Ca^{2+} and Mg^{2+} ions from hard water. These ions tended to precipitate out the surfactants and hence lead to a lower washing efficiency. Calcium also tends to precipitate out onto fibres as CaCO_3 or Ca-organic salts leading to encrustation and possible damage of garment fibres (3,11,14-16). Calcium is also detrimental to the washing process by its counter ion effect which reduces the extraction of other metal salts which are nearly always found on dirt and fibres (16).

Various zeolites have been used to replace the triphosphate agents, with the optimum being synthetic zeolite-A (3,15). Zeolite-A improves calcium chelation as the

temperature increases (11). However at high temperatures calcium tends to precipitate out and once insoluble the zeolite cannot exchange it. Consequently laundry detergents containing zeolite are usually formulated with a co-builder to help solubilise Ca^{2+} ions from dirt, fibre and precipitates(11,17-21). In countries where phosphate is not completely banned, a triphosphate agent is used as the co-builder, but in other countries soluble polycarboxylic acid, or citric acid are used. These act as transfer agents for metal ions to the zeolite and it is known as the “carrier effect” (11). The requirement for co-builders are far below the stoichiometric requirement for complexing (11). Diagram 2 illustrates the carrier effect of co-builders.

Diagram 2: The Carrier Effect (11)



Some of the advantages of using zeolite-A is the it has a small particle size distribution, 2-8 μm which falls between being too large, >15 μm (fabric encrustation), and too small, < 1 μm , leading to adhesion and encrustation of fibres by van der Waal's forces (11). Its low Si/Al ratio allows for large cation exchange capability. Zeolite-A can absorb dyestuff and dirt pigments, and can also act as a preferential substrate for deposition of sparingly soluble salts (15). On the disadvantage side, zeolite-A cannot

duplicate the full builder effect by itself and it has been reported that effectiveness of the bleach component (solid peroxy organic acid) is reduced with zeolite (19).

2.2.3: Zeolites and Pulp and Paper making.

The application of zeolites in pulp and papermaking is relatively recent. The first application in pulp and papermaking was as a pigment in fillers. Zeolite has been used to partially replace TiO_2 in the order of 10 to 90% replacement (25). Zeolite-A with a small size distribution in the order of $2\mu\text{m}$ is ideally suited for replacement of TiO_2 on both physical and economic reasons. The sodium zeolite-A can be exchanged with calcium ions to reduce the alkali load of the zeolites which may induce photo-yellowing or alkali darkening of lignin in the final paper product (25).

Zeolites have also been used in the peroxide bleaching of Pine TMP and deinked recycled fibre, ONP (old newsprint) (22-24,26,27). In particular the synthetic zeolites, A, X and Y have been used as a replacement for the organic chelating agents EDTA and DTPA. These agents are thought to be difficult to breakdown and may lead to mobilisation of heavy metal in the receiving waters (22). Results so far have shown that zeolite alone can not be used to replace DTPA. However zeolite with a small amount of biodegradable organic acid (such as citric, gluconic) or phosphoric acid can perform as well as DTPA in the chelation of detrimental metal ions in peroxide bleaching (23,24,26,27). Further studies have also shown that the strength properties of bleached deinked ONP is not significantly affected by the use of zeolites(23). Other advantages of using zeolites is a cleaner white water after a bleaching stage(23,24). However the overall cost is higher using the zeolite/ biodegradable acid than for DTPA (23,24).

2.3: Zeolites and the Environment

One of the advantages of zeolites is that they have no nutrient effect on wastewater, and therefore no eutrophication effect. Studies undertaken in Germany have shown that

there is no effect by zeolites from household detergents on the operation of the local municipal sewage treatment plant. The study carried out over one year found that 60% of zeolite was removed in the sand trap, 34% in biological clarifier and remaining 6% passed through the plant. The zeolite did not remobilise heavy metal ions in sediment unlike some organic agents, but conversely contributed to the detoxification of surface waters (11). Furthermore zeolite-A was not found to have a detrimental effect on fish, plants and microorganisms (11). In other studies rats survived a single dose of 32g/kg of body weight with zeolite A, X, and Y. Longer term studies feeding 5g/kg of body weight per day for 7 days also had no effect. Cold and warm water fish species exposed to a suspension of 680 mg/l showed no mortality (2).

2.4 References

- (1) Davis, M.E., *Ind. Eng. Chem. Res.*, **30**: 1675(1991)
- (2) Kirk - Othmer, **Encyclopedia of Chemical Technology** - 3rd edition, Vol 15, 638-669, John Wiley and Sons (1981)
- (3) Buchner, W., Schliebs, R., Winter, G., Buchel, K.H., **Industrial Inorganic Chemicals**, 321-330, translated by Terrel, D.R., Germany (1989)
- (4) Breck, D.W., **Zeolite Molecular Sieves: structure, chemistry and uses**: Wiley and Sons (1974)
- (5) Bhatia, B., Beltramini, J., Do D.D., *Catal. Rev. Sci. Eng.*, **31**(4): 431(1989-90)
- (6) Gottardi, G., Galli, E., **Natural Zeolites**: Springer-Verlag 1985
- (7) Sand, L.B., Mumpton, F.A., **Natural Zeolites - Occurance, Properties and Uses**: 353 Pergamon Press 1978
- (8) Ogawa, K., Masahiro, N., Aomura, K., *Zeolites*, **1**:169 (October 1981)
- (9) Breck, D.W., Eversole, W.G., Milton, R.M., Reed, T.B., Thomas, T.L., *J. Am. Chem. Soc.*, **78**(23):5963(1956)
- (10) Breck, D.W., Reed T.B., *J. Am. Chem. Soc.*, **78**(23):5972(1956)

- (11) **Technical Bulletin Pigments**, No 71 "Wessalith for Detergents", 4th edition ,
Degussa AG (1993)
- (12) Davis, M.E., *Chemtech*, :22-26 Sept 1994
- (13) Townsend, R.P., **The Properties and Applications of Zeolites**, Special
Publication No. 33, 102-119, The Chemical Society 1980
- (14) Layman, P.L., *C&EN*, :10 Sept 27 (1982)
- (15) Sand, L.B., Mumpton, F.A., **Natural Zeolites - Occurance, Properties and
Uses**: 487-493 Pergamon Press 1978
- (16) Townsend, R.P., **The Properties and Application of Zeolites**, Special
Publication No 33, 244-257, The Chemical Society 1980
- (17) Emery, W.D., Barnes, S.G., Sims, P.S., European Patent 0 313 143 (Unilever)
- (18) Emery, W.D., Barnes, S.G., Sims, P.S., European Patent 0 313 144 (Unilever)
- (19) Emery, W.D., Barnes, S.G., Sims, P.S., European Patent 0 319 053 (Unilever)
- (20) Schepers, F.J., Verburg, C.C., European Patent 0 339 997 (Unilever)
- (21) Hogan, P.J., International Patent WO 93/12217 (Ethyl Corp)
- (22) Leonhardt, W., German Patent DE 41 18 899 C1 (Degussa AG)
- (23) Rivard, J., Sain, M., Leduc, C., Daneault, C., 1997 *ISWPC*, P4-1
- (24) Volkel, H.G., Weigl, J., Ruf, F., *Woch. fur Papier.*, **21**: 952 (1995)
- (25) Rock, S.L., European Patent 0 257 304 (PQ Corp)
- (26) Sain, M.M., Daneault, C., 82nd Ann. meet. Tech. Sect., *CPPA* , B91-B95 (1997)
- (27) Sain, M.M., Daneault, C., *Appita*, **50**(1):61(1997)

Part 1:

Peroxide decomposition in the absence of pulp

Introduction:

As stated previously by various authors, the role of peroxide decomposition is a critical factor in determining the effectiveness of a hydrogen peroxide bleaching stage. In order to understand better what occurs when peroxide decomposes it was decided to investigate the effects of pH, transition metal ions and various chelating agents on a model system that does not contain any pulp. This model system only models peroxide decomposition reactions and eliminates the complication of other bleaching reactions. The model system will be used to evaluate chelating systems at two temperatures, 20°C (chapter 3) and 70°C (chapter 4). These temperatures have been chosen as they represent room temperature and typical conditions in a bleach plant for peroxide bleaching respectively.

Experimental:

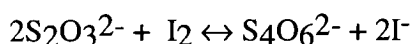
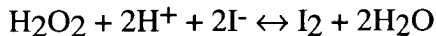
All glassware and plasticware were washed with 10 % w/w sulphuric acid made up with Milli Q water, before being rinsed twice with Milli Q water. This step was repeated before re-use of each piece of the labware.

Preparation of the metal ion solutions:

The metal ion solutions were made up to a concentration comparable with the concentrations found in a typical sample of peroxide bleached pine TMP (45 ppm Mn; 20 ppm Fe; 20 ppm Cu {4 times normal}). The appropriate amounts of the $\text{MnSO}_4 \cdot \text{H}_2\text{O}$, $\text{FeSO}_4 \cdot 7\text{H}_2\text{O}$, $\text{Cu}(\text{NO}_3)_2 \cdot 2.5\text{H}_2\text{O}$ were dissolved in Milli Q water before being made up into 1 litre to give the concentration of the metal ions as stated above.

Method 1: Peroxide decomposition measurement with metal ions only.

100 mL of the metal ion solution was added to a screw top polyethylene bottle in a water bath at 20 °C. The pH was adjusted throughout the experiment by the addition of sodium hydroxide or sulphuric acid. Decomposition experiments were run at constant pH's of 4.0, 7.5 and 11.0. The mixture was constantly stirred. 5 mL of stock peroxide (30 % w/w) was added to the mixture. The point of addition of peroxide was used as time zero. At regular intervals of 5 minutes thereafter, 5 mL aliquots of the peroxide/metal ion solution were withdrawn. This solution was added to a conical flask containing approximately 10 mL of 10 % sulphuric acid, 3 drops of 10% w/w ammonium molybdate(VI) $\{(NH_3)_6Mo_7O_{24}\}$ solution and 50 mL of Milli Q water. After the addition of the peroxide/metal ion solution, 1.0 g of potassium iodide was added to the conical flask. This solution was mixed before titration with standardised sodium thiosulphate(1). The residual peroxide was calculated from the thiosulphate.

**Method 2: Peroxide decomposition used for evaluation of chelating systems**

In a 1 litre polyethylene vessel, 475g of Milli Q water and 45 ppm manganese as solid manganese sulphate were mixed. This mixture was placed in a water bath over a magnetic stirrer. The appropriate chelating agent, 0.001% (1 mL of 5 g/L NaOH) or 0.01% sodium hydroxide (1 mL of 50 g/L NaOH solution) and 25 mL of stock (30% w/w) BDH hydrogen peroxide were then added in that order . Using the time of addition of hydrogen peroxide as time zero, 5 mL aliquots of solution were removed to determine the residual peroxide every five minutes for an hour. The pH of the solution was measured for all samples. The addition of 0.01% NaOH raises the initial pH to around 11, a similar initial pH to those used in peroxide bleaching studies (Part 2). Addition of 0.001% NaOH produces a pH in the range of 8.5-9.0.

A blank with only MilliQ water and hydrogen peroxide was used to determine the residual peroxide at time zero. This method was used to standardise the stock 30% w/v hydrogen peroxide solution obtained from BDH chemicals.

Residual peroxide determination:

5 mL aliquots were pipetted into a 250 mL conical flask containing 10 mL of 10% w/w sulphuric acid, 1 drop of 10% w/w ammonium molybdate (VI) $\{(NH_3)_6Mo_7O_{24}\}$ and 50 mL of distilled water. 2.0g of potassium iodide was added, swirled and titrated against standardised 0.1 M sodium thiosulphate(1). The residual peroxide was then calculated from the previous reactions by standard methods.

Table 1: Standard peroxide decomposition conditions (method 2)

Chemical	Chemical charge
Milli Q water	475 mL
Sodium hydroxide	0.01% (1 mL of 50 g/L NaOH solution)
manganese	45 ppm
Hydrogen peroxide	25 mL of 30 % w/v stock
Reaction time and temperatures	60 min at 20°C and 70°C

Each point in the figures for peroxide decomposition is the average of at least two experiments. In general, the experimental error for those systems that did not have a large decomposition rate was quite small at less than 5% from the mean. However, those systems which did have significant decomposition rates had variations of up to 15% from the mean and/or in some cases 5 minutes difference in peroxide exhaustion. The errors were higher at 70°C than 20°C as the relative rates of decomposition were faster.

RESULTS AND DISCUSSION: (PART 1)

CHAPTER 3: PEROXIDE DECOMPOSITION AT 20°C

This chapter will cover the various effects of pH, transition metal ions, sodium hydroxide charge, zeolite type and charge, citrate form and charge, DTPA form and the order of addition of chemicals on peroxide decomposition at 20°C.

3.1: Transition metal ions and peroxide decomposition.

The effect of iron, copper and manganese at pHs of 4, 8, 11 has been investigated in this section. Peroxide decomposition was studied using method 1 as outlined in the experimental section Part 1.

As shown in figure 1, manganese was found to have a dramatic effect on peroxide decomposition. Under alkaline conditions a brown precipitate was observed to occur.

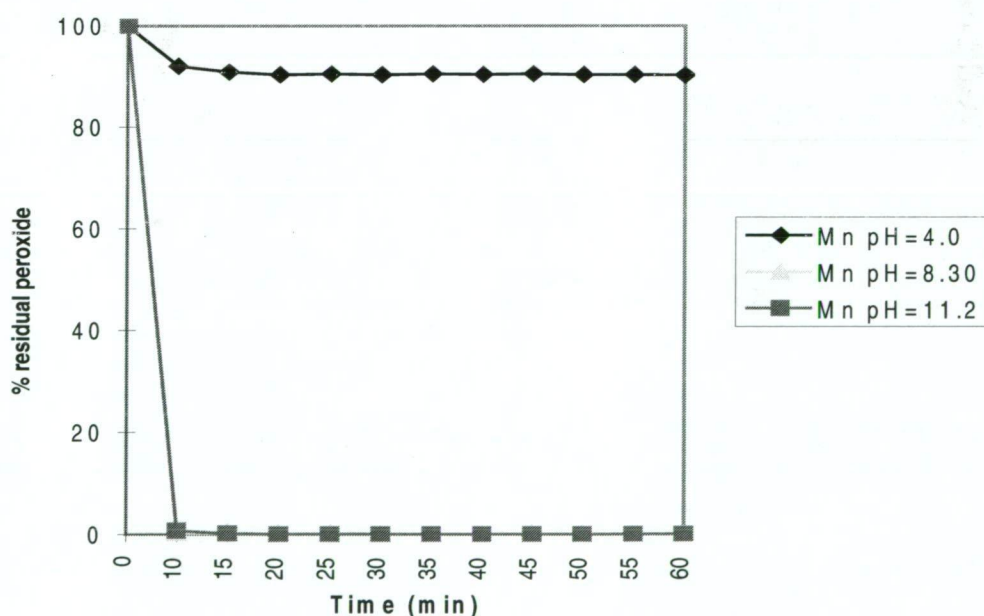


Figure 1: Peroxide decomposition at 20°C with manganese at various pHs.

This precipitate is believed to be involved in the rapid decomposition of all of the peroxide present within 10 minutes. Under acid conditions, no precipitate was observed

and also no peroxide decomposition occurred. Therefore, it is likely that manganese must be oxidised from its Mn^{2+} state (acid conditions) to a higher state such as Mn^{3+} , Mn^{4+} , Mn^{7+} , under alkaline and oxidation (peroxide) conditions (2-4) before peroxide decomposition can occur.

Copper has been shown to have little effect on peroxide decomposition in figure 2.

Furthermore, there is no significant effect of pH on the peroxide decomposition at 20°C over the reaction period of 1 hour.

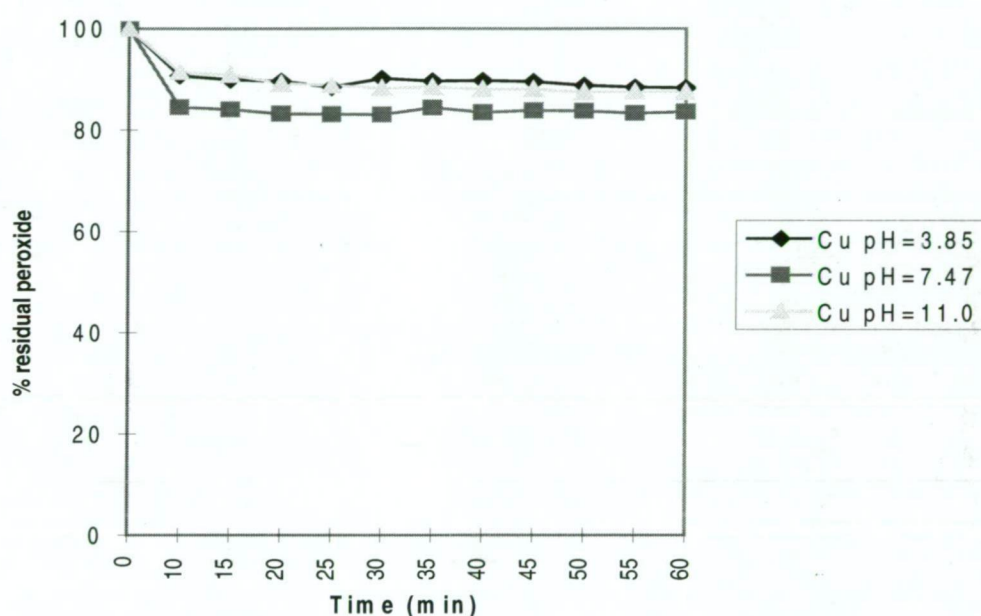


Figure 2: Peroxide decomposition with copper at various pHs.

The effect of iron on peroxide decomposition has been found to be minimal in figure 3. There is again no significant decomposition despite trying three different pHs. There was, however, a brown precipitate under strong alkaline conditions. This precipitate may however have some effect over longer reaction periods as shown in the literature(5). It would certainly lower the brightness of pulps that use alkaline white water with fillers such as calcium carbonate.

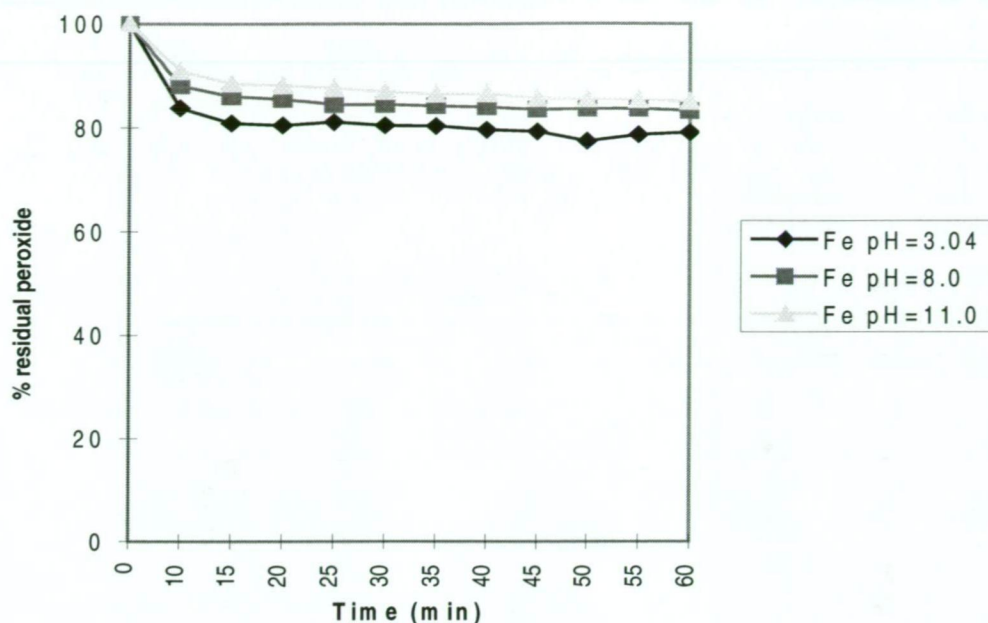


Figure 3: Peroxide decomposition at 20°C with iron at various pHs.

The results for the effects of transition metal ions at various pHs have shown that manganese under alkaline conditions was the only ion that produced significant peroxide decomposition over the time period investigated. Because this work is investigating the effect of zeolites as a chelating agent, the rest of this study will use only the alkaline manganese condition. Therefore, if zeolites are going to have any effect in prevention of peroxide decomposition, it will be very easy to evaluate if there is a large difference between the peroxide decomposition with and without zeolite.

It was decided to change to a system that added a constant alkali charge at the start of the reaction. One reason for this is that it mimics a bleach plant that generally adds a charge of alkali at the start of a bleaching stage rather than constant alterations to pH over the entire reaction time. Consequently, the method for peroxide decomposition was changed to “Method 2” as described in the experimental section.

3.2 Zeolite types with manganese.

The effect of manganese on peroxide decomposition at two alkali levels will be compared against three commercially available zeolites using “Method 2” with alkali addition after zeolite as stated above. The pHs before addition of peroxide for the systems containing the alkali charges 0.001% and 0.01% were approximately pH=8.5-9.0 and pH=11.0-11.5. However, addition of zeolites in their sodium form raises the pH (see table 2). It is important to note that addition of hydrogen peroxide lowers the pH. However, as the peroxide decomposes, the pH starts to rise back to the initial pH (table 2).

Table 2: Typical pH profile of a peroxide decomposition reaction.

Chemical	pH after addition	pH after addition	pH after addition
Mn/MilliQ H ₂ O	5.2	6.1	4.9
1% Z-A	-	-	11.1
0.001% NaOH	8.4	-	-
0.01% NaOH	-	11.2	12.3
H ₂ O ₂	7.4	8.7	9.8
Final pH	7.1*	10.9**	9.9 [#]

*: 100% decomposition after 50 minutes.

**: 100% decomposition after 5 minutes.

#: practically no decomposition after 60 minutes.

The effect of the high alkali charge (0.01% NaOH) on a system that does not contain manganese, ie peroxide under alkaline conditions, is shown in figure 4. This figure shows that there is a small initial breakdown of peroxide in the first 5 minutes. However, after that time there is no further decomposition over the whole reaction period. In the presence of manganese (45 ppm), all of the peroxide was found to decompose within the first 5 minutes.

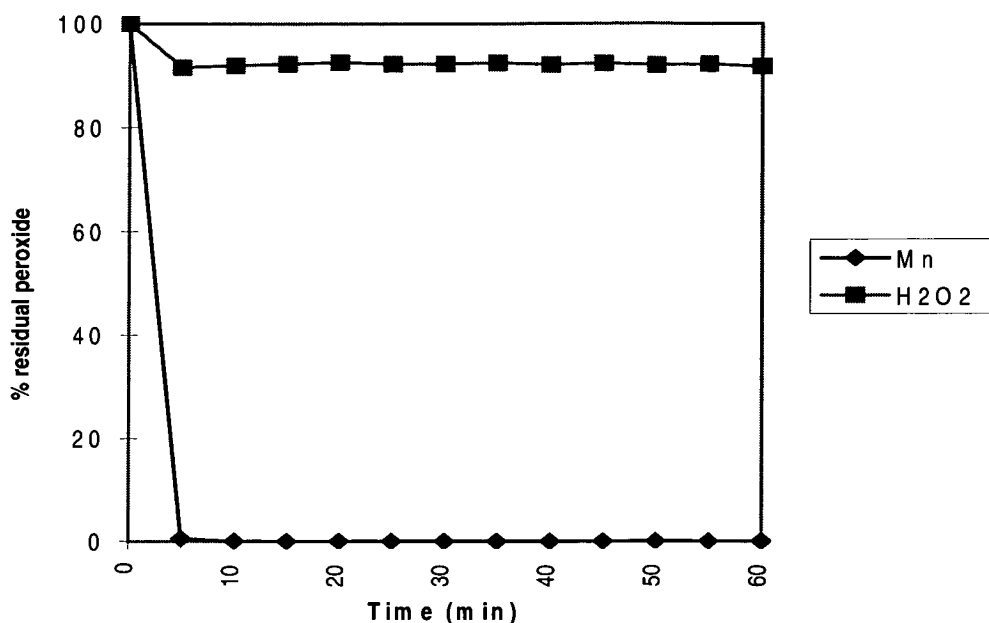


Figure 4: Peroxide decomposition with and without manganese at 0.01% alkali charge.

The effect of alkali charge on manganese induced peroxide is interesting. Figure 5 shows that as the alkali charge was reduced from 0.01% to 0.001% NaOH, the rate of peroxide decomposition decreased. Complete decomposition was obtained after 45 minutes at 0.001% as compared to 5 minutes at 0.01% NaOH. It was noted that the variation in experimental data was greater at 0.001% NaOH. This alkali charge produced pHs (see table 3) which were close to the equilibrium point for the oxidation of Mn^{2+} to Mn^{4+} (6).

Table 3: pH profile for manganese induced peroxide decomposition.

Chemical	pH after addition	pH after addition
Mn / MilliQ H ₂ O	5.4	6.1
0.001% NaOH	8.4	-
0.01% NaOH	-	12.1
H ₂ O ₂	7.4	9.2
Final pH	7.1	11.9

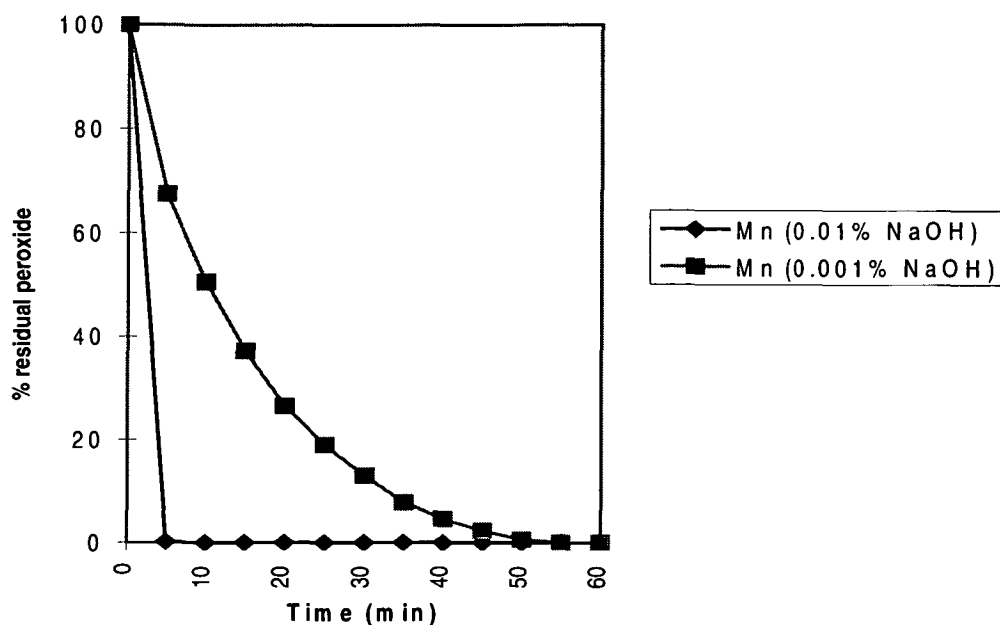


Figure 5: Peroxide decomposition with manganese at two alkali levels.

Zeolite-A

The effect of adding zeolite-A on alkaline manganese peroxide decomposition is shown in figure 6. At 1% zeolite-A charge (5g in 500mL) and 0.001% NaOH, a large decrease in the rate of peroxide decomposition occurs. The decrease is such that only approximately 15% of the original peroxide charge is decomposed over a hour, compared to 100% decomposition in around 50 minutes for the equivalent system not containing any zeolite-A (Figure 5).

The inhibition of peroxide decomposition by manganese with zeolite-A is even more significant at 0.01% NaOH charge despite the increase in reaction pH (table 4). The 1% zeolite-A system reduces decomposition to approximately 10% over the full reaction time compared to 100% decomposition with the first five minutes for the system that does not contain any zeolite-A.

Table 4: pH profile for peroxide decomposition involving zeolite-A.

Chemical	pH after addition	pH after addition
Mn / MilliQ H ₂ O	4.3	3.8
1% Z-A	11.4	11.1
0.001% NaOH	9.5*	-
0.01% NaOH	-	12.1
H ₂ O ₂	9.2	9.7
Final pH	9.8	9.9

* NaOH added before zeolite

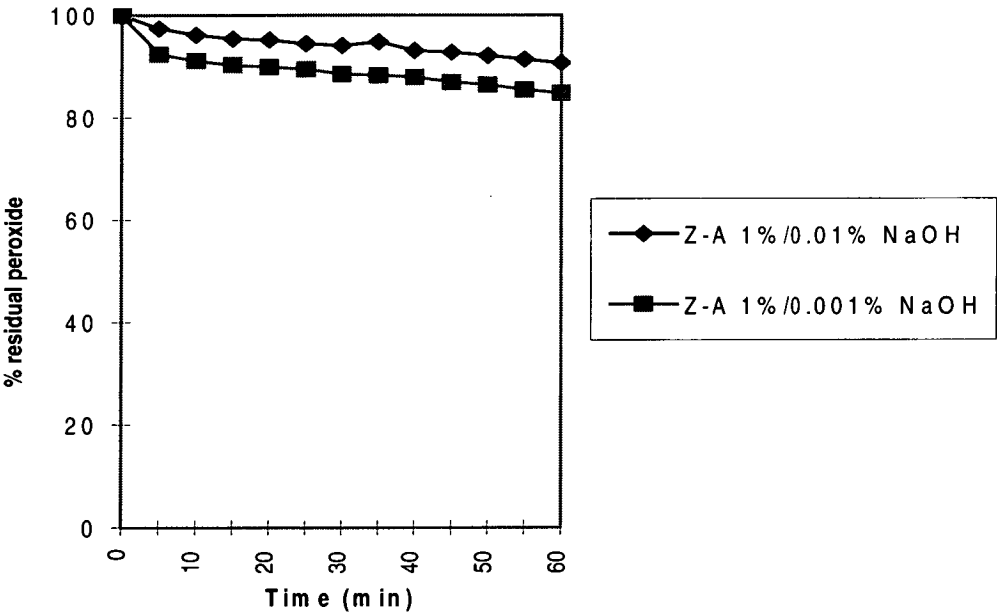


Figure 6: Peroxide decomposition with 1% zeolite-A at two alkali levels.

Zeolite-X

The use of zeolite-X at 1% charge was investigated against the manganese induced peroxide decomposition system in figure 7. Table 5 presents the change in pH of the solution for the addition of 0.001% and 0.01% alkali using zeolite-X. The use of zeolite-X was quite significant in reducing peroxide decomposition at the 0.001%

NaOH charge with slightly less than 10% of the original peroxide charge being decomposed of the full reaction time of 1 hour as compared to 100% in 50 minutes for manganese alone as shown in figure 5.

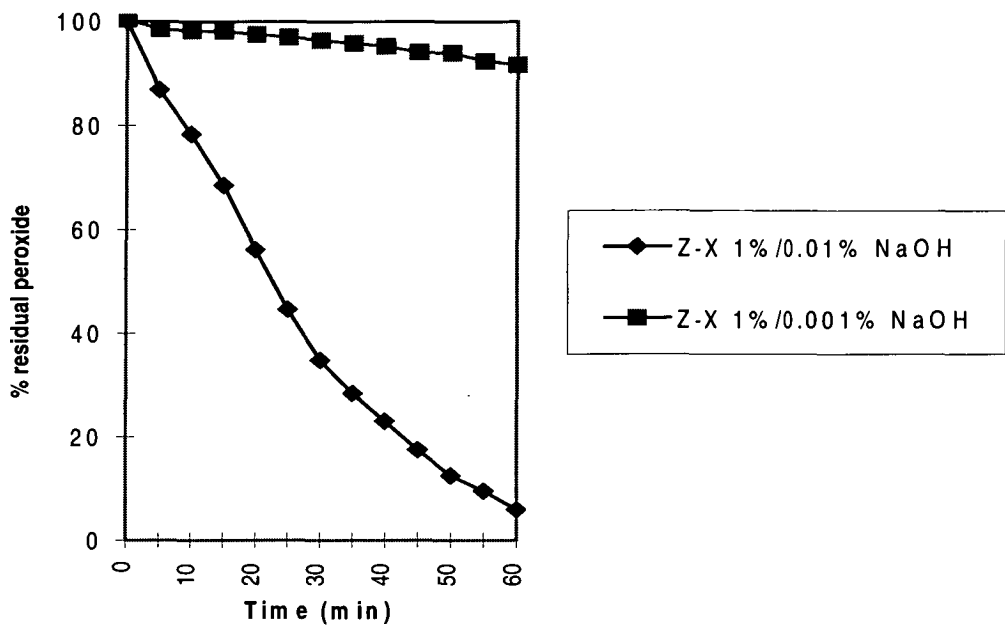


Figure 7: Peroxide decomposition with 1% zeolite-X at two alkali levels.

Table 5: pH profile for peroxide decomposition involving zeolite-X.

Chemical	pH after addition	pH after addition
Mn / MilliQ H ₂ O	4.9	4.2
1% Z-X	11.0	10.6
0.001% NaOH	9.1*	-
0.01% NaOH	-	12.2
H ₂ O ₂	9.2	9.8
Final pH	9.4	11.9

* NaOH added before zeolite

Zeolite-X, however, did not perform as well as at the 0.01% NaOH charge as that at 0.001% NaOH in preventing peroxide decomposition. Zeolite-X did still, however, have a beneficial effect over the system that did not contain any zeolite.

There was approximately 90% peroxide decomposition over the full hour with 1% zeolite-X compared to 100% decomposition within 5 minutes for the system containing manganese without any zeolite (figure 5). If the zeolite-X system is compared with that of zeolite-A at 0.01% NaOH charge (figure 6), there is a reduction of approximately 80 percentage units in the residual peroxide charge over the full 60 minutes reaction period, when using zeolite-X.

Zeolite-Y

The effect of zeolite-Y on manganese induced peroxide decomposition has been shown to be quite variable in figure 8. For instance at 0.001% NaOH charge there is essentially no peroxide decomposition over the full hour. This result is better than those for both zeolite-A and zeolite-X under the same conditions.

Table 6: pH profile for peroxide decomposition involving zeolite-Y.

Chemical	pH after addition	pH after addition
Mn / MilliQ H ₂ O	5.0	5.1
1% Z-Y	9.9	8.4
0.001% NaOH	8.9*	-
0.01% NaOH	-	11.7
H ₂ O ₂	8.4	9.2
Final pH	8.2	11.3

* NaOH added before zeolite

While zeolite-Y performs well at 0.001% NaOH charge, it does not perform very well under the higher alkali charge of 0.01% NaOH (table 6). In fact zeolite-Y at 0.01% NaOH virtually has no effect on manganese induced peroxide decomposition; 100% peroxide decomposition occurs after 10 minutes (figure 8) compared to 100% decomposition in 5 minutes for the system that does not contain any zeolite (figure 5).

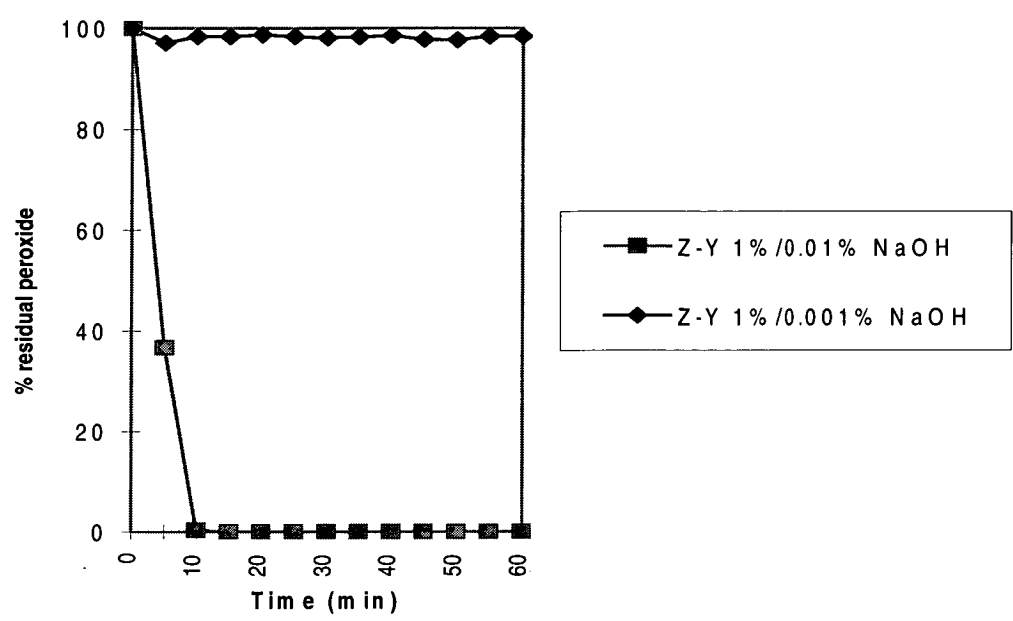


Figure 8: Peroxide decomposition with 1% zeolite-Y at two alkali levels.

It was also observed that the pH of the solution (Table 6) after the addition of zeolite-Y was almost 1 unit lower at the lower alkali charge than after the addition of the other zeolites.

Therefore, from this section it can be seen that as the alkali level is increased, manganese induced peroxide decomposition becomes more difficult to inhibit. All of the 3 commercially available zeolite types, at the lower alkali charge (0.001% NaOH), inhibited peroxide decomposition quite successfully. Zeolite-Y performed the best under these conditions. This alkali level is close to the pH required to oxidise manganese to the active decomposition species. Therefore it would seem from table 6 that zeolite-Y is buffering the pH of the system at the lower alkali charge or there is not

sufficient OH^- from the combined 0.001% NaOH and zeolite-Y in the system, so that the manganese active decomposition species is not formed. At the higher alkali charge, zeolite-Y did not seem to exchange manganese ions into the zeolite structure, based on the very rapid decomposition curve. However with the other two zeolites, when the results at the higher alkali charge are evaluated, it seems probable that the zeolites can easily remove and protect the Mn^{2+} in solution from being converted to the active decomposition species.

While zeolite-Y may have performed the best of the 3 zeolite types at 0.001% NaOH charge, it performed the worst of the zeolites at the higher alkali charge, 0.01% NaOH. Zeolite-X performed better than zeolite-Y, but still 90% of the peroxide was decomposed at the end of the 1 hour reaction period. Zeolite-A was the best of the 3 zeolite types in inhibiting peroxide decomposition with only 10% of the original peroxide charge being consumed over the 60 minute reaction period. It is interesting to note that these results follow the Si/Al ratio of the zeolite themselves, with the lower Si/Al ratio of zeolite-A (Si/Al=1) the best performer, zeolite-X (Si/Al=1.25) second best, and zeolite-Y (Si/Al=2.5) coming in last in terms of inhibiting manganese induced peroxide decomposition. Furthermore according to Breck(7) the lower the Si/Al ratio the greater the amount of ion exchange occurs due to the larger number of exchangeable sodium counterions. Consequently more Mn^{2+} ions are trapped and protected inside the internal structures of the zeolites with the lower Si/Al ratios. The manganese ions when exchanged into zeolite-A are preferentially located inside the β -cages or sodalite cages (see diagram 1, Chapter 2) often referred to as site I (7). Once inside the β -cages the manganese ions form ionic bonds with oxygen molecules of AlO_4^- groups. Therefore they are protected from attack by OH^- anions and peroxide. However there are another 2 sites at which manganese ions can be exchanged into the zeolite structure. Site II is located on the oxygen molecules of the six membered ring of the β -cages which face the internal void, often referred to as an α -cage(7). Manganese ions located in site II

positions are not protected by any overlapping zeolite structure as is the case in site I positions. Consequently alkali and peroxide can readily attack manganese ions in this location. Site III is adjacent to the rings forming the prisms which join the β -cages together; 4 member rings in zeolite-A, and 6 member rings in zeolite X and Y (see diagram 1). Zeolite-A mainly has manganese ions located in site I with the overflow filling up sites II and III. Zeolite-X can only partially fill up site I with sites II and III playing a more significant role in the location of manganese ions. Zeolite-Y does not have any manganese ions located in site I positions, rather they are mostly located in site II (7). The effectiveness of the zeolite in binding up manganese ions is also moderated by water as it effects the sites available for exchange, the chemistry of the exchange site and the mobility and form of manganese ions inside the zeolite. Water limits the availability of site I locations in hydrated zeolite-X such that the manganese ions are predominately located near site II and site III positions. The chemistry of the available exchange sites is changed from $\text{AlO}_3\text{-O}^-$ to $\text{AlO}_3\text{-O-H}$ by the hydrolysis of water by the sodium counterion. Consequently the bonding arrangement with manganese ions is changed from ionic and covalent to a weakened covalent state relying on dipole moments (7), producing a much less preferred bonding site. When zeolite-X and zeolite-Y are hydrated, it has been found that water forms a liquid phase inside the pores and voids of the zeolites. Zeolite-A has been found to contain complex water structures bound to the zeolite rather than a free liquid phase (7). Studies involving hydrated zeolite Na-X and Na-Y have shown that Mn^{2+} ions are fully hydrated and therefore those ions that are not bound to an exchange site are free to move through the zeolite structure. Therefore differences in decomposition rates between the lower and higher alkali charges particularly for zeolite-X and Y may be due to the manganese ions that are bound to the surface sites being attacked and consequently being involved in peroxide decomposition at the higher alkali charge. In particular for zeolite-Y with its low number of exchange sites it is likely that manganese ions are located inside its pore and channel system, but the manganese ions are predominately in the liquid phase.

Therefore when the alkali charge is raised, the manganese ions are converted to active decomposition species which lead to a peroxide decomposition curve as shown in figure 8.

3.3 Zeolites types and chemical addition order.

In section 3.2, the effect of the different zeolite types on manganese induced peroxide decomposition was investigated. Those results were based on the method of applying zeolite before sodium hydroxide followed by hydrogen peroxide as in “method 2”. However in a real world situation the sodium hydroxide may be applied before the zeolite. For example in the Cold Caustic Soda (CCS) process, eucalypt chips are impregnated with sodium hydroxide in a screw press before the first stage refining. In the CCS process, the zeolite would probably have to be added in or after the first stage of refining. Therefore, it would be important to evaluate the potential of zeolites to prevent peroxide decomposition when alkali is already present in the system, or in other words the ability of zeolite to deactivate the active manganese decomposition species.

The results reported in this section all use an alkali charge of 0.01%. At this alkali charge, the manganese will form the active decomposition species, and induce rapid peroxide decomposition. At the lower alkali charge of 0.001% NaOH the active decomposition species is not necessarily formed and could consequently defeat the purpose of this section of the investigation.

Zeolite-A

Zeolite-A's inhibiting effect on manganese induced peroxide decomposition is significantly affected when the chemical addition order is changed as shown by figure 9. When alkali is added after zeolite-A, as in the normal method, zeolite-A strongly prevents decomposition, such that approximately 90% of the original peroxide charge

remains after the 60 minutes reaction time. However when alkali is added before zeolite, the decomposition curve is the same as the case without any zeolite present. Therefore, zeolite-A has essentially no preventive effect on manganese induced peroxide decomposition when the active species has already been formed in the system.

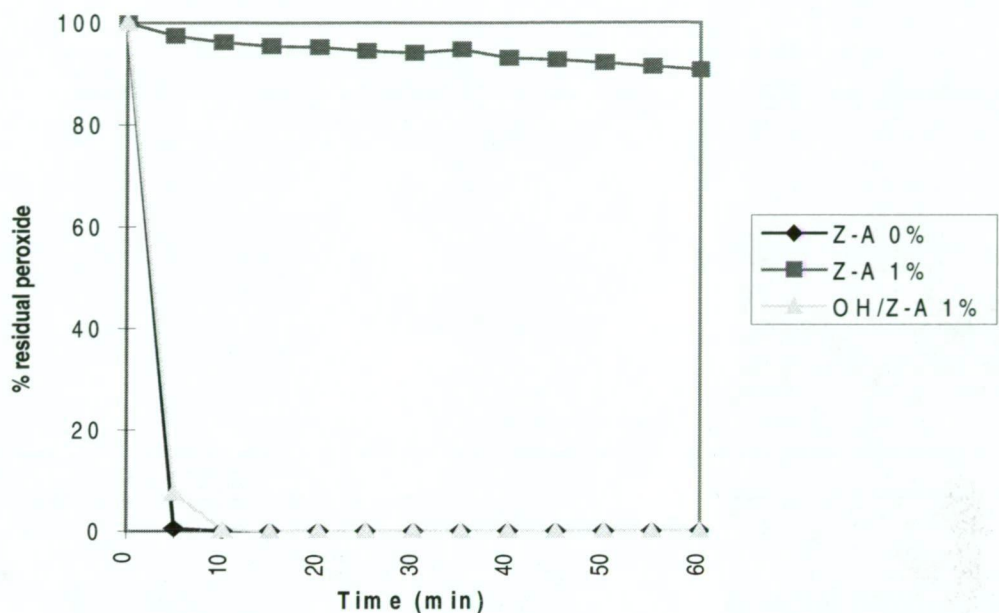


Figure 9: Zeolite-A and chemical addition order.

Table 7: pH profile for decomposition with various order of addition of zeolite-A.

Chemical	pH after addition	pH after addition	pH after addition
Mn/MilliQ water	5.0	4.2	4.2
0.01% NaOH	-	-	12.0
1% zeolite-A	-	12.0	12.3
0.01% NaOH	11.8	13.0	-
H ₂ O ₂	9.0	10.2	9.8
Final pH	11.6	10.4	12.5

Zeolite-X

The effect of chemical addition order on the ability of zeolite-X to prevent manganese induced peroxide decomposition is illustrated in figure 10. Zeolite-X when added before alkali does a reasonable job at preventing decomposition, although not as good as zeolite-A, with approximately 10% of the original peroxide charge remaining at the end of the 60 minute reaction period. However, when alkali is added before zeolite-X, the zeolite has little affect on manganese induced decomposition with all of the peroxide being decomposed within 15 minutes. Within experimental error, this result is essentially the same as in the absence of zeolite, with only alkaline manganese species present.

Table 8: pH profile for decomposition with various order of addition of zeolite-X.

Chemical	pH after addition	pH after addition	pH after addition
Mn/MilliQ water	5.0	4.2	4.2
0.01% NaOH	-	-	11.7
1% zeolite-X	-	11.3	11.7
0.01% NaOH	11.8	12.5	-
H ₂ O ₂	9.0	10.0	9.5
Final pH	11.6	11.1	11.6

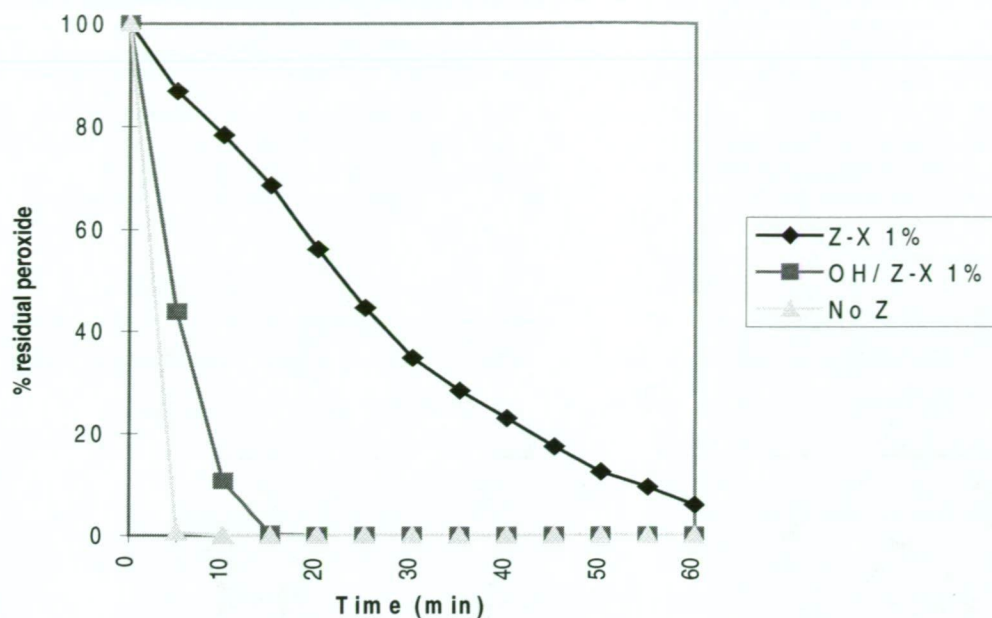


Figure 10: Zeolite-X and chemical addition order.

Zeolite-Y

The manganese induced peroxide decomposition with zeolite-Y is not affected by the change of chemical addition order. Zeolite-Y at the higher alkali charge (0.01% NaOH), regardless of alkali addition order, produced no reduction in manganese induced peroxide decomposition (figure 11). Therefore, these results could show that zeolite-Y does not exchange manganese into its structure regardless of the manganese ion form at this temperature. However it is more likely that zeolite-Y does exchange some Mn^{2+} into it when the zeolite is added before alkali, but it is in a free state and consequently forms the active decomposition species leading to peroxide decomposition. Therefore zeolite-Y does not have enough exchange capacity to effect manganese induced peroxide decomposition regardless of manganese form at 20°C.

Table 9: pH profile for decomposition with various order of addition of zeolite-Y.

Chemical	pH after addition	pH after addition	pH after addition
Mn/MilliQ water	5.0	4.2	4.3
0.01% NaOH	-	-	12.0
1% zeolite-Y	-	8.0	12.0
0.01% NaOH	11.8	12.2	-
H ₂ O ₂	9.0	9.6	9.4
Final pH	11.6	11.7	11.8

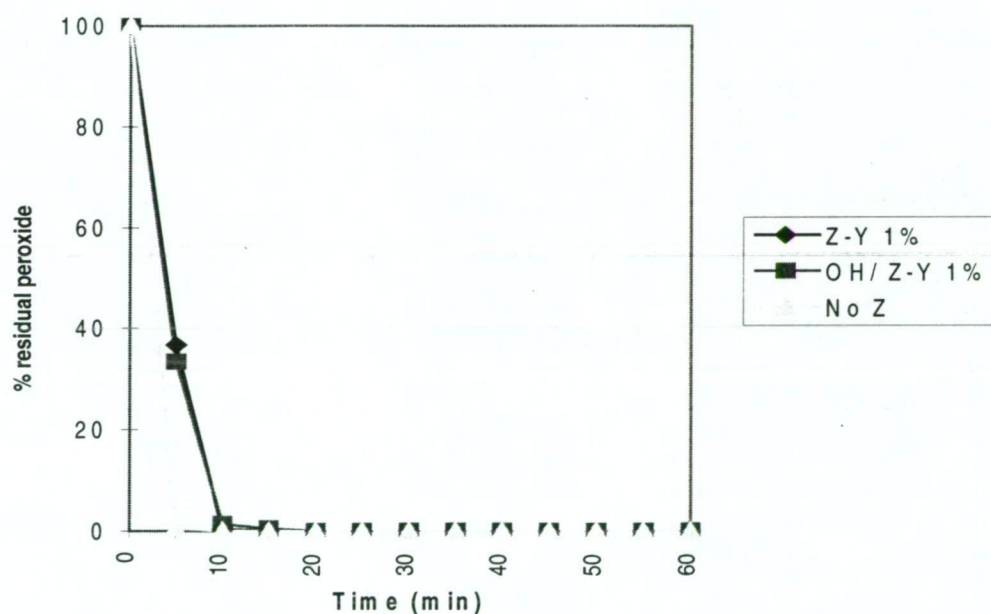


Figure 11: Zeolite-Y and chemical addition order.

The results in this system have shown conclusively that the order of chemical addition has a strong influence on the ability of the zeolites to prevent peroxide decomposition. Zeolite-A and Zeolite-X have shown that while they can prevent decomposition of peroxide to a certain extent when alkali is added after the zeolite, both perform poorly when alkali is added before the zeolite. Therefore, the zeolites A and X can exchange

soluble Mn^{2+} ions; they cannot ion exchange to any significant extent when the manganese species is more complex as manganese dioxide or some Mn-O-Mn type arrangement(8). Insolubility or slow kinetics between the complex manganese species and the zeolites are possible explanations for these observations. Zeolite-Y on the other hand has been shown to have no significant affect whatsoever on peroxide decomposition at the higher alkali charge, and it seems likely that it does not have enough exchange capacity to prevent peroxide decomposition by manganese of any species type to any great extent.

3.4 Zeolite-A and peroxide decomposition.

In section 3.2 and 3.3, zeolite-A at 1% charge was shown to perform the best of the 3 commercially available zeolite types in preventing manganese induced peroxide decomposition provided the alkali was added after zeolite as in “Method 2”. In bleaching studies involving Pine TMP (chapter 5), higher charges of zeolite-A were required for positive gains in brightness and residual peroxide values and therefore this section will investigate the effect of zeolite-A concentration on manganese induced peroxide decomposition at 0.01% NaOH using “Method 2”. 0.001% NaOH is no longer used as there was only minimal peroxide decomposition and the equivalent pH is not like anything used in peroxide bleaching conditions.

The effect of zeolite-A concentration on manganese induced peroxide decomposition is illustrated in figure 12 and the pH results are shown in Table 10. In the absence of any zeolite-A, a very rapid manganese decomposition curve is produced. Addition of 1% zeolite-A however significantly reduces total peroxide decomposition to such an extent that approximately 90% of the original peroxide charge remains after the full reaction period. Increasing the zeolite-A charge to 2% leads to an increase in the decomposition rate, with approximately 78% of the original peroxide remaining. Further addition of zeolite-A to 3% charge induces another increase in the rate of decomposition, with

approximately 70% of the original peroxide charge remaining. At zeolite-A charges of 4% and 5% the rate of peroxide decomposition, is approximately 55% of the original. There is no significant difference between the two charge levels. So the overall trend is that as zeolite-A charge is increased above 1% zeolite, increased decomposition occurs:

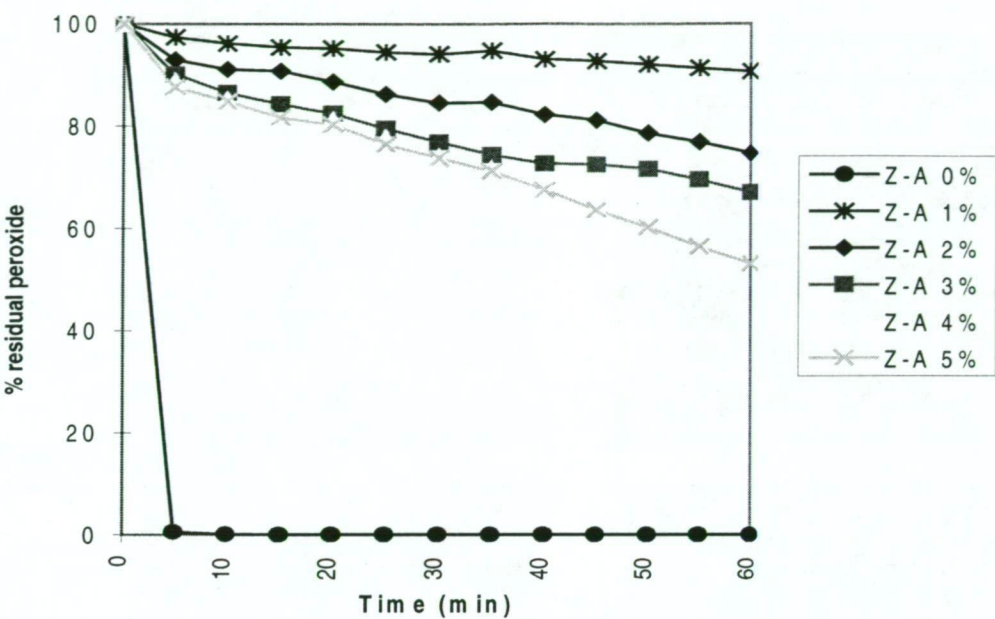


Figure 12: manganese induced peroxide decomposition with zeolite-A concentrations.

Table 10: pH profile for decomposition with various concentrations of zeolite-A.

Chemical	0% Z-A	1% Z-A	2% Z-A	3% Z-A	4% Z-A	5% Z-A
Mn/H ₂ O	5.0	4.9	4.4	4.1	4.4	4.3
zeolite-A	-	11.1	11.9	11.8	12.0	12.3
NaOH	11.8	12.3	12.2	12.8	12.8	13.0
H ₂ O ₂	9.0	9.8	9.9	10.2	10.3	10.4
Final pH	11.6	9.9	10.2	10.5	11.2	11.2

There are two possible explanations for these results; firstly that the increased zeolite charge produced more surface sites for manganese exchange. Consequently the

majority of manganese ions are located on the surface sites because there is an insufficient manganese concentration gradient to force the manganese ions to pass the surface sites (II and III) and absorb into the internal zeolite structure (site I). The manganese ions located on the surface can be attacked by alkali and participate to some extent in peroxide decomposition reactions. The other possibility is that the zeolite itself is involved in some decomposition reactions and that increasing the zeolite charge increases the amount of decomposition.

In order to investigate the mechanism of increased decomposition with increasing zeolite-A charge, figure 13 illustrates the results of a study into peroxide decomposition with zeolite-A, but without any manganese present. This figure shows that there is no significant difference between 1% zeolite-A and 5% zeolite-A with respect to peroxide decomposition. Therefore, it seems likely that zeolite induced decomposition is not responsible for increased decomposition at higher zeolite-A charges. Table 11 shows the pH results for the decomposition using zeolite-A without manganese ions.

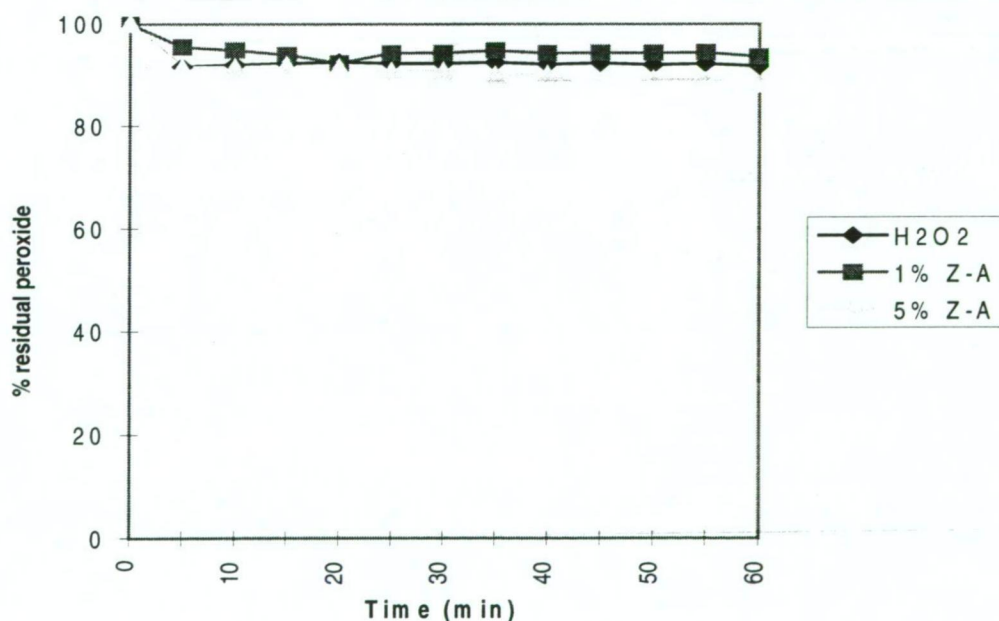


Figure 13: The effect of zeolite-A without any manganese on peroxide decomposition.

Table 11: pH profile for decomposition using zeolite-A without any manganese.

Chemical	No zeolite-A	1% zeolite-A	5% zeolite-A
MilliQ water	4.0	4.4	4.7
Zeolite-A	-	11.9	11.8
0.01% NaOH	12.8	12.3	12.4
H ₂ O ₂	10.0	9.9	10.0
Final pH	9.6	10.0	10.2

The results in this section have shown that lower charges of zeolite-A particularly 1% or less perform the best in preventing peroxide decomposition. The increased decomposition observed at higher zeolite charges is best described by the supposition that increasing the zeolite charge increases the number of surface cation exchange sites. Assuming also that the surface sites would be filled before the manganese ions migrate into inner cage sites, there would be a zeolite level at which most of the manganese ions would be bound on the outer surfaces rather than inside the zeolite. The surface bound manganese is less likely to be protected from alkali and peroxide attack. Therefore it is possible that these surface bound manganese can partially decompose peroxide. Under the conditions of this experiment, the level for 45 ppm manganese to be surface bound appears to be at 4% zeolite-A (figure 12) as the 5% curve is essentially identical to that at 4% zeolite-A.

3.5 Peroxide decomposition with citrate.

A patent(9) suggests that the use of low molecular weight organic acids may improve the zeolite system by what seems to be a transfer of metal ions based on the complex formation constants difference between the organic acid (low) and zeolite (higher). However, there could exist other possibilities such as an increase in total complexing power, or the organic acid- metal ion complex may have greater bonding to the inside of

the zeolite structure and therefore could increase the equilibrium towards metal ions staying inside the zeolite structure rather than migrating back into solution at some equilibrium point. Consequently, it is important to investigate the effects of sodium citrate without any zeolite on manganese induced peroxide decomposition.

Figure 14 illustrates the effect of sodium citrate charge on manganese induced peroxide decomposition while Table 12 shows the corresponding pH profile. The results indicate that when there is no citrate, manganese can decompose all the peroxide within 5 minutes. However, with the addition of 0.2% citrate to the system the rate of decomposition was reduced by a small margin when compared to the case without any citrate. The reduced rate was such that it took 25 minutes to completely decompose the peroxide compared to 5 minutes without any citrate. Further addition of citrate to 0.5% charge significantly reduced the rate of decomposition such that 90% to 95% of the original charge remained after the full 60 minute reaction period. There was no further gain in reducing decomposition by adding additional citrate up to a charge level of 3%.

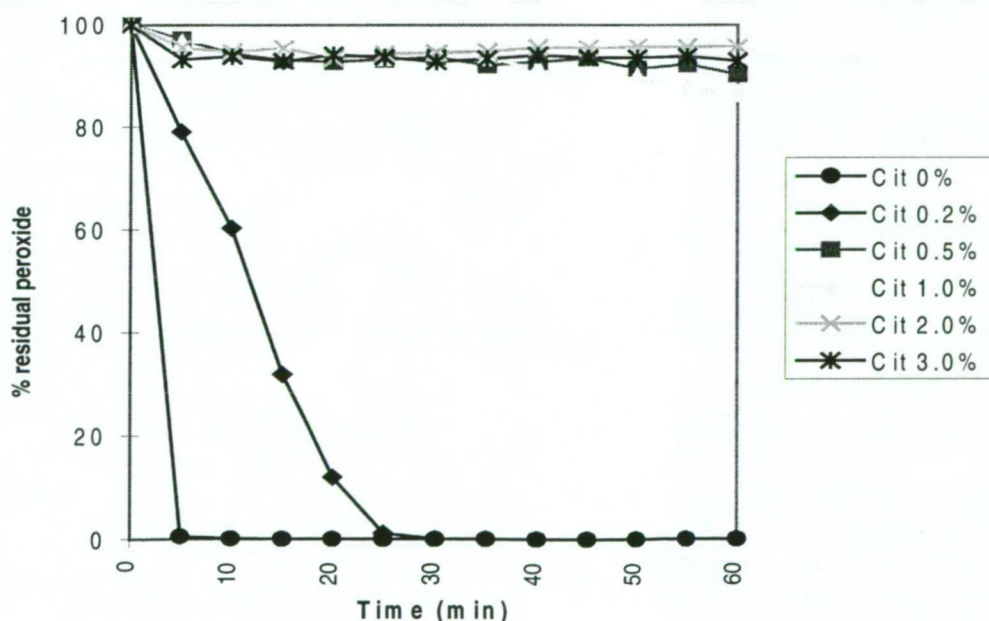


Figure 14: Peroxide decomposition with sodium citrate concentration.

Table 12: pH profile for decomposition with various citrate concentrations.

Chemical	0% Cit	0.2% Cit	0.5% Cit	1.0% Cit	2.0% Cit	3.0% Cit
Mn/H ₂ O	5.0	4.1	4.2	4.4	4.9	4.1
Citrate	-	7.8	7.6	8.0	8.3	8.1
NaOH	11.8	11.3	11.4	11.5	11.8	11.8
H ₂ O ₂	9.0	8.9	9.1	9.0	9.2	9.1
Final pH	11.6	11.3	9.3	8.9	9.1	9.0

Previously it has been shown that 1% zeolite-A performs well when alkali is added after the zeolite, but performs quite poorly when the order of alkali addition is reversed.

Figure 15 describes the effect when the order of alkali addition is changed with both the acid (citric acid) and alkaline (sodium citrate) forms of citrate. Sodium citrate is shown to behave similarly to the zeolite-A in that at 0.5% charge with alkali added after the citrate approximately 90% of the original peroxide charge remains after the 60 minute reaction period. However adding the alkali before the citrate dramatically increases the rate of decomposition such that the curve resembles that of a curve with manganese alone. This also occurred with zeolite-A when the order of alkali was reversed as shown in figure 9.

The citric acid, however, did not exhibit this alkali addition order effect, with no decomposition occurring with alkali added before or after citric acid. However, the main reason for no decomposition being exhibited with citric acid is that the pH of the system at 0.5% charge is around 1.7 (see Table 13). We have shown earlier that for any peroxide decomposition to occur with manganese, the solution must be alkaline. While there was no peroxide decomposed it was observed that the brown coloured active species was formed when the alkali was added first, but then it disappeared with the

addition of citric acid after about 1 minute reaction time. So obviously with acid and the chelating capacity present, the active alkaline species can be degraded back to the Mn^{2+} species.

Table 13: pH profile for decomposition with various forms of citrate.

Chemical	0.5% Na-Cit	0.5% Na-Cit	0.5% H-Cit	0.5% H-Cit
Mn/MilliQ	4.2	3.5	4.1	3.9
0.01% NaOH	-	11.8	-	11.3
Citrate	7.6	12.1	1.7	1.8
0.01% NaOH	11.4	-	1.8	-
H ₂ O ₂	9.1	9.5	1.7	1.7
Final pH	9.3	11.9	1.7	1.7

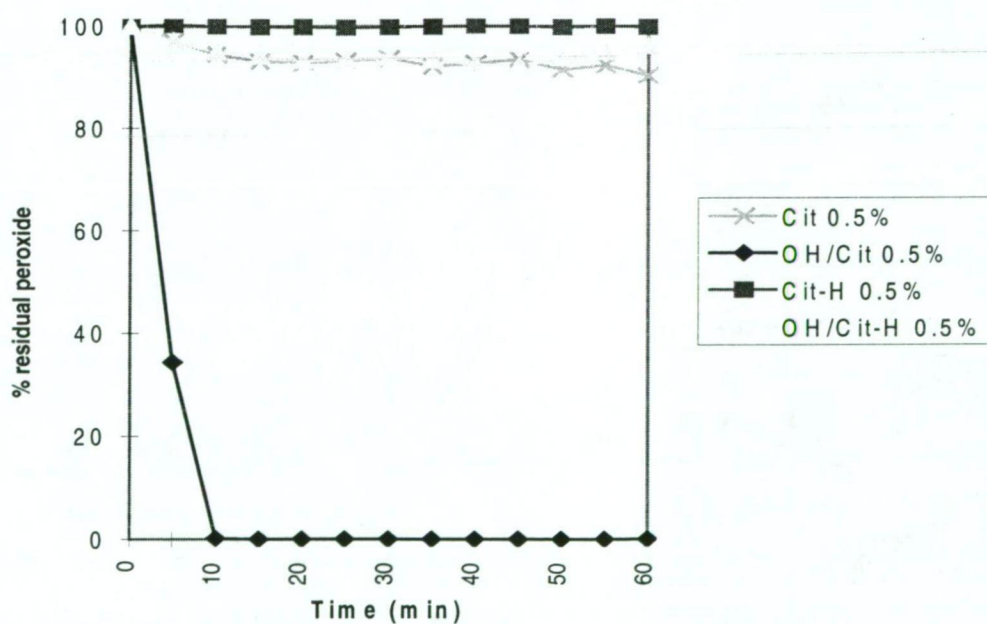


Figure 15: The effect of citrate type and addition order on peroxide decomposition.

This section has shown that sodium citrate dosed at a charge of 0.5% or higher can significantly inhibit peroxide decomposition induced by 45 ppm manganese with 0.01%

NaOH at 20°C. The results in figure 14 suggest that sodium citrate acts as a chelating agent in binding up the manganese and hence preventing the formation of the active species. The result observed at 0.2% citrate further suggests that the citrate was acting primarily as a chelating agent, although this concentration was not enough to chelate all of the manganese ions. The effect of citrate is dependent on the citrate being able to bind up the Mn^{2+} ions before they are converted by alkali into the active decomposition species. The acid form of citrate (citric acid) lowers the pH of the system into the acid region and therefore no manganese induced peroxide decomposition occurred. Citric acid would not find application in a real bleach plant unless a pre-existing acid wash step is used.

3.6 Peroxide decomposition with zeolite-A and sodium citrate.

In previous sections the effect of zeolite-A and sodium citrate alone have been investigated. This section will cover the combined effect of zeolite-A and citrate added together to the manganese induced peroxide decomposition system. Zeolite-A at low concentrations prevents most peroxide decomposition. Therefore high zeolite-A charges which allow for significant decomposition have been combined with citrate in figure 16 to evaluate if there could be a possible benefit with a combined system over that of zeolite-A alone. Furthermore it was found in bleaching studies involving Pine TMP (chapter 5) that higher amounts of zeolite were required to produce a positive effect on brightness and residual peroxide values.

The combined effect of both 5% zeolite-A and sodium citrate is illustrated in figure 16. Table 14 shows the corresponding pH profile. When a charge of 5% zeolite-A is applied without any citrate a decomposition curve ending with 55% of original peroxide charge. However when 0.2% citrate is added to the zeolite system significant reduction in peroxide decomposition occurs, such that about approximately 87% of the original peroxide charge remains after the full 60 minute reaction period. Further increases to

0.5% citrate charge lead to an increase in the rate of decomposition to such an extent that it performed worse than the system without any citrate present. The final residual peroxide was only 40% of the original charge. 1% citrate with 5% zeolite-A however produced a significant reduction in peroxide decomposition with 75% of the original peroxide charge remaining after the full 60 minute reaction period. It is interesting to note that for the first 25 minutes this curve performed the best in inhibiting decomposition, however after 25 minutes the rate of decomposition started to accelerate. This would indicate that an equilibrium point had been reached and the effect of citrate at the 1% charge was becoming less significant. Therefore these results tend to suggest that a small amount of sodium citrate is desirable when using zeolite-A to inhibit manganese induced peroxide decomposition. A possible explanation could be that at very low concentrations the citrate acts as a transfer agent for the manganese into the zeolite. At some point the citrate (0.5%) starts to exchange the ions between themselves forming short lived species which allow manganese to attack the peroxide. When the citrate level is increased the citrate may form longer and more stable complexes which prevent manganese attack on peroxide to a greater extent than the 0.5% citrate case.

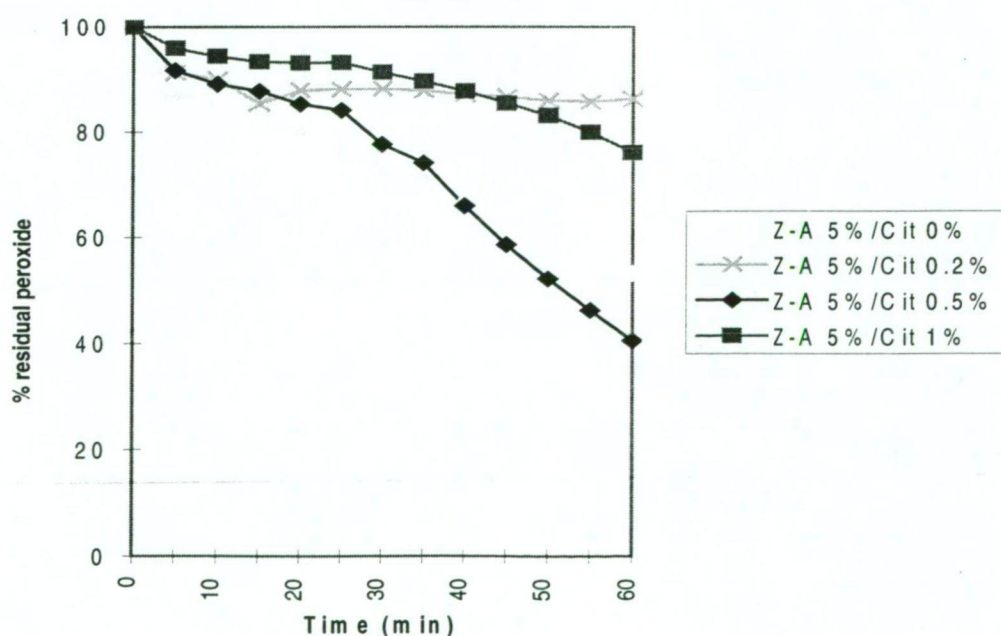


Figure 16: Combined effect of zeolite and sodium citrate on peroxide decomposition.

Table 14: pH profile for decomposition with zeolite and citrate.

Chemical	0% Citrate	0.2% Citrate	0.5% Citrate	1.0% Citrate
Mn/MilliQ	4.3	5.3	4.6	4.1
5% zeolite-A	12.3	11.4	11.4	11.1
Citrate	-	12.0	11.5	11.2
0.01% NaOH	13.0	13.1	12.6	12.3
H ₂ O ₂	10.4	10.4	9.9	9.6
Final pH	11.2	10.8	10.4	9.9

3.7 Peroxide decomposition with DTPA.

DTPA is the current chemical of choice for chelating metal ions out of pulp by many pulp and paper manufacturers around the world who use a peroxide bleaching stage whether it is being used in a chemical or mechanical pulp process. Therefore, it is important to compare the effect on decomposition with zeolites, citrate or a combined system against that of DTPA.

DTPA in either its acid or alkaline form prevents any significant peroxide decomposition induced by an alkaline species as shown by figure 17. The solution pH profiles are shown in Table 15. DTPA never lets the brown active decomposition species form when added before alkali. However the brown active decomposition species does form when alkali is added first but disappears within about 30 seconds leaving a clear solution which does not decompose peroxide. The reason for this is that DTPA forms an extremely strong complex(10,11) with manganese that excludes any peroxide reaching the manganese ion and reacting with its outer shell electrons.

Table 15: pH profile for decomposition with DTPA.

Chemical	Na-DTPA	Na-DTPA	H-DTPA	H-DTPA
Mn/MilliQ	4.8	5.0	4.4	4.4
0.01% NaOH	-	10.8	-	12.2
0.5% DTPA	11.7	12.0	1.7	2.8
0.01% NaOH	12.2	-	1.8	-
H ₂ O ₂	10.0	10.0	1.7	1.8
Final pH	9.8	9.8	1.7	1.2

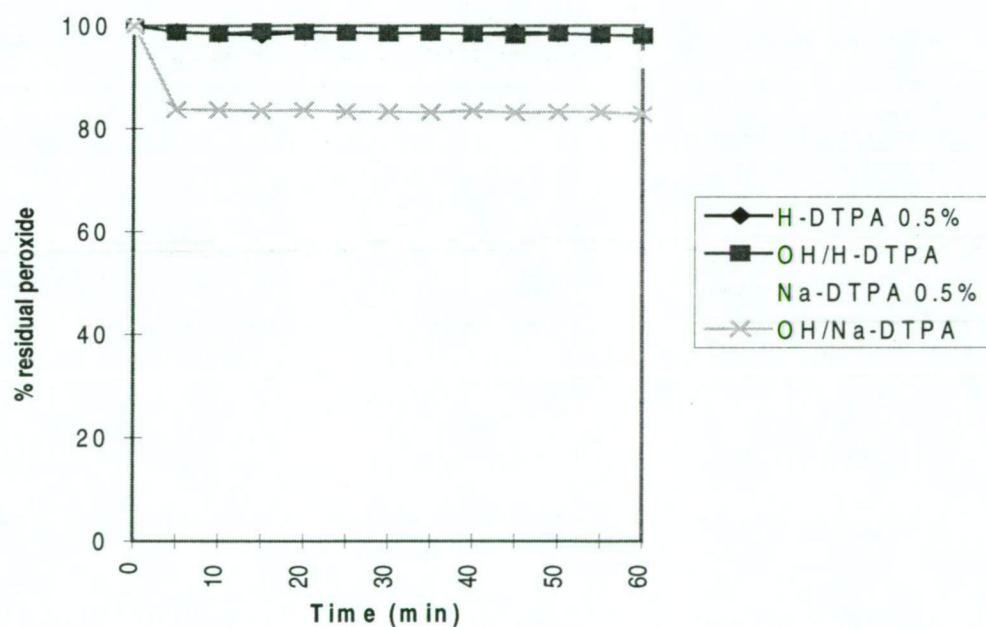


Figure 17: The effect of DTPA and alkali addition order on peroxide decomposition.

3.8 Conclusion:

- The experimental system of 45 ppm manganese at 0.001% NaOH readily decomposes peroxide and so provides a good system for investigating the effects of zeolite and other chelating systems.

- Under these conditions the active decomposition species is MnO_2 or a Mn-O-Mn type arrangement although $\text{Mn}(\text{OH})_2$ is also thought to play a role in the catalytic cycle.
- At 0.001% NaOH all of the 3 zeolite types inhibit decomposition, though it appears that formation of the active decomposition species was prevented due to possibly zeolites buffering the system.
- At the higher alkali charge (0.01%), zeolite-A was better than zeolite-X, while zeolite-Y performed poorly in inhibiting peroxide decomposition. These results appear to follow Si/Al ratio of the zeolites. This ratio has a bearing on the cation exchange capacity.
- Zeolite-A produced the best inhibition of peroxide decomposition at charges of 1% or less. Higher addition levels increased the rate of decomposition. A possible explanation of this increase in decomposition with zeolite charge could be that there are more surface sites. The surface sites are more readily accessible and the manganese more readily exchanges on the surface than in the β -cages at higher zeolite charges. Furthermore manganese bound on the surface sites may to some extent decompose peroxide.
- It is important that the active manganese species is not formed prior to zeolite addition. If the active species is present then zeolite is unable to inhibit peroxide decomposition.
- Sodium citrate was found to inhibit peroxide decomposition at 0.5% or greater addition levels. Like zeolite, citrate required the Mn^{2+} species to be present otherwise if $\text{Mn}^{4+}/\text{Mn}^{3+}$ decomposition species were present then the citrate was unable to inhibit peroxide decomposition.
- Citrate and zeolite combined produced a synergistic effect on peroxide decomposition. 5% zeolite-A and 0.2% sodium citrate greatly enhanced the inhibition of the decomposition reaction.

CHAPTER 4: PEROXIDE DECOMPOSITION AT 70°C

This chapter will cover the various effects of pH, zeolite type, zeolite concentration, citrate type and concentration, zeolite and citrate combined, and DTPA type on peroxide decomposition at 70°C. This chapter will use only the alkali charge of 0.01% NaOH based on the results observed in the previous chapter, "Peroxide decomposition at 20°C".

4.1 Peroxide decomposition with manganese

The effect of manganese on peroxide decomposition at 70°C is shown in Figure 18. As noted previously in chapter 3, the effect of pH on the action of manganese on peroxide decomposition is quite significant. Under acid conditions, manganese is not converted to the active species, so despite the increase in reaction temperature there is no significant peroxide decomposition. When the pH is however changed to alkaline conditions, extremely rapid decomposition occurs. All the peroxide was decomposed within the first 5 minutes, no bubbles (oxygen gas) were observed after about 3 minutes so it is likely that all of the peroxide was consumed then, rather than at the first sample time of 5 minutes. At high pH, manganese undergoes reactions which form a brown precipitate with destructive catalytic properties. It seems likely that this species is manganese dioxide (MnO_2), as manganese is known to oxidise from Mn^{2+} to various states such as Mn^{3+} , Mn^{4+} , and Mn^{7+} under alkaline conditions via a catalytic cycle involving $\text{Mn}(\text{OH})_2$ (2-4). However manganese can form more complex ions such as Mn_3O_4 and it has been proposed by Abbot(8) that the catalytic species may actually be an Mn-O-Mn type complex species.

The manganese catalysed decomposition of peroxide at high pH is ideal for the study of the effect of additives on peroxide decomposition because it produces very rapid decomposition.

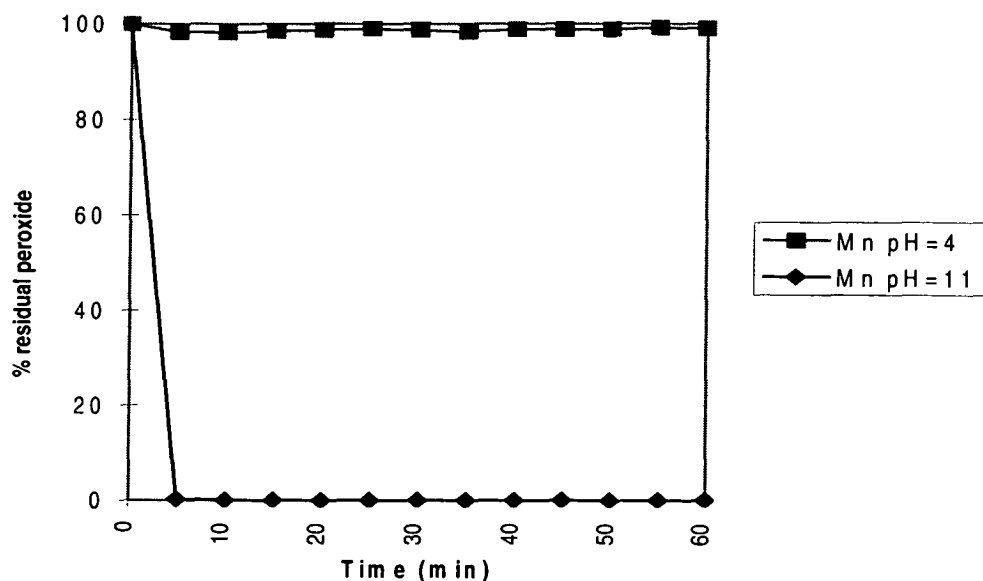


Figure 18: Peroxide decomposition with manganese at various pH's.

Hydrogen peroxide is shown to be quite stable under alkaline conditions (0.01% NaOH) at 70°C in figure 19 over the 60 minute reaction period used in this study. Figure 19 also highlights the dramatic effect of adding manganese (45 ppm) to the system with all the peroxide destroyed within 3 minutes (as previously stated), compared to essentially no decomposition when manganese is absent.

The results in this section show that manganese under alkaline conditions rapidly decomposes peroxide, while under acid conditions manganese has no effect on peroxide decomposition. The only difference between 70°C (figures 18,19) and 20°C (figures 1,4) is the slight decrease in the time at which full peroxide decomposition occurred of 3 minutes at 70°C compared to 5 minutes at 20°C. There were no significant effects at both temperatures on peroxide decomposition under acid conditions. Furthermore, peroxide itself did not decompose under alkaline conditions at both temperatures. Therefore, it seems that the pH of the system is important in forming the active

decomposition species, whereas the temperature only accelerates the performance of the active decomposition species once formed.

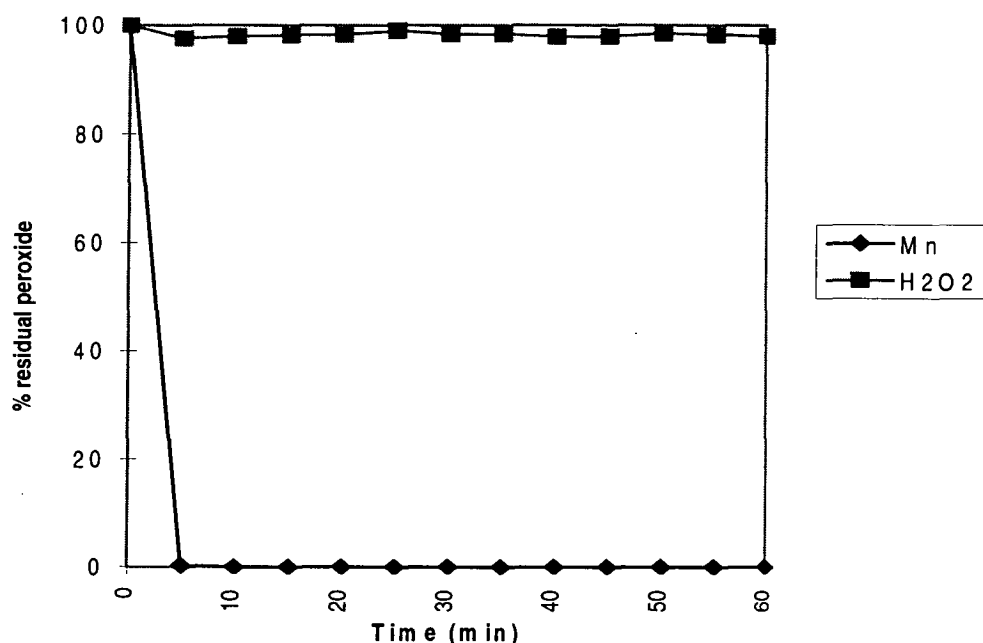


Figure 19: Peroxide decomposition with and without manganese at 0.01% NaOH.

4.2 Peroxide decomposition with zeolite type

The three commercially available zeolites were used to investigate the effect of zeolite type on manganese induced peroxide decomposition at 70°C. Figure 20 illustrates the effect of zeolite-A, X and Y on peroxide decomposition while Table 16 shows the corresponding pH profile. The manganese curve has been used to show the effect of not having any zeolite in the system. Obviously, not having any zeolite produces no significant reduction in the rate of peroxide decomposition and hence all of the peroxide is decomposed within five minutes. Addition of 1% zeolite-A however provides quite a large reduction in the decomposition rate with 50% of the original peroxide charge remaining after the full 60 minute reaction period. Zeolite-X did not perform as well as zeolite-A with approximately 10% of the original charge remaining after the full reaction period. The reaction with zeolite-X seems to be different to both zeolite-A and zeolite-Y with a fast initial decomposition rate that slows down with lower residual

peroxide charges. The reactions with zeolite-A and zeolite-Y were roughly linear. Zeolite-Y proved to be the worst performer of the 3 zeolite types with all of the peroxide decomposed within 45 minutes.

Table 16: pH profile for decomposition with various zeolite types.

Chemical	No zeolite	zeolite-A	zeolite-X	zeolite-Y
Mn/MilliQ	4.6	4.1	4.1	4.1
1% zeolite	-	10.7	10.3	7.8
0.01% NaOH	11.3	11.4	11.3	9.8
H ₂ O ₂	8.6	9.4	9.0	7.9
Final pH	11.0	9.5	10.1	10.0

The rise in reaction temperature from 20°C to 70°C has had different consequences on the rate of peroxide decomposition for the 3 different zeolite types. For instance when comparing figure 20 with figure 6 (0.01% NaOH) for zeolite-A there is a drop of 40% units in the residual peroxide at the end of the reaction period, from 90% to 50%, when

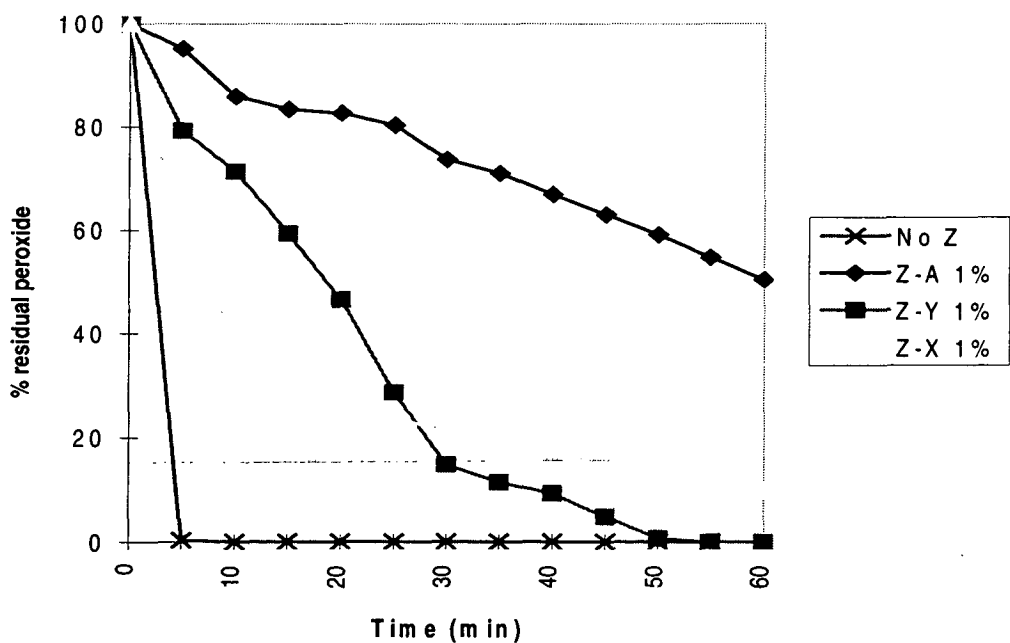


Figure 20: Peroxide decomposition with 3 zeolite types.

the temperature is raised to 70°C. Zeolite-X was less affected with essentially no difference between the curves at 20°C (figure 7) and 70°C (figure 20). However the curve at 70°C was less linear suggesting that there may be a change in the decomposition rate order.

The rise in reaction temperature actually produced a significant reduction in the decomposition rate with an increase of 35 minutes before all of the peroxide decomposed from 10 minutes at 20°C (figure 8) to 45 minutes at 70°C (figure 20) for zeolite-Y.

Zeolite-A was found to be the best performer of all the zeolite types. Zeolite-A has a lower Si/Al ratio (Si/Al=1.0) than both zeolite-X (Si/Al=1.3) and zeolite Y (Si/Al=2.5) which allows for more rapid and complete ion exchange provided that the ion diameters are small enough to enter the zeolite structural cages(7). When the reaction temperature was raised from 20°C to 70°C, it had a negative effect on the performance of zeolite-A , negligible effect on zeolite-X and a positive effect on zeolite-Y. These results are likely due to the higher energy levels at 70°C which affect the ion exchange equilibrium. The higher energy levels allow the exchange of manganese to overcome some of the structural energy barriers in zeolite-Y. Greater ion exchange and consequently a lower rate of peroxide decomposition occur. A possible explanation why zeolites A and X behave differently to zeolite-Y could be that the higher energy levels reduce the stability of the bonding that keeps the manganese inside the zeolite structure.

4.3 Peroxide decomposition with zeolite-A charge.

In the previous section, zeolite-A was shown to be the best of the 3 zeolites types in inhibiting manganese induced peroxide decomposition at 70°C. This section will investigate the effects of zeolite-A charge on peroxide decomposition with and without

manganese at 70°C. Furthermore the results presented in this section can be directly related to studies involving the peroxide bleaching of Pine TMP(chapter 5) as the experiment conditions are the same with the exception of pulp fibres.

Figure 21 illustrates the effect of zeolite-A charge on the manganese induced peroxide decomposition system while Table 17 presents the pH profile. The absence of any zeolite produces a very rapid decomposition with all of the peroxide decomposed within the first five minutes (3 minutes observed). When the 1% zeolite-A charge was added to the system the decomposition rate was reduced such that 50% of the original charge remained. Addition of up to 2% zeolite, increased the rate of decomposition compared to 1% zeolite-A with approximately 30% of the original charge remaining. 3% zeolite-A charge produced a further increase in the rate of decomposition with approximately 17% of the original peroxide charge remaining. Further additions to 4% and 5% zeolite-A produce further increases in the rate of decomposition with all of the peroxide decomposed at 60 and 45 minutes respectively. Therefore, as the zeolite-A charge is increased, the rate of peroxide decomposition is increased. These general observations for zeolite-A charge are comparable to those at 20°C (figure 12), however the amount of decomposition is larger at 70°C (figure 21). For instance a comparison at 1% and 5% zeolite-A between the two temperatures highlights the increased rate of decomposition at the higher temperature; 90% (20°C) compared 50% (70°C) original peroxide charge remaining at 1% zeolite

Table 17: pH profile for decomposition with various zeolite-A concentrations.

Chemical	0% Z-A	1% Z-A	2% Z-A	3% Z-A	4% Z-A	5% Z-A
Mn/H ₂ O	4.6	3.3	4.1	3.8	4.1	3.7
Zeolite-A	-	10.8	11.5	11.4	11.4	11.3
NaOH	11.3	11.6	11.9	11.8	11.6	11.7
H ₂ O ₂	8.6	9.3	9.8	9.7	9.8	9.6

Final pH	11.0	10.0	10.9	10.4	11.4	11.6
----------	------	------	------	------	------	------

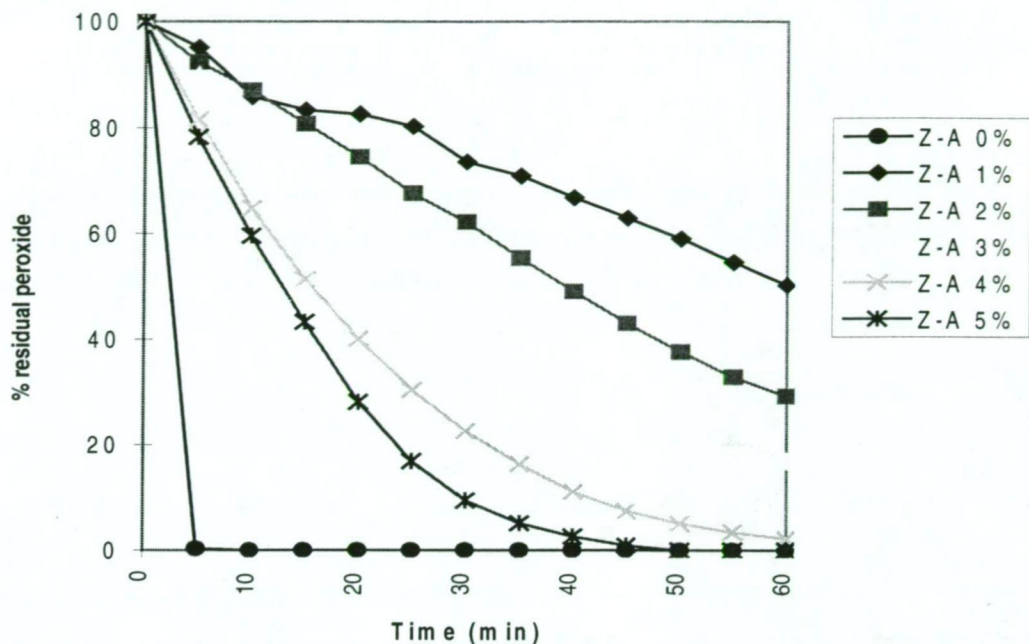


Figure 21: Peroxide decomposition with zeolite-A charge.

charge, and 55% (20°C) compared to 0% at 45 minutes (70°C) of the original peroxide charge for 5% zeolite-A.

In order to clarify the effect of zeolite-A charge on peroxide decomposition, the residual peroxide results in figure 21 at 30 minutes have been plotted against zeolite charge rather than time in figure 22. Figure 22 highlights the effect of zeolite charge on peroxide decomposition, with increasing zeolite charge producing a significant increase in the rate of decomposition. For instance, at 1% zeolite-A charge approximately 75% of the original peroxide charge remains after 30 minutes compared to only about 10% of the original peroxide concentration left at 30 minutes with 5% zeolite-A charge, a loss of around 65% units.

Figure 21 and figure 22 illustrate the effect of zeolite-A charge on peroxide decomposition. These results show that increasing the zeolite charge actually increases the rate of peroxide decomposition. This observation might be explained by peroxide

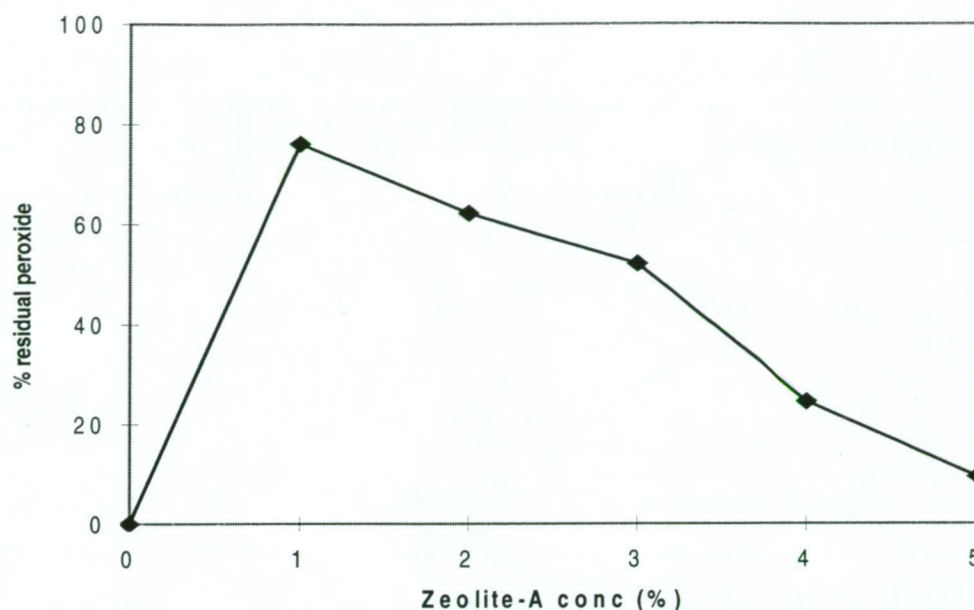


Figure 22: Peroxide decomposition with zeolite-A charges at 30 minutes reaction time.

decomposition with manganese bound on the outer surfaces of the zeolite structure. Some authors note that the performance of laundry detergents which use inorganic/organic peroxides has been reduced when triphosphate chelating agents were replaced with zeolites (12). Schepers and Verburg (13) observed gas release, which they concluded was oxygen, one of the primary peroxide decomposition products. The addition of zeolite-A to the decomposition system without any manganese present, at 70°C has quite a significant effect on peroxide decomposition. At 1% zeolite charge approximately 60% of the original peroxide charge is decomposed over the 60 minutes reaction period. The addition of 5% zeolite-A induces a greater rate of decomposition than 1% zeolite-A with essentially all of the peroxide being consumed within the reaction time of 55 minutes. Therefore, these results confirm that increasing the zeolite-A charge increases the rate of decomposition. In comparison to the results obtained at

20°C (figures 12, 13) the mechanism of decomposition would seem to be different at 70°C (figures 21,22,23). At 20°C the results suggested that the most likely explanation for the increased rate of decomposition with increased zeolite charge was that at the higher zeolite charges the manganese was absorbed onto the outer surfaces rather than being bound deep inside the zeolite structure. However, the results at 70°C, in particular figure 23, suggest that the zeolite itself plays a more significant role in the mechanism of peroxide decomposition. The decomposition curves with zeolite-A alone (figure 23), have shown that the rate of decomposition is equal to or greater than the curves with manganese present (figure 21). A possible explanation of how the zeolite operates in preventing manganese induced decomposition could be that the manganese is rapidly absorbed onto the inner exchange sites (site I) within the zeolite structure leaving the

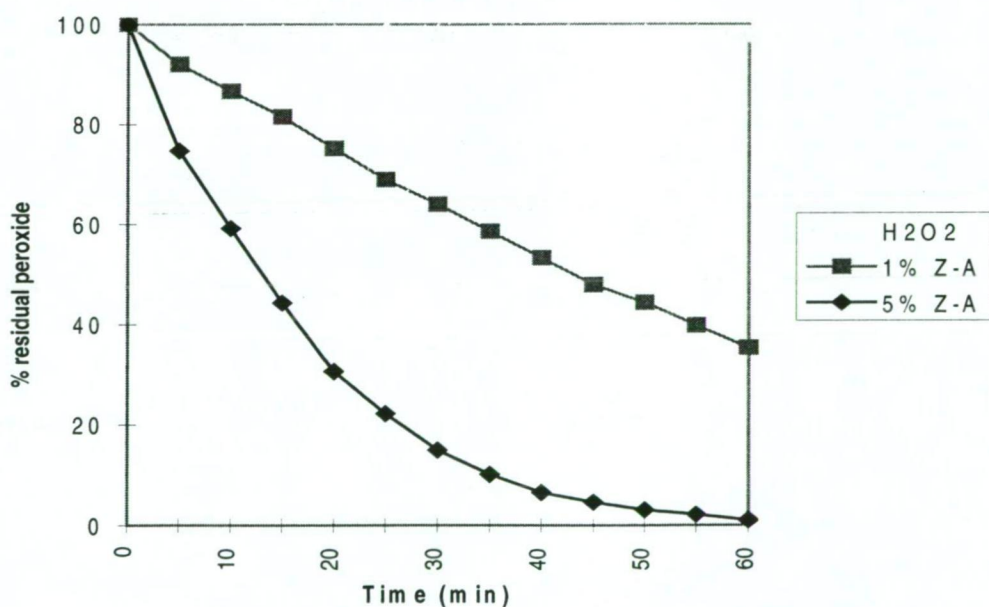


Figure 23: Peroxide decomposition with zeolite-A without any manganese.

Table 18: pH profile for decomposition using zeolite-A without any manganese.

Chemical	No zeolite-A	1% zeolite-A	5% zeolite-A
MilliQ water	4.8	4.3	4.0
Zeolite-A	-	11.3	11.0
0.01% NaOH	11.4	11.8	11.9
H ₂ O ₂	8.8	9.5	9.5
Final pH	8.8	10.1	11.5

outer surface sites (site II) available for interaction. The explanation can be taken one step further to explain why at 1% zeolite charge there is greater decomposition without manganese present than with. It might be that the manganese is tightly bound to the cation exchange site, and it acts to block the site from reaction with peroxide. Therefore the number of active decomposition sites in the zeolite is lower when manganese is exchanged and hence a lower decomposition rate may occur. Furthermore as the amount of zeolite is increased there are more sites available for interaction with peroxide as there is a fixed concentration of manganese and consequently the rate of decomposition increases with the zeolite charge.

The rise in reaction temperature from 20°C to 70°C has significantly increased rate of manganese induced peroxide decomposition with zeolite-A present. Increasing the zeolite-A charge only further increases the rate of peroxide decomposition. However, at the higher temperature, the rate at which peroxide decomposition due to zeolite alone is significantly increased. It would appear that the mechanism by which peroxide decomposition occurs in the presence of zeolite-A is different at the higher temperature, with zeolite-A itself playing a more significant role.

4.4 Peroxide decomposition with organic chelating agents.

4.4.1 Peroxide decomposition with sodium citrate charge.

The effect of sodium citrate on peroxide decomposition at 70°C is illustrated in Figure 24. Addition of 0.5% sodium citrate significantly reduces the rate of peroxide decomposition from 5 minutes to 40 minutes before peroxide exhaustion. However, when sodium citrate was increased to 1%, an increase in the rate of decomposition occurred from 40 minutes at 0.5% charge to 20 minutes at 1% charge. As the addition was further increased, peroxide decomposition was again reduced with 10% peroxide after 60 minutes with 2% charge and approximately 80% peroxide after 60 minutes at 3% charge. This local minimum at 1% sodium citrate is particularly interesting. In the 1% case after 5 minutes, a thin black film was observed to form over all surfaces in the reactor (polyethylene) and over the pH probe (polyethylene and glass). It should be noted that the result at 1% was the average of 2 experiments, with the black surface film forming in both runs.

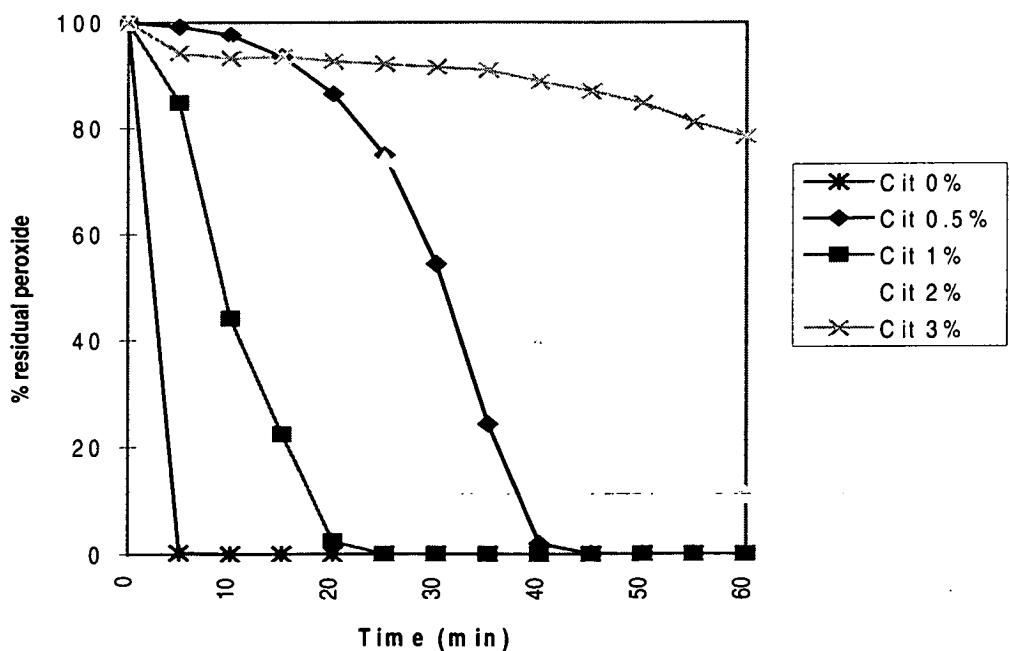


Figure 24: Peroxide decomposition with sodium citrate charge.

Table 19: pH profile for decomposition with various citrate concentrations

Chemical	0% Cit	0.5% Cit	1.0% Cit	2.0% Cit	3.0% Cit
Mn/H ₂ O	4.6	4.2	4.6	4.5	4.5
Citrate	-	8.0	8.6	8.5	8.7
NaOH	11.3	10.7	11.0	10.7	11.1
H ₂ O ₂	8.6	8.3	8.8	8.8	8.7
Final pH	11.0	9.9	9.9	9.9	9.0

The film coating all of the surfaces in the reaction vessel could not be scratched off with a spatula. The only way to remove the surface coating was to dissolve the coating by 3 hours of stirring in 10% sulphuric acid and DTPA solution. If the sodium citrate charge is increased even further, this surface activated decomposition species can be bypassed, as shown by the 3% sodium citrate curve where no film formation occurred.

Figure 25 has been included to highlight the effect of sodium citrate concentration, particularly at 1% charge on peroxide decomposition. The residual peroxide values at 30 minutes have been taken from figure 24 and converted to a residual peroxide vs citrate concentration in figure 25. Figure 25 highlights that there is a beneficial reduction in peroxide decomposition at 0.5% charge, significant gain in the rate of decomposition at 1% followed by additional reductions in decomposition rate as the citrate charge is increased above 1%.

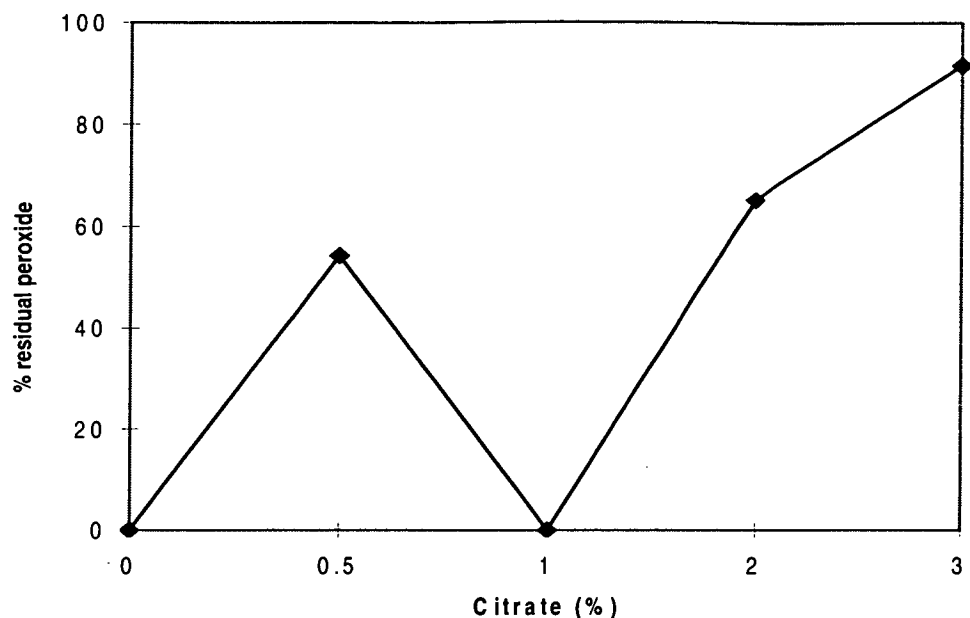


Figure 25: Peroxide decomposition with sodium citrate charge at 30 minutes reaction time.

4.4.2 Effect of chelating agent under acid and alkaline conditions on peroxide decomposition.

The effect of the organic chelating agents under acid or alkaline conditions, is shown in figure 26. In both cases of the acid form of the chelating agents, the pH (table 20) for the experiments was around 1.0, and therefore no catalytic manganese species was formed. No peroxide decomposition was observed. These results have also shown that the sodium form of the chelating agent can behave differently from that of the acid form. The efficiency of DTPA as a chelating agent for manganese was independent of form. Both the acid and sodium form behaved similarly due to DTPA's ability to form highly stable complexes(10,11). Sodium citrate on the other hand did not perform as well as its acid form. For the sodium citrate, manganese was oxidised by alkali and hence its weak complex formation constant(9) could not prevent peroxide decomposition.

The rise in reaction temperature from 20°C to 70°C has had a significant effect on peroxide decomposition with sodium citrate. At 20°C (figures 14 and 15) there was no peroxide decomposition above a citrate charge of 0.5%, however at 70°C (figures 24,25,26) the results were quite different with a very poor inhibition effect at 1% citrate charge. However, higher levels of citrate were able to produce significant reductions in peroxide decomposition. The citric acid produced no decomposition as the pH was low and no manganese decomposition species were formed. DTPA in either form was not affected by temperature in the prevention of peroxide decomposition.

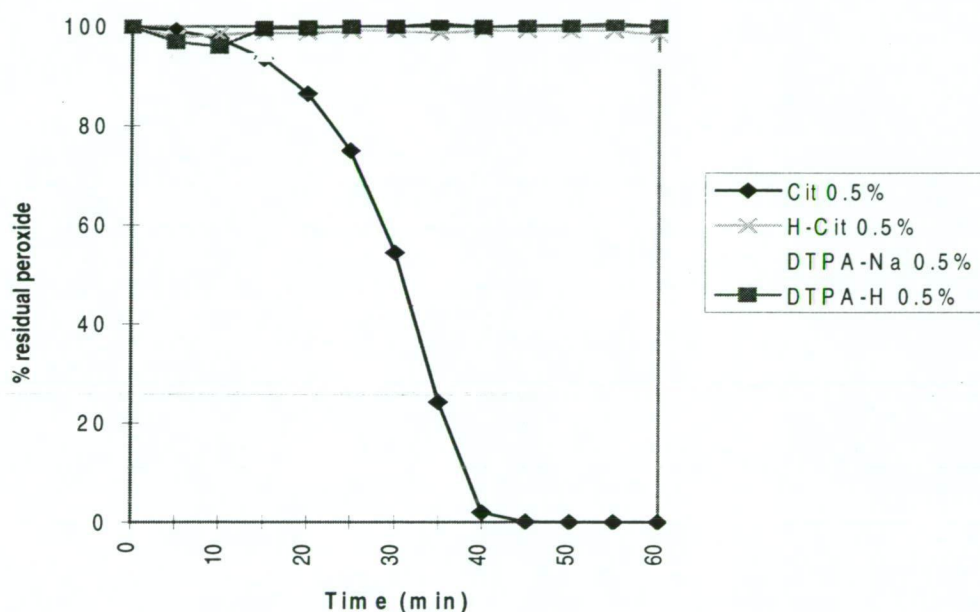


Figure 26: Peroxide decomposition with acid/base forms of citrate and DTPA.

Table 20: pH profile for decomposition with organic chelating agents

Chemical	pH (Na-cit)	pH (H-cit)	pH (Na-DTPA)	pH (H-DTPA)
Mn/MilliQ	4.2	3.5	3.5	3.3
Citrate	8.5	0.3	-	-
DTPA	-	-	12.5	1.4
0.01% NaOH	11.0	0.4	12.7	10.8*
H ₂ O ₂	9.0	0.3	10.4	1.3
Final pH	10.2	0.2	9.9	0.7

*: NaOH added before H-DTPA

4.5 Peroxide decomposition with a system of zeolite-A and sodium citrate.

The combined effect of zeolite-A and sodium citrate on peroxide decomposition is illustrated in figure 27. These results show that increasing the sodium citrate concentration is detrimental to peroxide stability. Small amounts of citrate can dramatically improve the effect of zeolite as compared to figure 21, where 5% zeolite had no residual peroxide after only forty minutes. The addition of 0.2% citrate to 5% zeolite-A raised the final peroxide concentration to 40% of the original charge after 60 minutes. There is not only an improvement over 5% zeolite alone, but the final result is only a 10% lower final peroxide charge than the optimum of 1% zeolite-A in figure 21. Therefore, it would seem most likely that citrate at small charges helps transfer the manganese ions into the zeolite structure. A possible explanation for the poor reduction in peroxide decomposition at the higher citrate charges could be that, as the citrate charge is increased, more manganese/citrate complex is bonded to the surface of the zeolite forming a catalytic species rather than allowing the metal ions to migrate into the porous zeolite structure.

Table 21: pH profile for decomposition with zeolite-A and citrate

Chemical	0% citrate	0.2% Citrate	0.5% Citrate	1.0% Citrate
Mn/H ₂ O	3.7	3.3	4.3	4.5
5% zeolite-A	11.3	10.4	10.4	10.6
Citrate	-	10.7	10.6	10.8
0.01% NaOH	11.7	11.4	11.3	11.6
H ₂ O ₂	9.6	9.2	9.1	9.3
Final pH	11.6	9.7	11.0	11.3

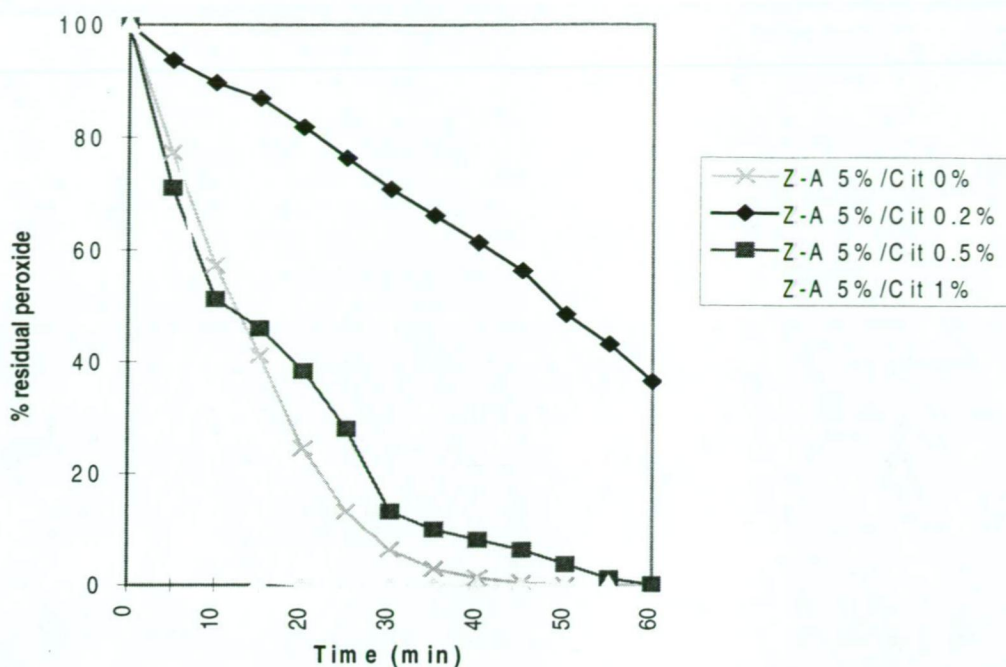


Figure 27: Peroxide decomposition with 5% zeolite-A and sodium citrate.

4.6 Conclusion:

- Manganese (45 ppm) decomposed peroxide within 3 minutes at 0.01% NaOH charge at 70°C. Under acid conditions no peroxide decomposition occurred.
- Inhibition of manganese induced peroxide decomposition with zeolites again followed the Si/Al ratio of the zeolites. Zeolite-A was the best performer of the three zeolite types at inhibiting manganese induced peroxide decomposition.
- Raising the temperature affected the kinetics of each of the zeolites differently. Zeolite-A performed worse at 70°C than 20°C with a loss in the final residual peroxide concentration of 40% units. Zeolite-X lost about 5% units in residual peroxide with the increase in temperature. Zeolite-Y improved its performance with a gain of 40 minutes at the higher temperature before peroxide exhaustion occurred.
- Increasing the zeolite-A charge significantly increased the rate of peroxide decomposition. 1% zeolite-A performed the best.
- In the absence of manganese, zeolite-A itself produced a significant amount of peroxide decomposition. The system with manganese actually performed a little

better than the system without manganese at the 1% zeolite-A level. Therefore at higher temperatures zeolite-A has a more significant role in peroxide decomposition reactions.

- Sodium citrate was found to inhibit peroxide decomposition, with the higher charges (3%) producing a significant reduction in decomposition.
- At 1% sodium citrate addition, a local minimum occurred with no substantial inhibition of peroxide decomposition. A black film which formed on all surfaces of the reaction vessel was responsible for the poor performance rather than the usual brown precipitate. The black film was not present at other citrate concentrations.
- The combined system of zeolite-A and sodium citrate also produced a synergistic effect on the inhibition of peroxide decomposition at 70°C. The system worked best when small amounts of citrate (0.2%) were added with 5% zeolite-A. These results suggest that citrate is most likely acting as a transfer agent for manganese into the zeolite.
- DTPA is not affected by temperature or form in the prevention of manganese induced peroxide decomposition.

References: (Part 1)

- (1) Bassett, J., Denney, R.C., Jeffrey, G.H., Mendham J., **Vogel's textbook of quantitative inorganic analysis**- 4th edition: Longman (1978)
- (2) Durrant, D.J., Durrant, B., **Introduction to advanced inorganic chemistry**- 2nd edition: Longman group Ltd (1970)
- (3) Cotton, F.A., Wilkinson, G., **Advanced Inorganic chemistry: a comprehensive text**- 3rd edition : Interscience Publishers (1972)
- (4) Kutney, G.W., Evans T.D., *Svensk Papperstidning*, **88**(9):84(1985)
- (5) Abbot, J., Brown, D.G, *Appita*, **43**(6):415(1990)
- (6) Galbacs, Z.M., Csanyi, L.J., *J. Chem. Soc., Dalton Trans.*, :2353 (1983)
- (7) Breck, D.W., **Zeolite Molecular Sieves: structure, chemistry and uses**: Wiley and Sons (1974)
- (8) Abbot, J., *J. Pulp Paper Science*, **17**(1):10(1991)
- (9) Leonhardt, W., Suss, H.U., Glaum, H., German Patent DE 41 18 899 C1 (1992)
- (10) Richardson, D.E., Ash, G.H., Harden, P.E., *J. Chromatography*, **47**:688(1994)
- (11) Durham, E.J., Ryskiewich, D.P., *J. Amer. Chem. Soc.*, **80**:4812 (1958)
- (12) Emery, W.D., Barnes, S.G., Sims, P.S., European Patent 0 319 053 : (1988)
- (13) Schepers, F.J. and Verbury, C.C., European Patent 0 339 997 : (1989)

Part 2:

Peroxide bleaching of Pine TMP and Eucalypt CCS

Introduction:

In Part 1 we explored the role of the various chelating agents in prevention of manganese induced peroxide decomposition without pulp. This section will investigate the effects of the various chelating agents on the peroxide bleaching of Pine TMP and Eucalypt CCS pulps. Chapters 5 and 6 describe the effect of chelation on the brightness and residual peroxide concentration for Pine TMP and Eucalypt CCS respectively. Brightness values are not the only important parameters to measure when a new chelating system is being evaluated for overall performance. For instance a high brightness pulp may have low strength properties, which could fail customer parameters, leading to a loss in sales. Furthermore addition of a filler like material such as zeolite may affect optical and strength properties. Therefore strength and optical properties have also been measured for the various chelating agents under evaluation in this study. Chapters 7 and 8 illustrate the effects of bleaching conditions on these properties with Pine TMP and Eucalypt CCS respectively.

Experimental:

All glassware and plasticware were washed with ~10 % w/w sulphuric acid made up with Milli Q water, before being rinsed twice with Milli Q water. This step was repeated before re-use of each piece of the labware to remove any residual metal ions.

Materials

Pinus Radiata TMP (Thermo-Mechanical Pulp) and Eucalypt CCS (Cold Caustic Soda) pulps were obtained from Australian Newsprint Mills (ANM), Boyer Tasmania. The pulp was dewatered to approximately 20% consistency and crumbed before storage

in a freezer at -9°C until use. All chemicals were analytical grade quality, except for laboratory grade potassium iodide, a commercial sample of sodium diethylenetriaminepentaacetic acid (Na₅-DTPA), zeolite-A, X and Y, and MilliQ water.

Method 3: Brightness of Pine TMP and Eucalypt CCS model systems with favouring decomposition conditions.

Preparation of chelated Pine TMP (PulpQ_{TMP}) and Eucalypt CCS pulp (PulpQ_{CCS}).

Into a 20 L stainless steel mixing bowl were placed approximately 1000 g oven dried defrosted pulp, 10 L of MilliQ water and 2% DTPA on o.d. fibre. The contents were mixed using a Hobart mixer with a paddle like stirrer at gear 1 (101 rpm) for 1 hour. The pulp slurry was placed in a pneumatic pulp dewatering press to remove as much liquid as possible. (A schematic of the press and further information about its design and operation are given in Appendix 1). A further 10L of MilliQ water was added onto the pulp cake in the press. Surface water was removed by vacuum before further pressing. The pulp was crumbed and stored in a freezer at -9°C until use. There was no attempt at retaining or recirculating fines washed out in the dewatering process as the filtrate contained DTPA which could interfere with bleaching experiments. While fines are important in brightness of bleached mechanical pulps all experiments including the controls were conducted using the same pulp and bleaching conditions.

Bleaching with hydrogen peroxide.

Pulp was bleached at 5% consistency in 500 mL polyethylene bottles with a reaction volume of 400 mL. PulpQ_{TMP} samples (20 g oven dried) were mixed with 135 ppm manganese (on pulp) as manganese sulphate (MnSO₄.H₂O) and MilliQ water in a waterbath at 70°C for 5 minutes. PulpQ_{CCS} samples were mixed with 40 ppm manganese in a similar manner. The appropriate chelating agent was added (zeolite, citrate or DTPA, w/w % on pulp) and stirred for a further minute before addition of sodium hydroxide (2.5% w/w on pulp) and hydrogen peroxide (2% w/w on pulp). The

mixture was then stirred for 3 hours at 70°C. After bleaching, the required amount of pulp for brightness sheets was placed in a separate 1L beaker. The unused pulp was filtered before residual peroxide measurements were made. Before the brightness handsheets were made the pH of the pulp was adjusted to pH 4.5 with a solution of 10% sulphuric acid. The handsheets were allowed to dry overnight before brightness testing with a Elrepho 2000. Standard bleaching conditions are summarised in Table 22.

Table 22: Standard peroxide bleaching conditions (method 3 - Brightness).

Chemical Charge	PulpQ _{TMP}	PulpQ _{CCS}
Stock Consistency	5%	5%
sodium hydroxide	2.5% w/w on pulp	2.5% w/w on pulp
manganese	135 ppm on pulp	40 ppm on pulp
hydrogen peroxide	2.0% w/w on pulp	2.0% w/w on pulp
Bleaching time and temp	3 hours @ 70°C	3 hours @ 70°C
Initial Pulp Brightness	60.9 ISO	46.2 ISO

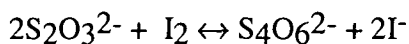
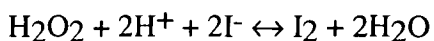
Brightness Handsheet Preparation.

Brightness handsheets were prepared in accordance with section 4.1.3 of AS/NZS 1301.446s:1992 “Measurement of diffuse blue reflectance factor (brightness) of pulp, paper, and paperboard” with only the modifications required to produce handsheets with a diameter of 95 mm.

Residual peroxide determination in pulp samples.

After removing the required amount of pulp for brightness handsheets from the bleached pulp slurry, the unused pulp was filtered using a Buchner funnel and no.4 filter paper for determination of residual peroxide. A 10 mL aliquot of the filtrate was pipetted into a 250 mL conical flask containing 10 mL of 10% w/w sulphuric acid, 1 drop of 10% w/w ammonium molybdate and 50 mL of distilled water. Potassium iodide (2.0 g) was

added to the flask, swirled and the contents titrated against standardised (0.01 M) sodium thiosulphate (1). The residual peroxide was then calculated from the formula below.



Method 4: Strength evaluations of peroxide bleached Pine TMP and Eucalypt CCS pulps.

Preparation of Pine TMP.

Pine TMP from the medium consistency stock pump (TMP plant) at ANM Boyer was dewatered in a pneumatic pulp dewatering press, removing as much liquid as possible. The pulp was crumbed in a Hobart mixer and stored in a freezer at -9°C until use.

Preparation of Eucalypt CCS pulp.

Stock Eucalypt CCS from the alkaline washers (pH=9.0) at ANM Boyer was treated the same as PulpQ_{CCS} as described in method 3. Eucalypt CCS at ANM Boyer is treated with DTPA in the unwashed stock chest, therefore it was washed to ensure any residual DTPA, metal ions or metal-DTPA complex were removed from the pulp.

Bleaching with hydrogen peroxide. (No pretreatment)

The pulp was bleached at 5% consistency in 500 mL polyethylene bottles with a reaction volume of 400 mL. Pulp (TMP and PulpQ_{CCS}) samples (20 g oven dried) were mixed with MilliQ water in a waterbath at 70°C for 5 minutes. 10 ppm manganese was added to PulpQ_{CCS} samples before addition of MilliQ water, to account for normal levels of Mn (5 ppm by Atomic Absorption Spectrometry) and any sundry metal ions (eg Mg, Ca, Cu, Fe etc) in the bleaching process. The appropriate chelating agent was added and stirred for a further minute before addition of sodium hydroxide (1.75% w/w on pulp) and hydrogen peroxide (2% w/w on pulp). The mixture was then stirred for 3

hours at 70°C. After bleaching, the pH of the pulps was adjusted to pH 4.5 before strength handsheets were made. Standard bleaching conditions are listed in Table 23.

Bleaching with hydrogen peroxide. (Pretreatment with chelating agents)

The bleaching of both TMP and CCS was conducted under the same conditions (table 23) as bleaching with no pretreatment except for the following modifications. To the 5% S/C pulp slurry containing either Pine TMP or Eucalypt CCS (10 ppm Mn added) after mixing for 5 minutes at 70°C, the appropriate chelating agent was added and stirred for a further 30 minutes. The pulp was washed with 1 litre of MilliQ water before dewatering using a Buchner funnel arrangement. The volume was readjusted to 400 mLs with MilliQ water (5% S/C) before placement back into the waterbath.

Sodium hydroxide (1.75% w/w on pulp) and hydrogen peroxide (2% w/w on pulp) were added. The mixture was stirred for 3 hours at 70°C. After bleaching the pH was adjusted to 4.5 using 10% w/w solution of sulphuric acid before strength handsheets were made.

Table 23: Standard conditions of peroxide bleaching of Pine TMP and Eucalypt CCS (no pretreatment and pretreatment) for Strength evaluations (method 4).

Chemical charge	Pine TMP	Eucalypt CCS
Stock consistency	5%	5%
sodium hydroxide	1.75% w/w	1.75% w/w
manganese (added)	0 ppm	10 ppm
hydrogen peroxide	2.0% w/w	2.0% w/w
Bleaching Time and Temp	3 hours @ 70°C	3 hours @ 70°C

The chemical levels used in method 4 (Table 23) are slightly different to those used in method 3 (Table 22). The conditions in Table 22 were chosen in order to induce decomposition reactions when manganese is not chelated. Those conditions produce

large differences between chelated and non chelated brightness readings, so it is easy to evaluate the effect of a particular chelating agent in pulp systems. The conditions in Table 23 take into account evaluation for strength properties of the bleached pulp, particularly the excessive alkali charge in Table 22 could have lead to a swamping of any effect of the chelating agents. Furthermore conditions in Table 23 are closer to a real mill situation than the model system used in Table 22.

Strength handsheet making and testing.

Strength handsheets were made in accordance with AS/NZS 1301.203s: 1993 “Forming of handsheets for physical testing of pulp”, using equipment in accordance with AS/NZS 1301.214s:1993 “Equipment for preparation of handsheets”. The strength handsheets were tested in accordance with AS/NZS 1301.208s:1997 “Methods of test for pulp and paper - Physical testing of pulp handsheets” and all references contained therein. The strength handsheets were also tested for optical properties using AS/NZS 1301.454s:1992 “Determination of opacity (paper backing) diffuse reflectance method”.

Preparation of acid zeolites:

50g of dry commercial sodium zeolite was added to 75g of ammonium nitrate (NH_4NO_3) dissolved in 100 mL of MilliQ water. The mixture was stirred for 24 hours at room temperature. The mixture was filtered and washed with MilliQ water using a Buchner funnel arrangement with no.4 filter paper. The zeolite slurry was dried at 400°C for 24 hours in a muffle furnace. The acid zeolite was stored in a dessicator before use.

Results and Discussion: (Part 2)

CHAPTER 5: BRIGHTNESS EVALUATIONS OF PEROXIDE BLEACHING WITH PINE TMP.

This chapter will investigate the effect of various chelating agents on the brightness and residual peroxide after a peroxide bleaching stage using Pine TMP. A model system containing Pine TMP and manganese as described in “Method 3” will be used to evaluate the effectiveness of zeolites, citrate, a combination of zeolite and citrate, and DTPA with respect to brightness and residual peroxide concentrations. This system with 135 ppm manganese, 2.5% NaOH and 2% hydrogen peroxide rapidly decomposes peroxide. A loss of approximately 6% in brightness and no residual peroxide concentration was found to occur. The loss in brightness occurred as a result of hydrogen peroxide decomposing, leaving the remaining alkali to attack lignin in the pulp. This produces alkali darkened chromophores and hence lowers the pulp brightness.

5.1: Zeolite-A and peroxide bleaching.

Figures 28 and 29 show that zeolite-A can have a beneficial effect on both brightness and residual peroxide concentration in peroxide bleaching of Pine TMP in the presence of manganese. A large charge (~5%) of zeolite-A is required to bring the system back to the manganese free pulp brightness ($PulpQ_{TMP}$) of 60.9. Addition of sodium citrate further improves both pulp brightness and residual peroxide. The zeolite charge required to reach the initial pulp brightness ($PulpQ_{TMP}$) after bleaching is lowered to 2% for the system containing zeolite-A and citrate as compared to 5% for that with zeolite-A alone. Furthermore, the brightness at a charge of 5% zeolite-A and 0.5% citrate is comparable to 10% zeolite-A in the system without citrate, which represents a saving of about half the chemical charge. The optimum brightness was obtained at 7.5% zeolite-A and 0.5% citrate, where as 10% zeolite-A produced the highest brightness of the experiments containing zeolite-A alone. The curve for zeolite-A alone is still increasing, but the zeolite-A and citrate curve at 10% zeolite-A has leveled off and it is

probable that the upper limit for brightness under these experimental conditions is nearly reached with the high zeolite-A charges. These results are opposite to those in figures 21 and 22 (chapter 4) where increasing the zeolite-A charge increased the rate of peroxide decomposition. One possible explanation for this difference is that more zeolite is needed to compete with lignin and cellulose for the metal ions. Higher levels of zeolite are needed to reduce metal catalysed peroxide decomposition arising from metal ions in solution or metal ions on fibre surfaces. Furthermore, peroxide can react with the pulp fibres which might lower the overall ratio of peroxide to zeolite in solution and hence lower decomposition due to peroxide/zeolite interactions.

Table 24: pH profile for bleaching of Pine TMP with various zeolite-A concentrations.

Zeolite-A (%)	Zeolite-A (Initial/final pH)	Zeolite-A + 0.5% Citrate (Initial/final pH)
0	10.9 / 9.7	11.8 / 9.7
1	11.7 / 10.0	11.7 / 9.8
2	11.8 / 9.8	11.8 / 9.6
3	11.8 / 9.8	11.6 / 9.4
5	11.8 / 9.8	11.7 / 9.5
7.5	11.8 / 9.8	11.6 / 9.5
10.0	11.9 / 10.0	11.9 / 9.8

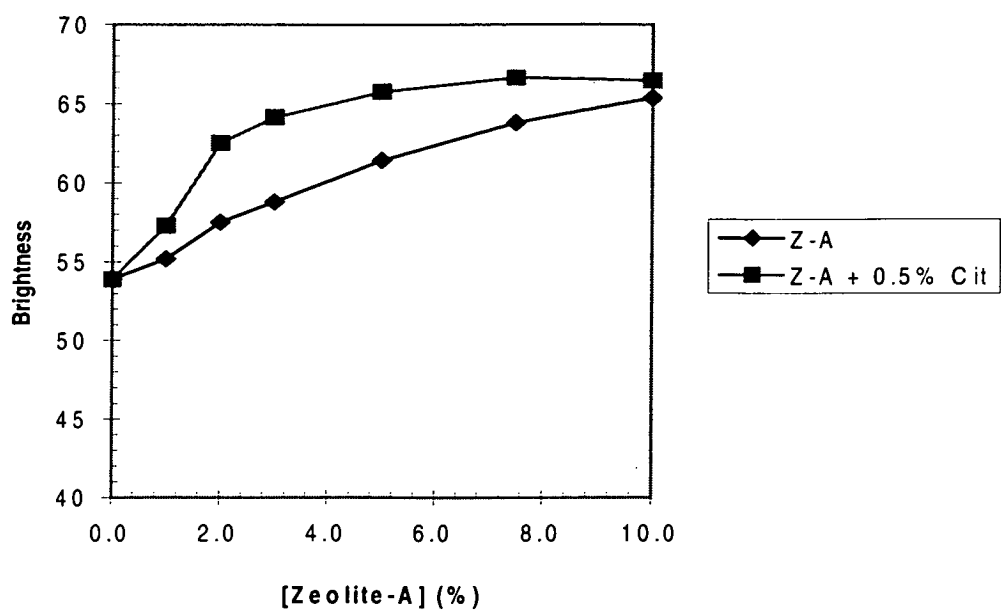


Figure 28: The effect on brightness of bleached Pine TMP by zeolite-A concentration.

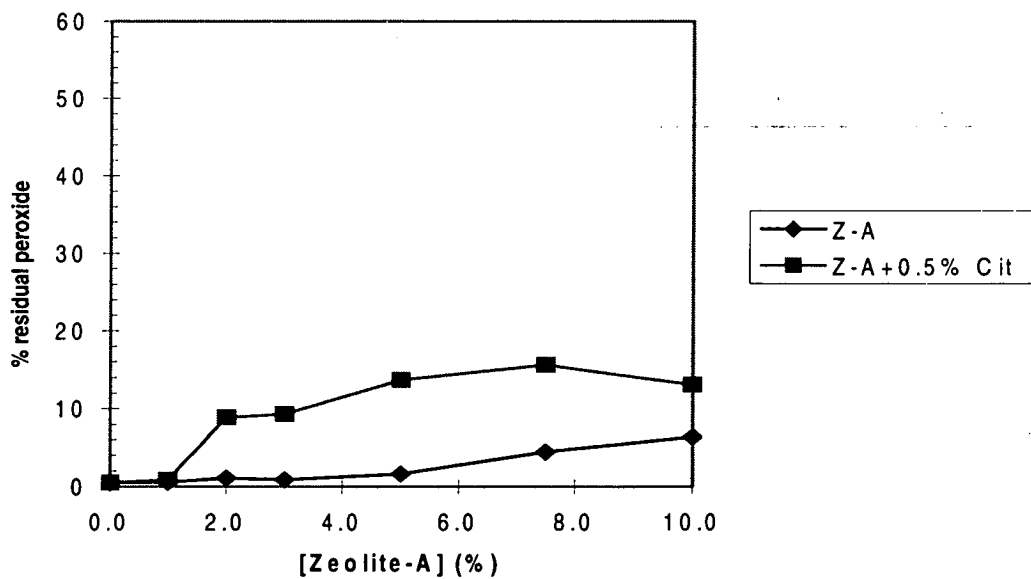


Figure 29: The effect on the residual peroxide of bleached Pine TMP by zeolite-A concentration.

Figure 30 illustrates the effect on brightness of unbleached Pine TMP by increasing amounts of zeolite-A. Zeolite has a high brightness and may be acting as a filler. These

results show that at the 95% confidence level, 5% zeolite produces only a small beneficial increase in brightness. Addition of 7.5% zeolite-A produces a gain of around 1% to 1.5% in brightness while with 10% zeolite-A a gain of 2.5 brightness can occur over the system with no zeolite present. These small gains indicate that the large brightness gains achieved after a bleaching sequence as shown in figure 28 are not due just to the presence of the zeolite alone acting as a filler, but are due to the zeolite preventing the peroxide from decomposing.

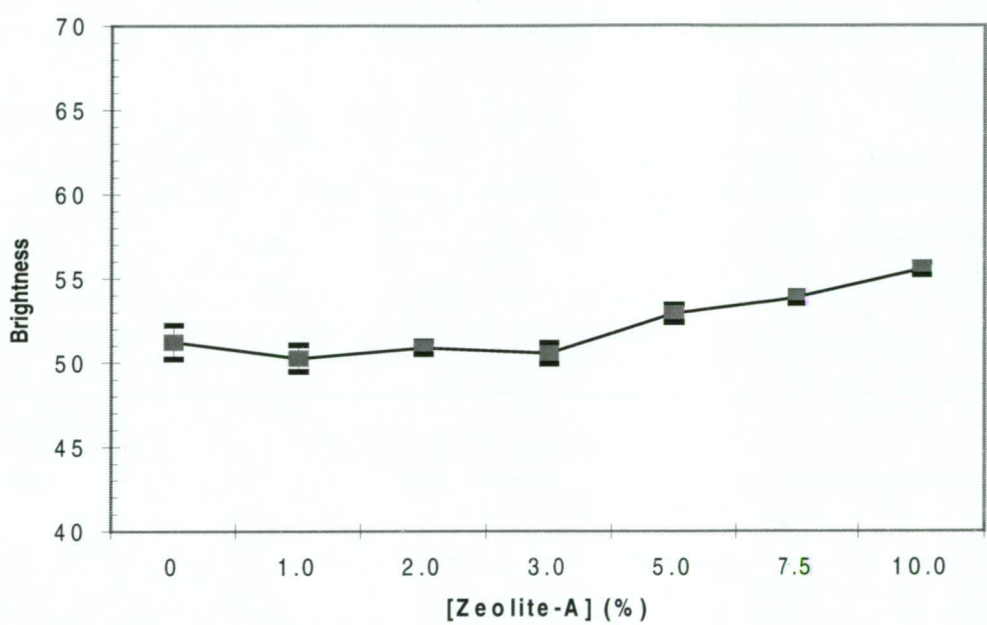


Figure 30: The effect on the brightness of unbleached Pine TMP containing no manganese and various zeolite-A charges at 95% confidence intervals.

5.2: Sodium citrate and peroxide bleaching.

The effect of sodium citrate on peroxide bleaching of Pine TMP is shown in Figures 31 and 32. Both brightness (figure 31) and residual peroxide concentration (figure 32) increased with increasing sodium citrate charge, with around 2% citrate being needed to reach the initial pulp brightness after bleaching. At this point, a significant increase in residual peroxide concentration occurred. Therefore it seems that citrate at high

concentrations is also able to chelate manganese ions and hence prevent peroxide decomposition.

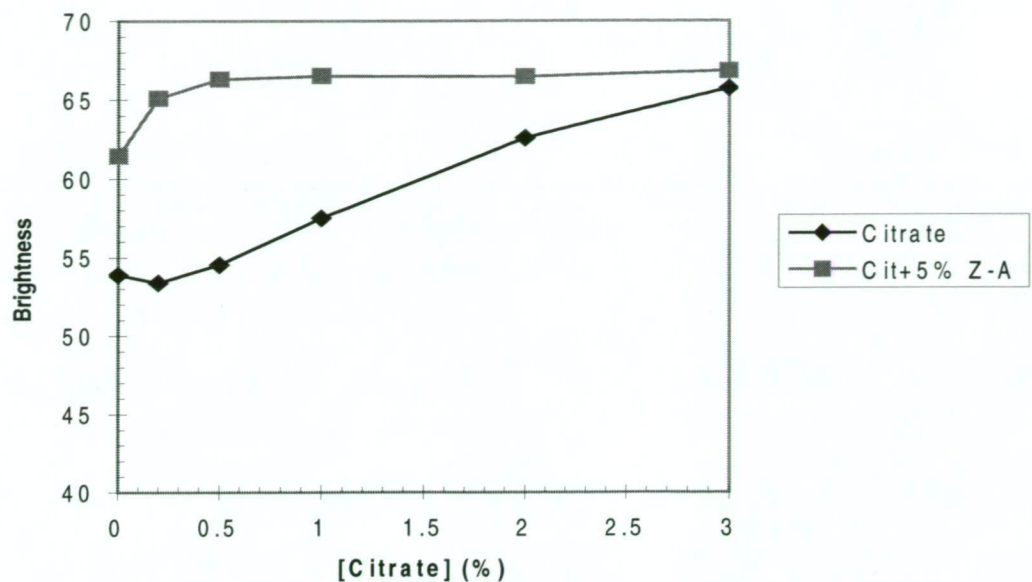


Figure 31: The effect on brightness of peroxide bleached Pine TMP by citrate charge.

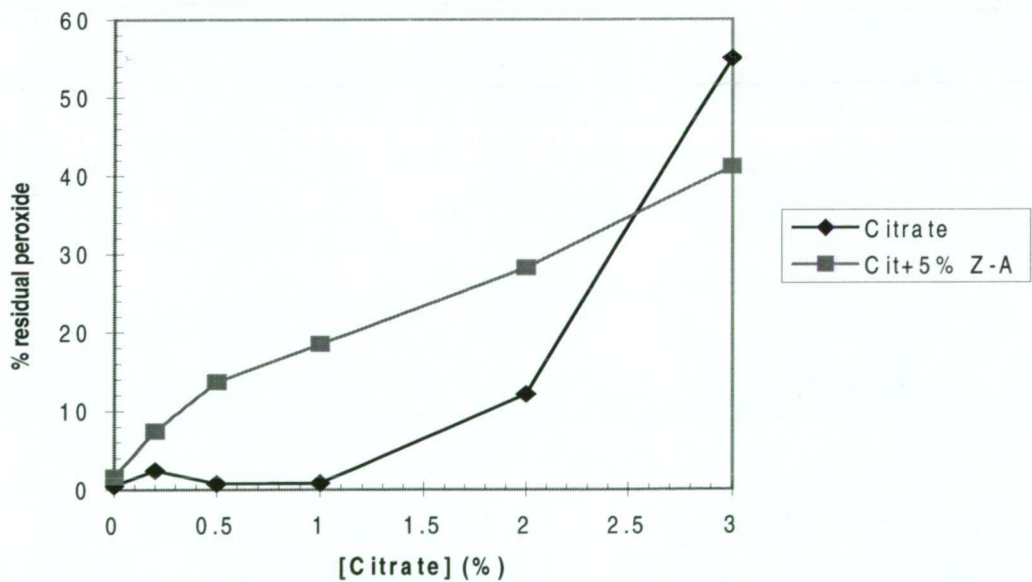


Figure 32: The effect on residual peroxide concentration of a peroxide bleached Pine TMP with sodium citrate charge.

Table 25: pH profile for bleaching of Pine TMP with various citrate concentrations.

Citrate (%)	Citrate (Initial/final pH)	Citrate + 5% zeolite-A (Initial/final pH)
0	10.9 / 9.7	11.8 / 9.8
0.2	11.8 / 10.1	11.5 / 9.9
0.5	11.8 / 9.7	11.3 / 9.4
1.0	11.5 / 8.6	11.1 / 9.4
2.0	10.7 / 7.9	10.6 / 8.9
3.0	9.2 / 6.7	10.1 / 8.7

Addition of zeolite-A to the system dramatically improved both residual peroxide and brightness response of the bleaching stage. Figure 31 shows that the system containing both zeolite-A and citrate reaches a limit in brightness after addition of 0.5% sodium citrate. There are no further gains in brightness above this level, however there is an improvement in the residual peroxide (figure 32). At low levels of citrate (< 0.5%) in the absence of zeolite-A, the pulp brightness does not increase and there is no residual peroxide. Consequently the citrate added at these levels is not able to prevent peroxide decomposition. However as the citrate charge is increased, the brightness increases. The citrate reduces the rate of peroxide decomposition. At a charge of 3% citrate, a large residual peroxide occurs and the brightness approaches the brightness limit obtained in the citrate/zeolite system.

In contrast, figure 28 shows that addition of citrate to the zeolite system caused a relatively constant improvement in brightness as the level of zeolite increased over that of zeolite alone until maximum was obtained. The results in figures 28, 29, 31 and 32 suggest that a brightness limit of 66 ISO occurs under the standard conditions employed in this study. This brightness limit appears to be “pulp limited” rather than “reagent limited” as high residual peroxides occur at the maximum brightness level. The

bleaching stock consistency, chemistry and structure of the pulp are major factors in determining the maximum brightness level achieved for “pulp limited” bleaching (2).

5.3: Pretreatment time of zeolite-A systems with peroxide bleaching.

The effect of pretreatment time on the performance of zeolite based chelation of Pine TMP is shown in figures 33 and 34. It should be noted with these results that there was no washing stage between the pretreatment and the bleaching stage. Bleaching chemicals were added directly to the pulp containing chelating agents. The washing stage was omitted in an attempt to model the refiner bleaching process at ANM Albury which does not have a washing stage between pretreatment and bleaching stages.

Table 26: pH profile for bleaching of Pine TMP using various pretreatment times.

Pretreatment Time (hours)	5% Zeolite-A (Initial/final pH)	5% Zeolite-A + 0.5% Cit (Initial/final pH)
0	11.8 / 9.8	11.3 / 9.4
1	11.3 / 10.1	11.6 / 9.4
1.5	11.4 / 10.4	11.5 / 10.0
2	11.3 / 10.2	11.6 / 8.9
2.5	11.3 / 10.1	11.5 / 9.4
3	11.4 / 10.0	11.6 / 8.9

Optimum pretreatment time occurs within an hour for both zeolite and zeolite/citrate systems in terms of brightness and residual peroxide. Therefore it seems likely that the chelation of manganese occurred within the first hour, so there is no need to extend the pretreatment reaction time.

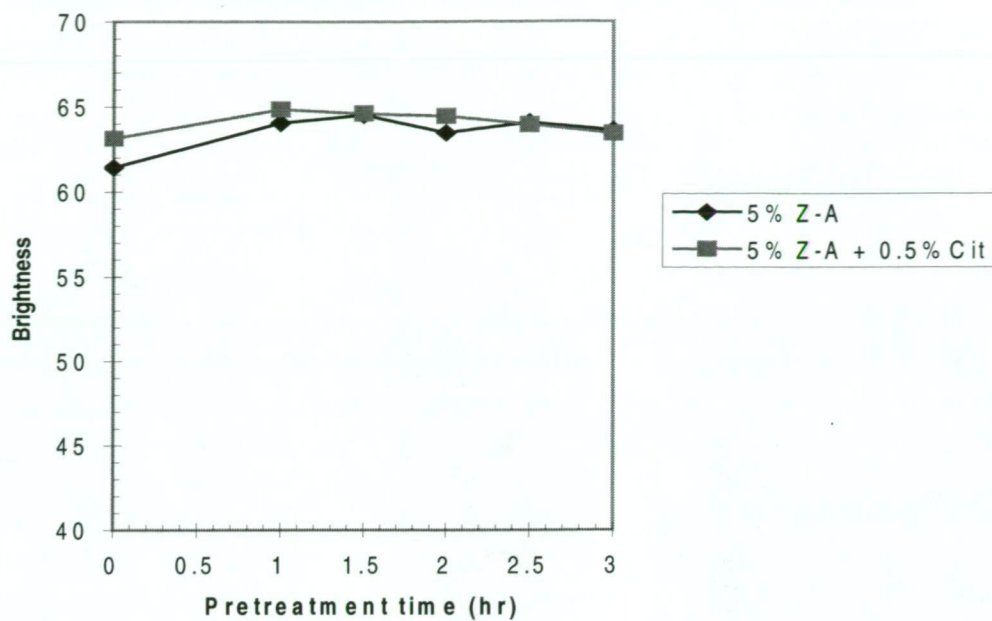


Figure 33: The effect on brightness of peroxide bleached Pine TMP by pretreatment time.

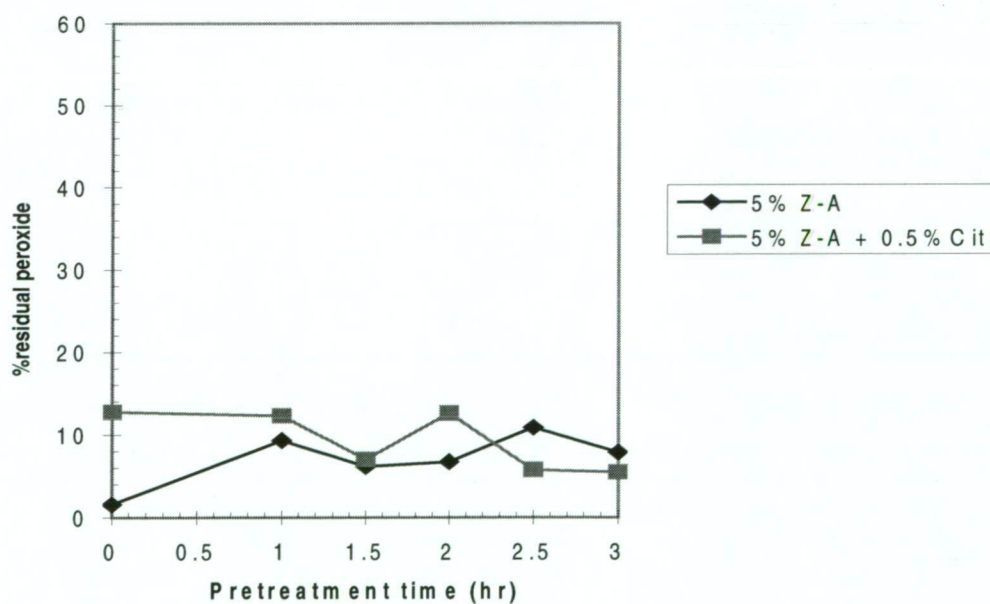


Figure 34: The effect on the residual peroxide concentration of a peroxide bleached Pine TMP with pretreatment time.

5.4: DTPA and zeolite-A systems at various peroxide charges.

Figures 35 and 36 show the effect of peroxide charge on the standard bleaching conditions (5% S/C, 2.5% NaOH) of Pine TMP. The curves of 5% zeolite-A and 0.5% citrate, and 0.5% DTPA also contain 135 ppm Mn (see table 22). Brightness and

Table 27: pH profile for bleaching of Pine TMP using various chelation systems.

H₂O₂ (%)	PulpQ- no Mn (Initial/final pH)	5% Z-A + 0.5% Cit (Initial/final pH)	0.5% DTPA (Initial/final pH)
0	11.8 / 11.0	11.3 / 10.1	11.9 / 10.9
1	11.1 / 9.6	10.8 / 9.0	11.5 / 8.9
2	11.1 / 10.1	11.8 / 9.8	10.8 / 9.2
3	10.9 / 8.6	10.5 / 8.8	11.3 / 8.5
4	10.8 / 8.5	10.4 / 8.8	11.2 / 8.3
5	10.7 / 8.5	10.5 / 8.6	11.3 / 8.2

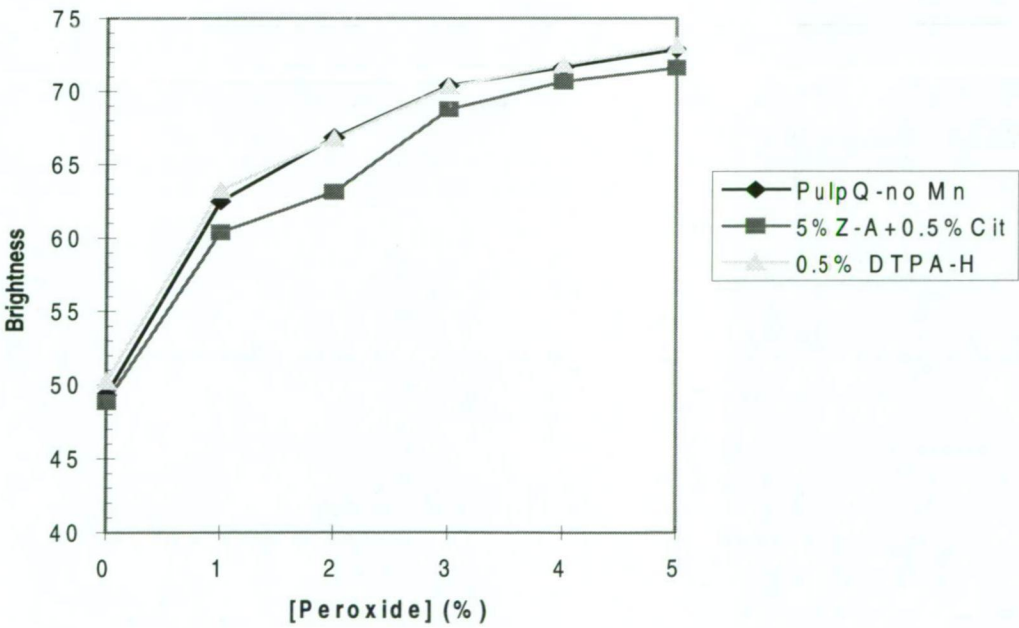


Figure 35: The effect on brightness of bleached Pine TMP by initial peroxide charge.

residual peroxide concentrations increase with increased peroxide charge. These results also show that the combined zeolite/citrate system performs only marginally less effectively than DTPA with respect to brightness over the whole range of peroxide charges. DTPA does produce a large improvement in the residual peroxide concentrations over that of the zeolite/citrate system due to the faster rate and a higher complexing stability. On that basis, DTPA would be a better choice if white water was being recycled in a bleach plant.

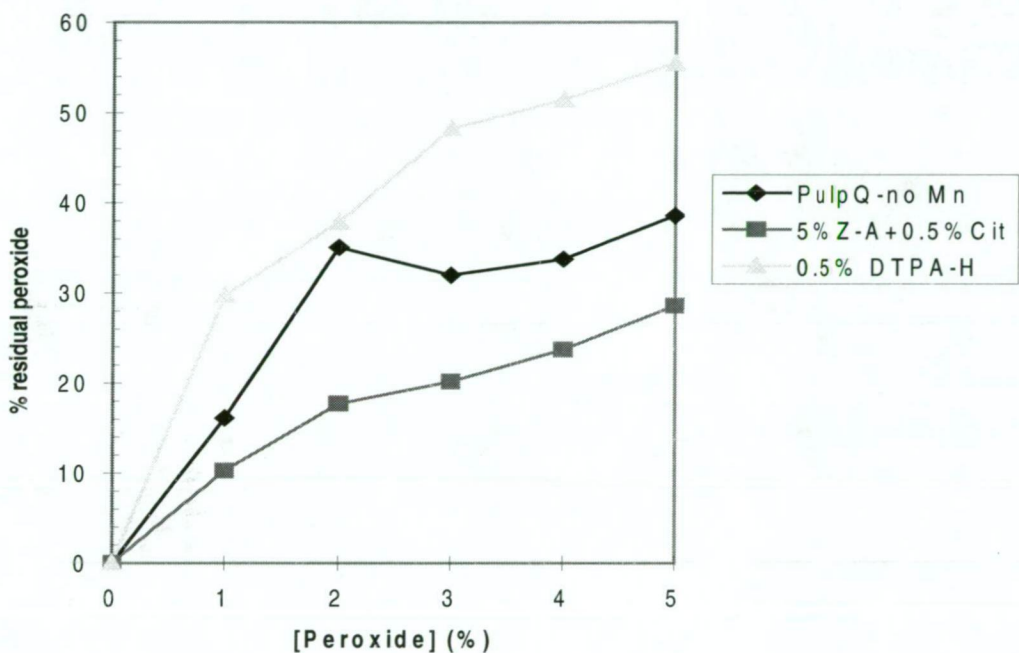


Figure 36: The effect on the residual peroxide concentration of a chelated bleached Pine TMP by the initial peroxide charge.

5.5: Zeolite types and peroxide bleaching.

The effect of zeolite type under various conditions on peroxide bleaching of Pine TMP is illustrated in Figures 37 and 38. These results show that both residual peroxide and brightness increased with zeolite charge, particularly when citrate is added to all of the zeolite types with exception of sodium zeolite-X. The acid form of zeolite-X performs better than the sodium form in the development of brightness and residual peroxide for bleached Pine TMP. This effect might be related to pH (see table 28), as acid from the

zeolite may be neutralising some of the alkali, thus reducing metal catalysed decomposition and alkali darkening. Furthermore figures 35 and 36 show that without manganese (PulpQ) the optimum peroxide charge was about 4% for 2.5% NaOH. The results in figures 37 and 38 use 2% peroxide with 2.5% NaOH so it is likely that NaOH has been overdosed. Therefore the alkali neutralising effect of H-X zeolite lowers the alkali charge towards the optimum required with 2% peroxide. Thus higher brightness and residual peroxide concentrations can occur. There is also an alternate explanation which may account for the difference in response between the zeolite types despite a similar pH drop from alkaline to acid forms with the peroxide bleaching of Pine TMP. The response of the acid forms particularly H-X is related to the effect of water on the bonding sites of the zeolite. Typically for the surface sites (sites II and III) when sodium is exchanged from the zeolite in to liquid phase, water is hydrolysed. Consequently the chemistry of the exchange site undergoes a change from AlO_4^- to $\text{AlO}_4\text{-H}$ (4). The $\text{AlO}_4\text{-H}$ chemistry reduces the possible bonding with hydrated Mn^{2+} species to partial dipole moments rather than a combined ionic and covalent nature. The difference between the two forms is that in the acid form there is no sodium ions present in the liquid phase at the point of hydration of the exchange site in the zeolite. Therefore the hydrogen ions can migrate in the liquid phase, which reverts the site back to more preferred chemistry of AlO_4^- for exchange of manganese ions. This effect is more significant for zeolite-X because it improves the bonding in surface sites (site II), making manganese ions in these position more resistant to attack from alkali and peroxide. Zeolite-Y which has the same type of sites available for exchange as zeolite-X, is unaffected by the change to the acid form because it does not have enough exchange sites for any difference in site chemistry to become significant. There is little change for the use of acid zeolite-A as the manganese ions are already located in the most preferred position, the sites (site I) inside the β -cages(4).

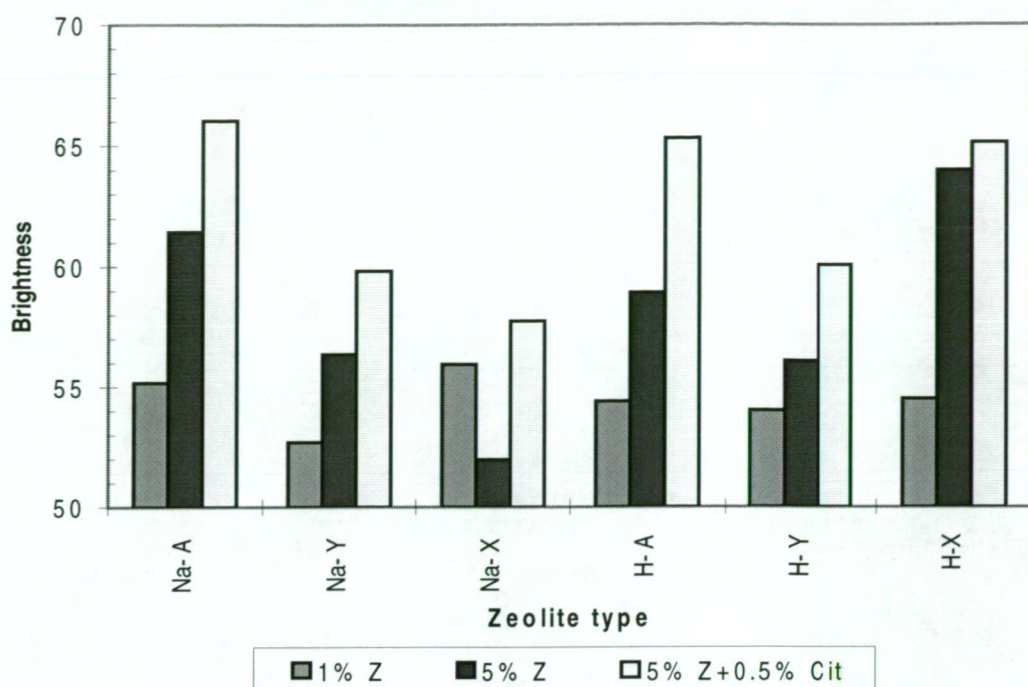


Figure 37: The effect on brightness for peroxide bleached Pine TMP by zeolite type.

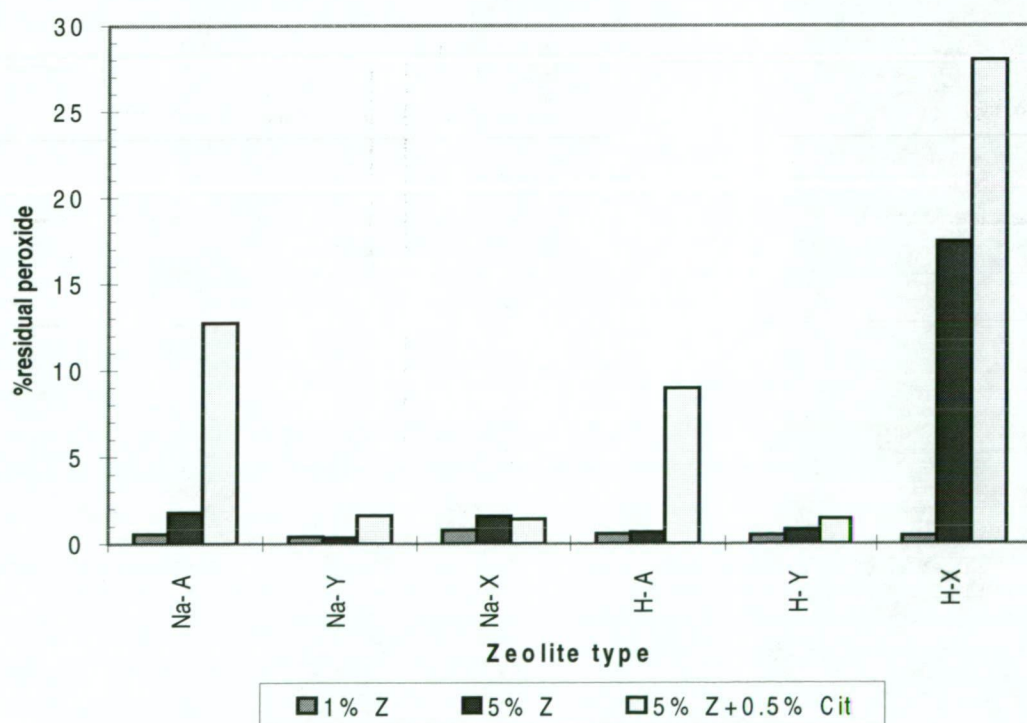


Figure 38: The effect on the residual peroxide concentration obtained after a peroxide bleaching stage for Pine TMP by zeolite type.

Table 28: pH profile of bleached Pine TMP using various chelating agents.

Chemical	pH of acid form (initial / final)	pH of sodium form (initial / final)
1% zeolite-A	11.4 / 9.8	11.3 / 9.9
1% zeolite-X	11.5 / 9.8	11.5 / 9.6
1% zeolite-Y	11.4 / 9.9	11.5 / 9.8
5% zeolite-A	11.1/8.6	11.8/9.8
5% zeolite-X	11.2/9.2	11.7/10.0
5% zeolite-Y	11.3/9.0	11.6/10.1
5% Z-A and 0.5% Cit	10.3/8.8	11.3/9.4
5% Z-X and 0.5% Cit	10.3/9.2	10.9/9.3
5% Z-Y and 0.5% Cit	10.8/9.0	10.9/9.3

Figures 37 and 38 confirm that zeolite-A is the best of the three commercial zeolites for use in peroxide bleaching.

5.6: Conclusions.

- Zeolite-A does provide a beneficial effect on peroxide bleaching of Pine TMP. The highest brightness for zeolite alone occurred at 10% zeolite charge although the trend was still rising at a reduced rate. However addition of a small amount of citrate provided a synergistic effect with the zeolite. The addition of 0.5% citrate lowers the dose of zeolite required for an equivalent brightness down to a charge of 5%, a saving in the order of 50% of the chemical charge. The optimum brightness for peroxide bleached Pine TMP under conditions of this experiment was 7.5% zeolite-A and 0.5% citrate.
- Zeolite-A itself only contributes around 1 to 2% in brightness at the higher charge levels.

- Higher amount of zeolites are required than those in decomposition studies (chapter 4) to prevent decomposition and increase brightness as the zeolite has to compete with pulp fibres for metal ions.
- Sodium citrate can produce beneficial effects in the bleaching of Pine TMP. The optimum charge for citrate addition occurred at 3% for citrate alone. The optimum charge of citrate with 5% zeolite occurred at 0.5%. Further addition of citrate had no additional effect on brightness but did increase residual peroxide.
- Pretreatment time had only a marginal effect on both brightness and residual peroxide concentrations with 5% zeolite-A and 5% zeolite-A with 0.5% citrate.
- The combined system of 5% zeolite-A with 0.5% citrate only performed slightly worse than DTPA in respect to brightness, however DTPA was far superior with respect to the residual peroxide concentrations.
- Zeolite-A performed better than types X and Y in the sodium form for both brightness and residual peroxide values. Zeolite-X was the best at 5% charge of the acid forms, but zeolite-A was equivalent at 5% zeolite with 0.5% citrate. This effect in the acid form with zeolite-X is most likely related to a change in exchange site chemistry rather than pH which was equivalent with the other two types in the acid form.

CHAPTER 6: BRIGHTNESS EVALUATIONS OF EUCALYPT CCS BLEACHING WITH PEROXIDE.

The effect of various chelating systems on the brightness and residual peroxide after a Eucalypt CCS peroxide bleaching stage will be investigated in this chapter. Eucalypt CCS (hardwood) is chemically different from Pine TMP (softwood) and consequently might behave differently to peroxide bleaching. The effects of peroxide, alkali and manganese levels on bleaching of Eucalypt CCS have been studied and the results are used to determine the reaction conditions needed to induce rapid decomposition. Consequently a model system containing Eucalypt CCS and 40 ppm manganese as described in “Method 4” will be used to evaluate the effectiveness of zeolite-A, sodium citrate, a combination of zeolite-A with citrate, and DTPA with respect to brightness and residual peroxide.

6.1 Peroxide charge and Eucalypt CCS bleaching.

Figures 39 and 40 show the effect of initial peroxide charge on brightness and residual peroxide concentrations of bleached Eucalypt CCS without manganese (PulpQ_{CCS}). Table 29 shows the pH profile for bleaching pine TMP with various peroxide charges. Eucalypt CCS brightness rapidly increases from approximately 46 ISO to 68 ISO up to a peroxide charge of 2%, before leveling out at the higher peroxide charges. The alkali charge has a more significant effect on the residual peroxide concentrations than brightness values. The optimum initial peroxide charge for residual peroxide concentrations occurs at 3% for 1.75% NaOH, whereas 1% peroxide is optimum for an alkali charge of 2.5% based on figure 40 with residual peroxide expressed as a percentage of applied peroxide. The results in figure 40 for 2.5% NaOH show strange behaviour as generally increasing the alkali charge, increases the optimum charge of peroxide. A good compromise for reasonable brightness targets and residual peroxide concentrations would be an initial peroxide charge of 2%.

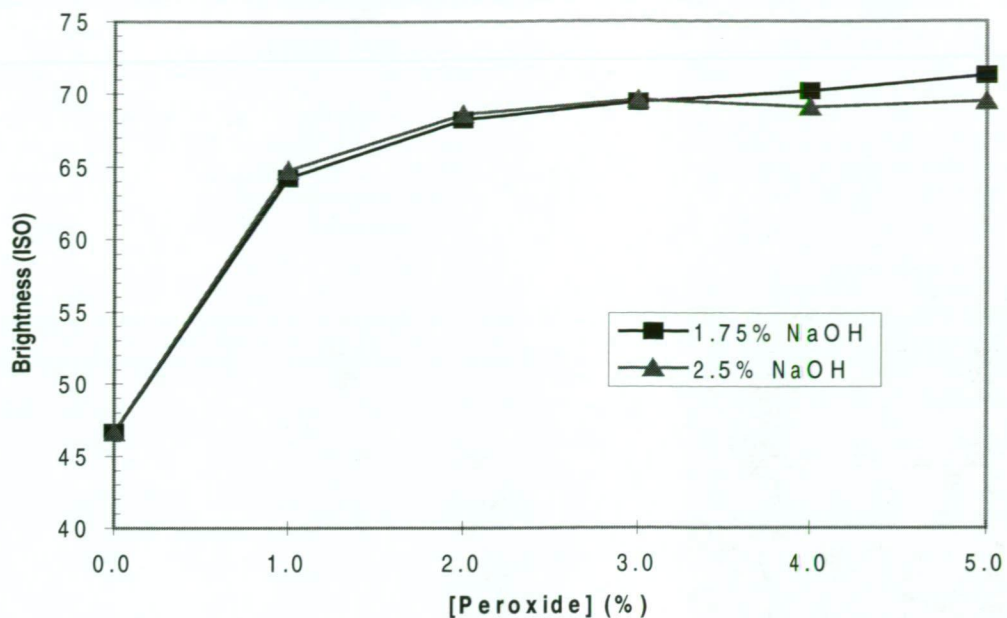


Figure 39: The effect on Brightness of PulpQ_{CCS} by peroxide charge with no manganese present.

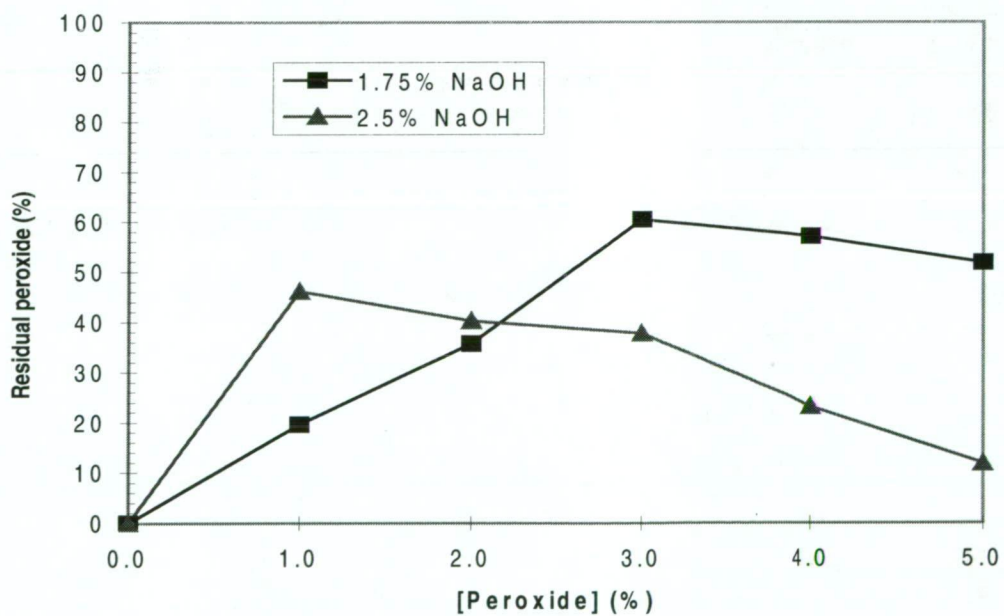


Figure 40: The effect on residual peroxide of bleached PulpQ_{CCS} by peroxide charge.

A comparison between Pine TMP and Eucalypt CCS show that Eucalypt CCS is easily bleached initially, but brightness levels off and reaches a upper limit despite higher

addition of peroxide as shown by figures 39. However the brightness response for Pine TMP slowly increases with high peroxide charges as shown by figure 35. The difference in behaviour of the two pulps could be due to different bleaching chemistry with different chromophores being present. It should also be noted that the final pH during CCS bleaching is very high, due to the alkaline treatment during pulping neutralising acidic groups in the wood/pulp. This high alkalinity during bleaching will affect the bleaching response.

Table 29: pH profile for bleaching of Eucalypt CCS with various peroxide charges.

H₂O₂ (%)	1.75% NaOH (Initial/final pH)	2.5% NaOH (Initial/final pH)
0	11.9 / 11.9	12.3 / 12.3
1	11.7 / 11.6	12.1 / 11.9
2	11.5 / 11.4	11.7 / 11.7
3	11.3 / 11.2	11.6 / 11.6
4	11.2 / 11.2	11.5 / 11.4
5	11.1 / 10.9	11.4 / 11.2

6.2 Manganese and peroxide bleaching of Eucalypt CCS.

Figures 41 and 42 illustrate the effects of manganese concentration on the brightness and residual peroxide concentrations of Eucalypt CCS (PulpQ_{CCS}) bleached with 2% peroxide. Table 30 presents the pH profile for bleaching of CCS with various manganese concentrations.

Figures 41 and 42 show that increasing manganese content at either alkali charge reduces brightness and a corresponding drop in residual peroxide also occurs. The rate of brightness decrease increases as manganese addition increased from 20 to 30 ppm. At 40 ppm a brightness drop of 13 ISO units occurs with complete exhaustion of residual

peroxide, indicating that manganese has decomposed all the peroxide and prevented bleaching from occurring. The set of values at 40 ppm Mn are ideal for evaluation of the effectiveness of chelating systems for peroxide bleaching.

Table 30: pH profile for bleaching of CCS with various manganese concentrations.

Manganese (ppm)	1.75% NaOH (Initial/final pH)	2.5% NaOH (Initial/final pH)
0	11.5 / 11.4	11.9 / 11.6
10	11.5 / 11.3	12.0 / 11.9
20	11.5 / 11.3	12.0 / 12.0
30	11.5 / 11.4	12.0 / 12.0
40	11.6 / 11.3	12.1 / 12.3

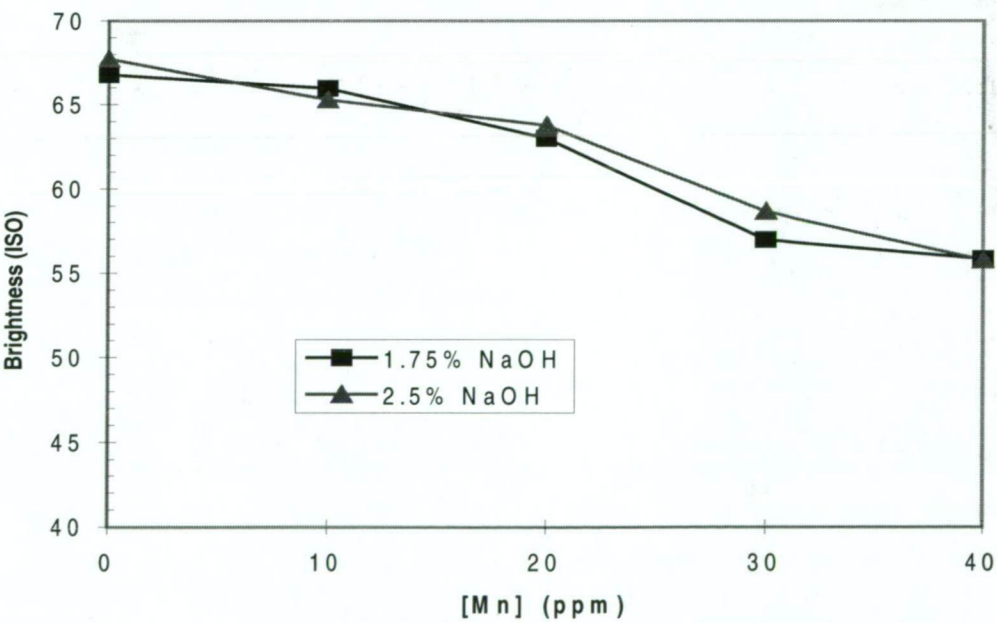


Figure 41: The effect on brightness of PulpQ_{CCS} bleached with 2% peroxide by manganese charge.

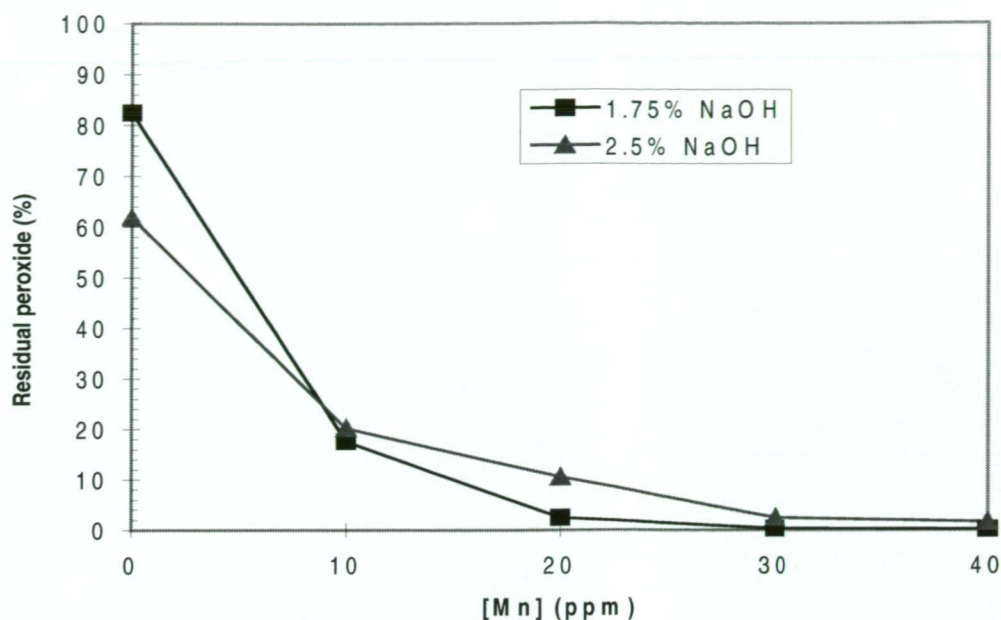


Figure 42: The effect on residual peroxide of PulpQ_{CCS} bleached with 2% peroxide by manganese.

6.3: Sodium hydroxide and bleaching of Eucalypt CCS.

The effect of alkali charge on brightness and residual peroxide concentrations of bleached Eucalypt CCS (PulpQ_{CCS}) with 2% peroxide and 0, 20, and 40 ppm manganese is shown in figures 43 and 44 respectively. The corresponding pH profiles for the bleaching of CCS at various alkali charges is shown in Table 31.

In figure 43 with no manganese, brightness increases with alkali charge such that the optimum brightness (69 ISO) occurs at an alkali charge of 2.5%. Addition of 20 ppm Mn lowers the optimum brightness to 64 ISO at an alkali charge of 1.25%. CCS pulp with 40 ppm Mn has a maximum brightness of 57 ISO at 1% NaOH. However the most striking feature about figure 43 is the comparison between 0 ppm Mn and 40 ppm at an alkali charge of 2.5%. Very little bleaching occurs at 40 ppm. Peroxide residuals as shown in figure 43 at 40 ppm Mn are very low suggesting that bleaching does not occur because of manganese induced decomposition.

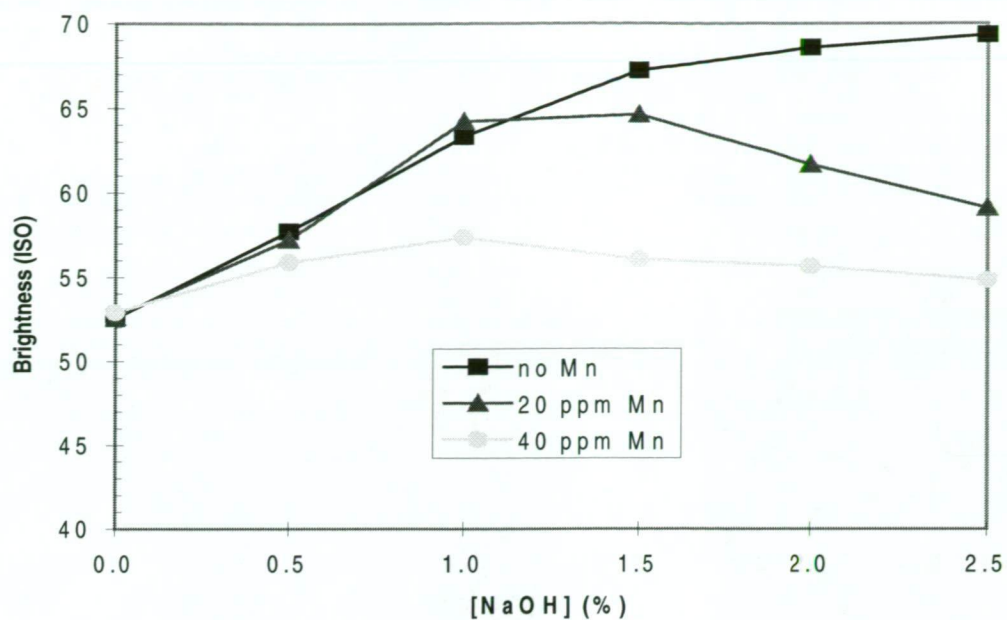


Figure 43: The effect on brightness of bleached PulpQ_{CCS} by alkali charge.

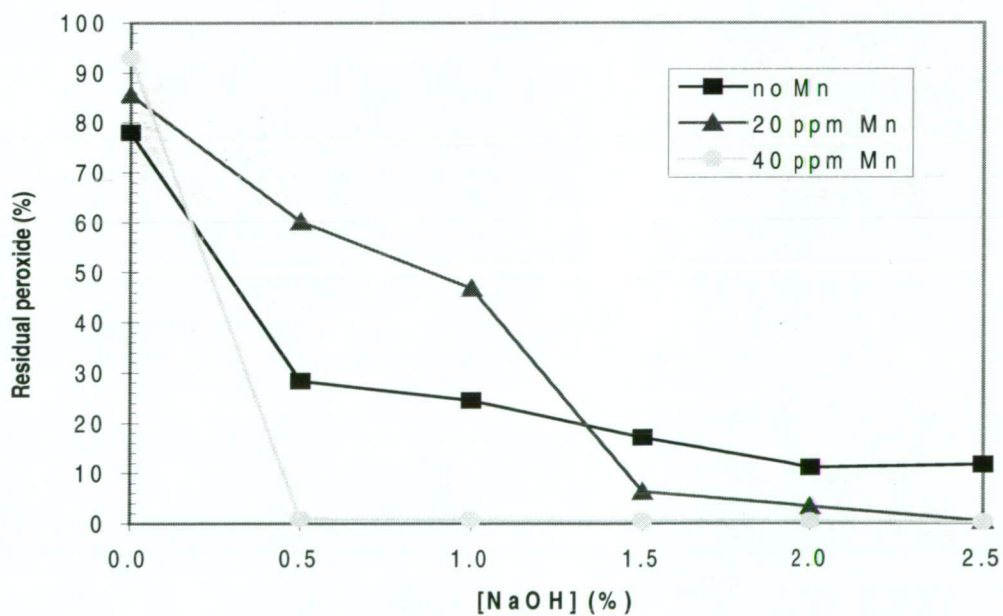


Figure 44: The effect on residual peroxide from bleached PulpQ_{CCS} by alkali.

It is known that alkali drives peroxide bleaching reactions, and that alkali also reacts with lignin to produce chromophores (alkali darkening). The curves at 20 ppm and 40 ppm Mn are due to the competition between these two reactions. Optimum NaOH

levels are found to decrease as the manganese level increases. This is because at the higher manganese levels, peroxide decomposition increases. As peroxide is consumed the alkali darkening reactions predominate causing a loss in brightness. It is expected that the results at 0 ppm Mn would also produce a similar curve to the other results at even higher alkali levels than those in this set of experiments.

The large gap in brightness values between 40 ppm Mn (55 ISO) and 0 ppm Mn (69 ISO) would be ideal to evaluate the effectiveness of chelating systems to protect peroxide from decomposing and hence increase the brightness of the bleached pulp.

High residual peroxide and brightness of 53 ISO rather than 46.2 ISO for Eucalypt CCS at 0% NaOH occurs because the pulp is alkaline (pH=8.5 after preparation) and consequently a small amount of bleaching occurs with 2% peroxide addition.

Table 31: pH profile for bleaching of CCS with various alkali charges.

NaOH (%)	No Mn (Initial/final pH)	20 ppm Mn (Initial/final pH)	40 ppm Mn (Initial/final pH)
0	8.2 / 8.2	8.1 / 8.1	8.2 / 8.2
0.5	9.7 / 9.5	9.8 / 9.4	9.8 / 9.6
1.0	10.9 / 10.4	10.7 / 10.5	10.8 / 10.7
1.5	11.2 / 11.1	11.3 / 11.2	11.2 / 11.1
2.0	11.4 / 11.3	11.4 / 11.5	11.5 / 11.3
2.5	11.6 / 11.2	11.8 / 11.7	11.9 / 10.8

6.4: Zeolite-A and peroxide bleaching of Eucalypt CCS.

The effects of using zeolite-A as a chelating agent for use in peroxide bleaching of Eucalypt CCS using the conditions as described in Method 4 on brightness and residual

peroxide are highlighted in figures 45 and 46 respectively. The pH profile for the bleaching experiments are given in Table 32.

Figure 45 shows that increasing zeolite-A charge has no effect on the brightness of bleached Eucalypt CCS. Furthermore if figure 45 is compared to figure 43 at 2.5% NaOH and 40 ppm there is no improvement in brightness. Figure 46 also confirms that zeolite-A has no effect on peroxide bleaching of Eucalypt CCS as there is no residual peroxide at any zeolite-A charge. These results were not entirely unexpected, as in the decomposition studies (section 3.3, figure 23) with zeolite-A, the zeolite had no effect in prevention of manganese if alkali was added before the zeolite.

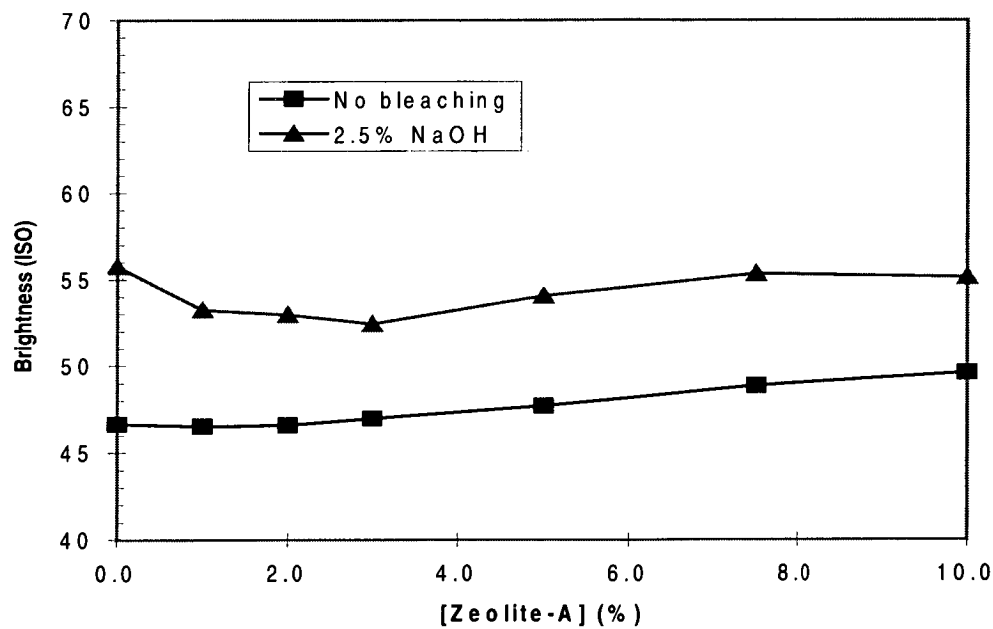


Figure 45: The effect on Brightness of bleached Eucalypt CCS by zeolite-A charge.

Figure 45 also shows that the addition of zeolite-A at high charges has only a small effect on brightness of unbleached Eucalypt CCS. Zeolite-A is a very white fine powder and the small increase in brightness is most likely to be related to a filler like effect.

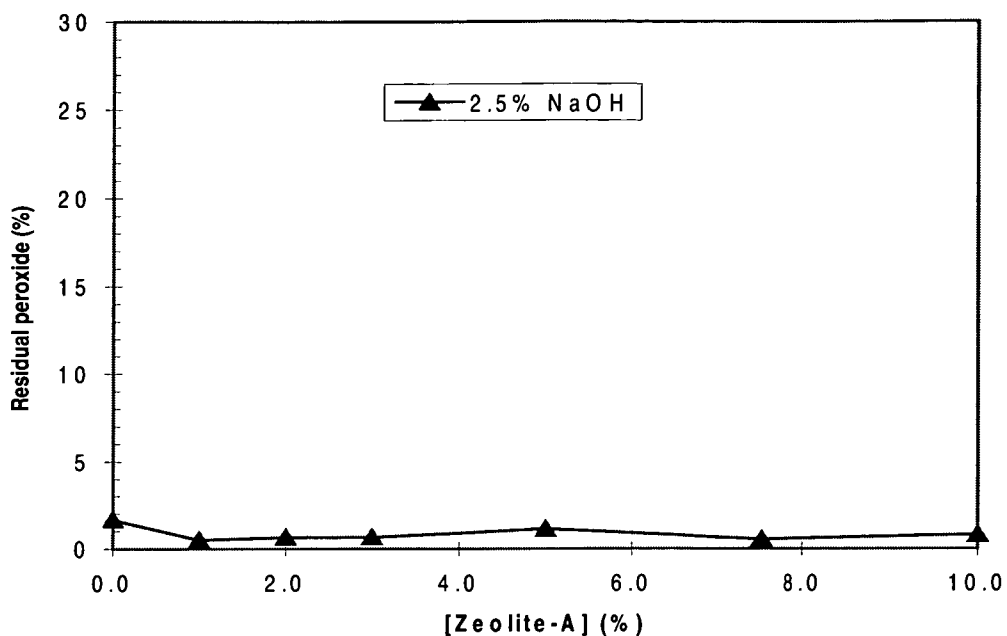


Figure 46: The effect on the residual peroxide of bleached Eucalypt CCS by zeolite-A charge.

Table 32: pH profile for bleaching of CCS using various concentrations of zeolite-A.

Zeolite-A (%)	No bleaching	Zeolite-A (initial/final pH)
0	8.6	11.9 / 11.8
1	8.7	11.9 / 11.6
2	8.9	12.0 / 11.9
3	9.2	12.1 / 12.0
5	9.4	12.2 / 12.3
7.5	9.7	12.3 / 12.1
10	9.9	12.5 / 12.3

6.5: Sodium citrate and peroxide bleaching of Eucalypt CCS.

Figure 47 and 48 show the effect of addition of chelating systems containing sodium citrate to peroxide bleaching of Eucalypt CCS. Figure 47 shows that citrate alone or

citrate with 5% zeolite-A has no effect in preventing brightness loss due to manganese decomposition of peroxide. Table 33 shows the pH profile for the bleaching of CCS with various concentrations of citrate.

Table 33: pH profile for bleaching of CCS with various concentrations of citrate.

Citrate (%)	Citrate (Initial/final pH)	Citrate + 5% Zeolite-A (Initial/final pH)
0	11.5 / 11.3	12.2 / 12.3
0.2	11.9 / 11.8	12.0 / 12.0
0.5	12.0 / 11.9	12.0 / 11.9
1.0	11.9 / 12.0	12.1 / 12.0
2.0	11.9 / 11.9	12.3 / 12.2
3.0	12.0 / 11.8	12.4 / 12.3

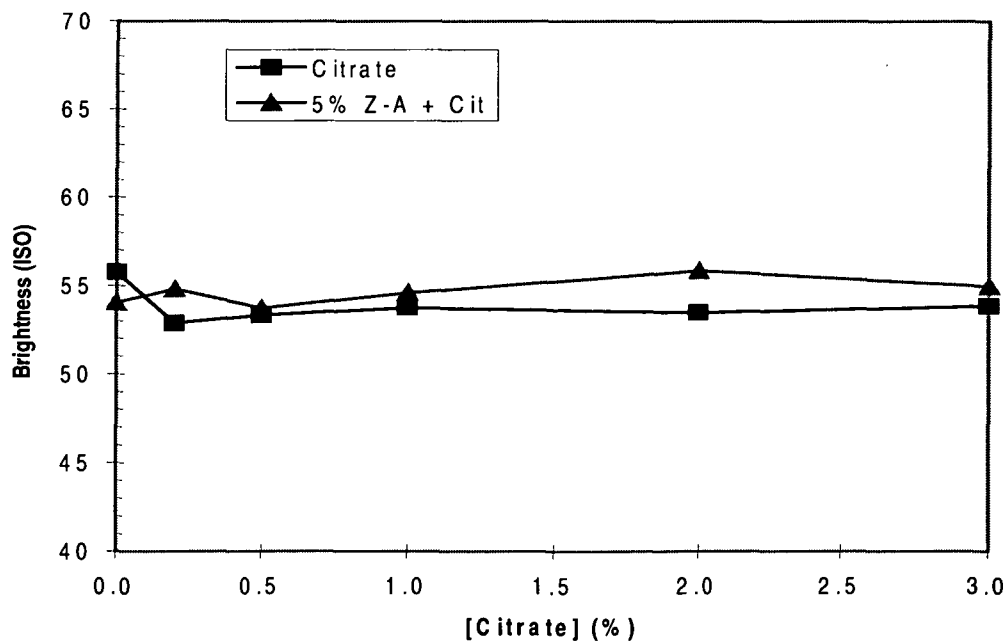


Figure 47: The effect on brightness of a bleached Eucalypt CCS pulp by citrate charge.

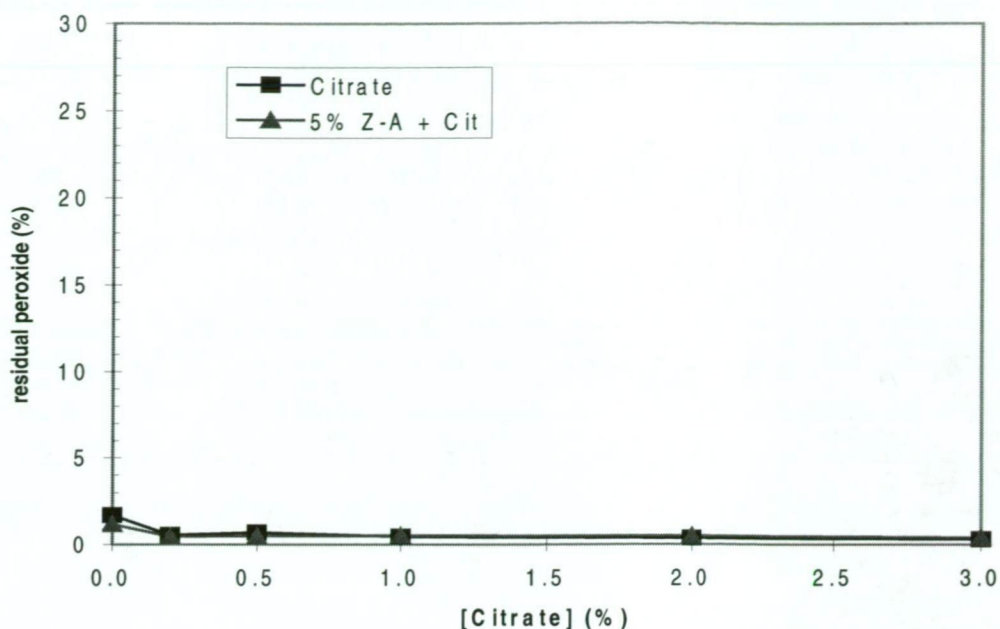


Figure 48: The effect on residual peroxide concentration of bleached Eucalypt CCS by citrate charge.

Figure 48 highlights the inability of citrate systems to prevent manganese decomposition with no peroxide remaining after the bleaching stage with any charge of citrate or 5% zeolite-A and citrate. As was the case with zeolite-A alone, citrate has already been shown (section 3.5, figure 15) to behave poorly when alkali is added before citrate in chelating manganese.

6.6: DTPA and peroxide bleaching of Eucalypt CCS.

The effect of DTPA on brightness and residual peroxide for peroxide bleaching of Eucalypt CCS is highlighted in Table 34. Table 34 shows that DTPA significantly outperforms the zeolite-A, citrate and 5% zeolite-A with 0.5% citrate in both brightness and residual peroxide. DTPA significantly reduces manganese induced peroxide decomposition and hence leads to large brightness gains and reasonable residual peroxide concentrations. This result is not unexpected as previously in figure 17 (chapter 3, section 3.7) DTPA has been shown to readily break down (dark brown to

clear solution) the active manganese decomposition species due to its large formation constant with manganese.

Table 34: Comparison of chelating agents for Eucalypt CCS bleaching.

Chelating system	Brightness [mean] (ISO)	Residual peroxide (%)	(Initial / Final) pH
0.5% DTPA	67.0	15.08	12.0 / 11.6
5% Z-A + 2% Cit [#]	55.9	0.49	12.3 / 12.2
1% Cit [#]	53.8	0.46	11.9 / 12.0
7.5% Z-A [#]	55.4	0.55	12.3 / 12.1
no chelating agent [*]	55.8	1.68	11.9 / 10.8

Best value in series

• with 2.5% NaOH, 40 ppm Mn and 2% H₂O₂

6.7: Conclusion.

- The best model system for inducing peroxide decomposition with manganese and evaluating the effectiveness of chelating systems under these conditions for peroxide bleaching of Eucalypt CCS is a system containing 2.5% NaOH, 40 ppm Mn and 2% peroxide.
- Zeolite-A and systems containing citrate do not prevent peroxide decomposition and consequently perform poorly as chelating systems for bleaching of Eucalypt CCS with peroxide because the pulp is alkaline before addition of the chelating agent. Therefore these systems can not interact with the active manganese species and prevent it from decomposing the peroxide.
- DTPA is a good performer as a chelating agent for Eucalypt CCS pulps with both high brightness and residual peroxide concentrations occurring after the bleaching stage.

CHAPTER 7: STRENGTH PROPERTIES OF BLEACHED PINE

TMP

This chapter will investigate the effects on strength and optical properties of peroxide bleached Pine TMP using the various chelating agents. Tear, tensile, roughness, porosity, opacity and light scattering co-efficient parameters have been measured on bleached Pine TMP as described in “Method 4”. Brightness values have already been reported in chapter 5. The results for the strength properties for pretreatment and no pretreatment with chelating agents have all been quoted with error bars to the 95% confidence interval, ie 2 standard deviations. The confidence intervals relate to measurements carried out on the same stock pulp, prepared under the same conditions on different days.

7.1: Peroxide bleaching and tear index

Figure 49 shows the effect of various chelating agents on tear index of bleached Pine

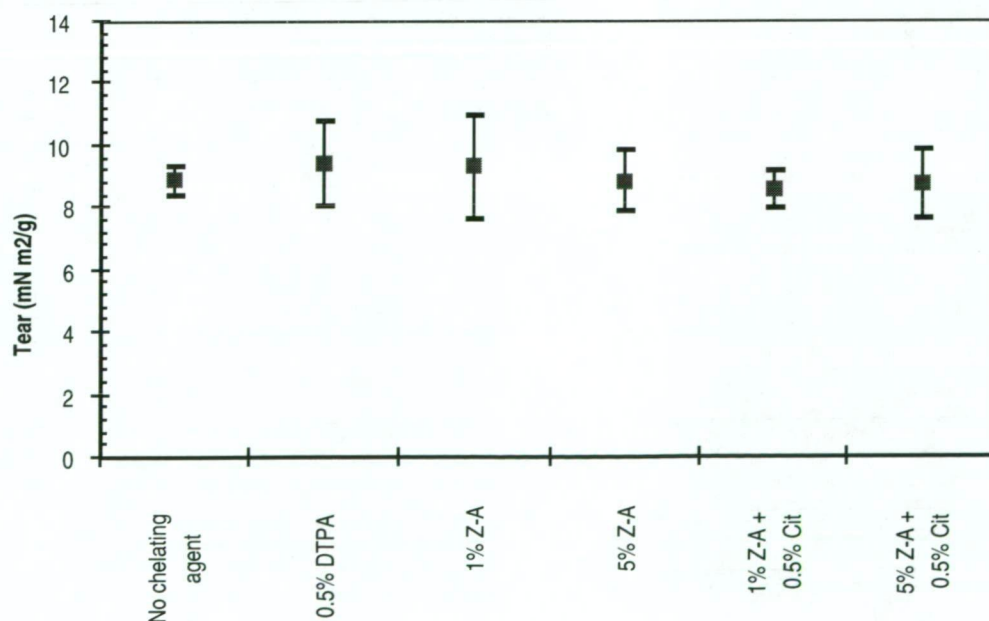


Figure 49: The effect on the tear index of bleached Pine TMP at the 95% confidence level by various chelating agents.

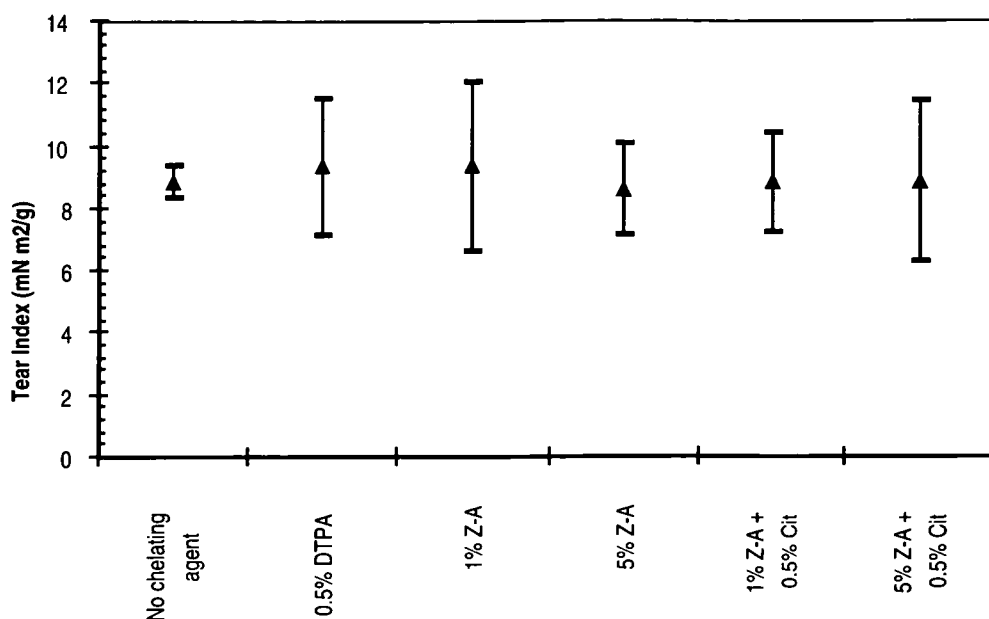


Figure 50: The effect on tear index of a bleached Pine TMP at the 95% confidence level by pretreatment with chelating agents.

TMP. No significant change in tear index was observed to occur. Figure 50 shows the effect of pretreating with the chelating agents on tear index of bleached Pine TMP. The only difference between the two sets of results is the extra variation for the results involving pretreatment. In the pretreatment case, chelating agent was applied then washed out prior to addition of bleaching chemicals.

7.2: Peroxide bleaching and tensile index

The tensile index of bleached Pine TMP as shown by figures 51 and 52 has not been statistically affected at the 95% confidence level by the various chelating systems, with or without pretreatment, employed in this study.

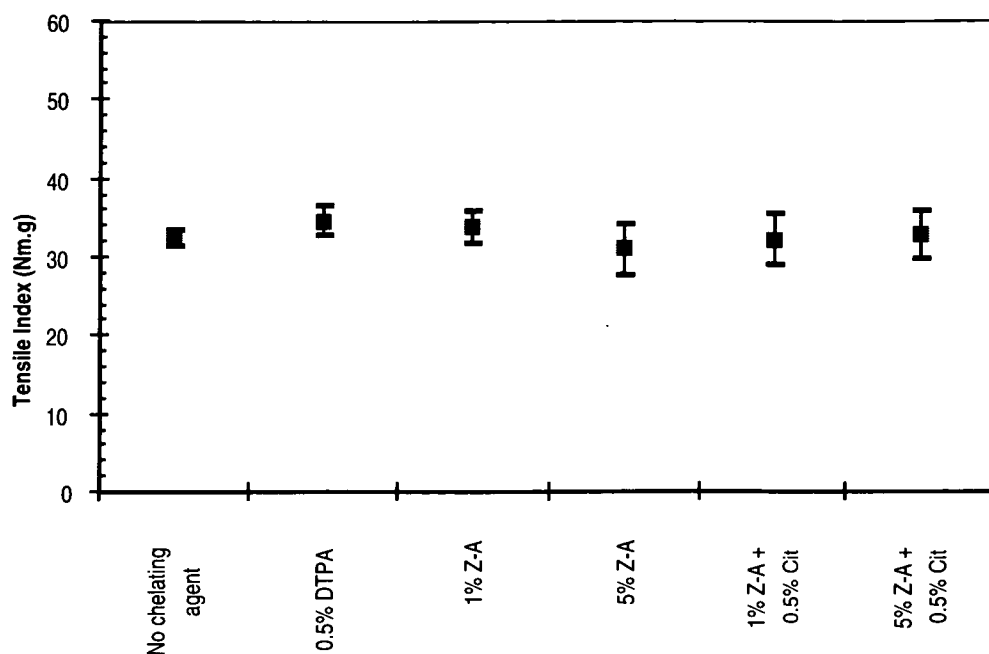


Figure 51: Tensile index of bleached Pine TMP at 95% confidence level.

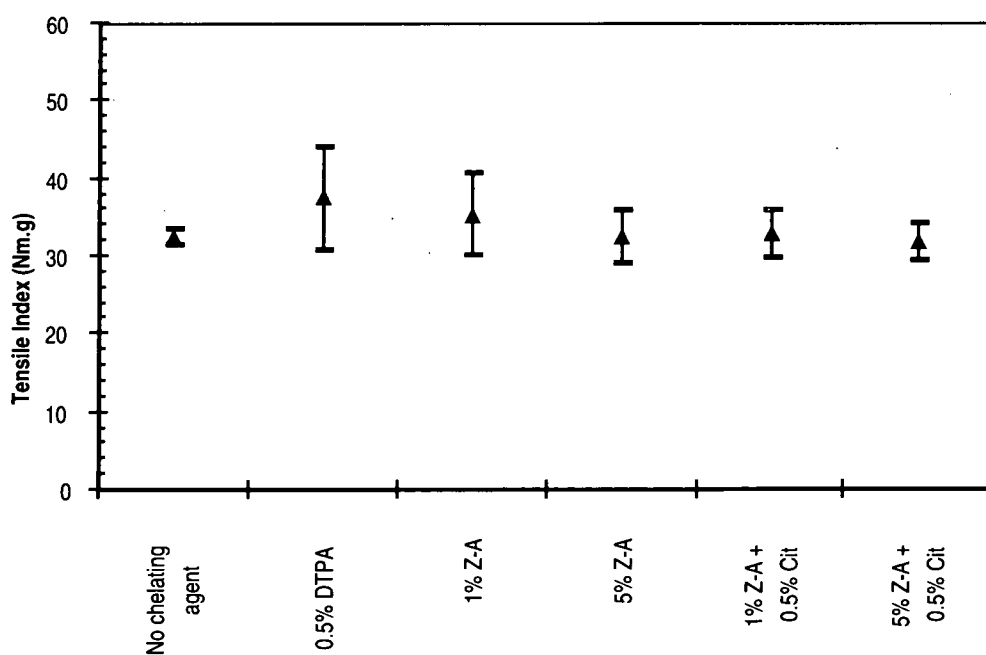


Figure 52: Tensile index of bleached Pine TMP by pretreatment with chelating agents.

7.3: Peroxide bleaching and roughness

The surface roughness of bleached Pine TMP as shown in figures 53 and 54 has not

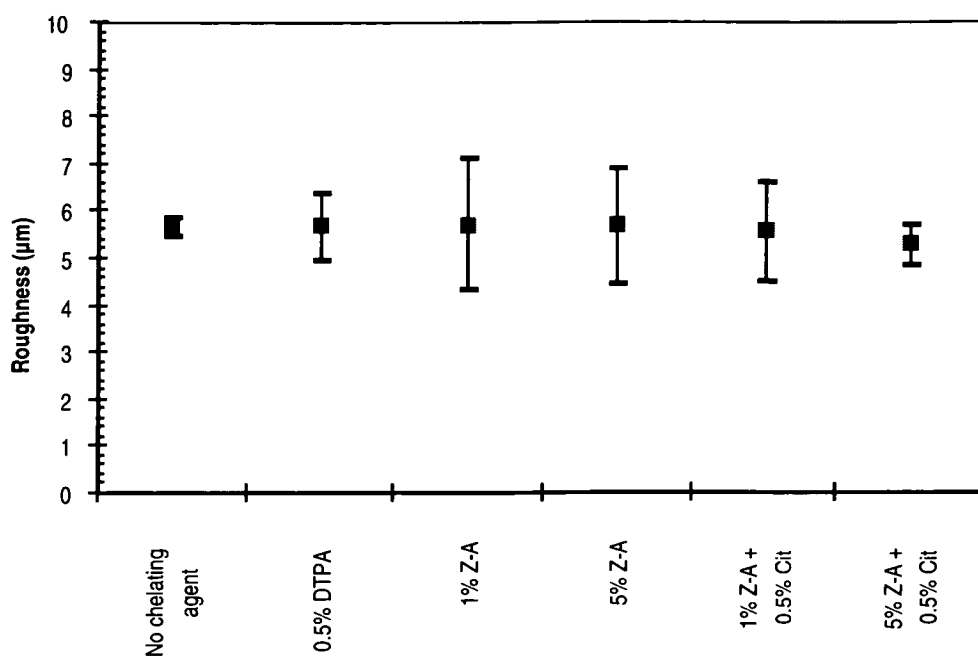


Figure 53: Roughness of bleached Pine TMP at the 95% confidence level.

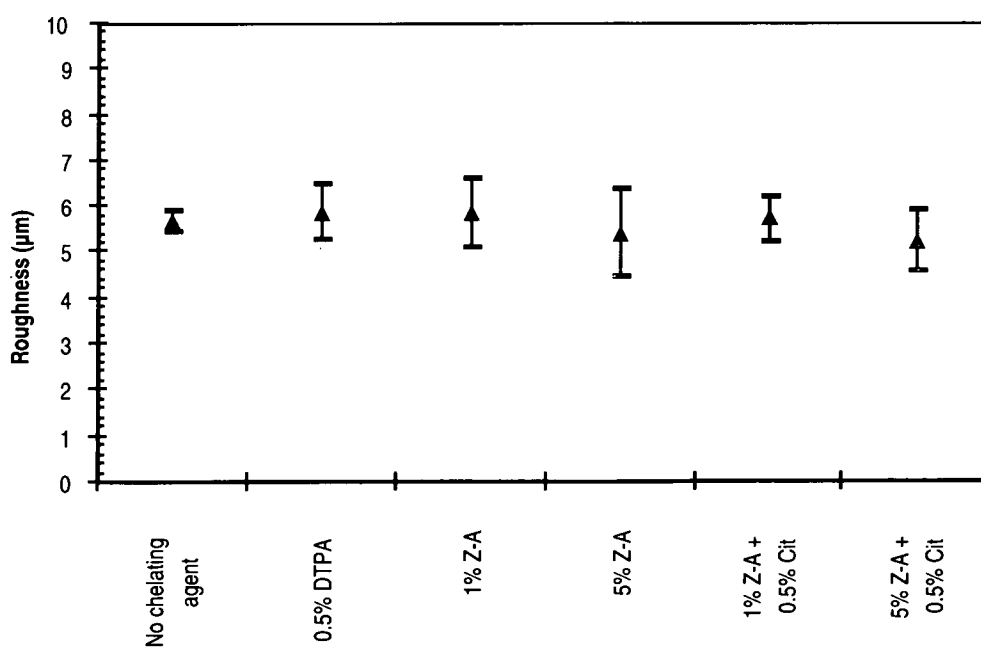


Figure 54: Pretreatment with chelating agents and roughness of bleached Pine TMP.

been affected by the use of chelating agents in the production of the bleached pulp, employed in this study.

7.4: Peroxide bleaching and porosity

Figures 55 and 56 show that the porosity of handsheets produced from bleached Pine

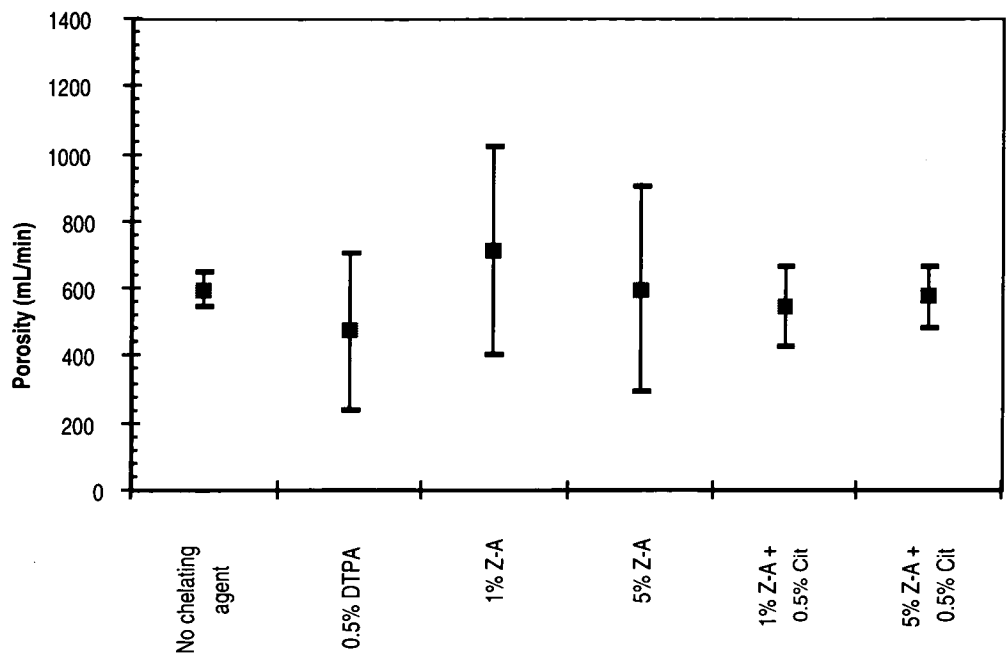


Figure 55: Porosity of bleached Pine TMP at the 95% confidence level.

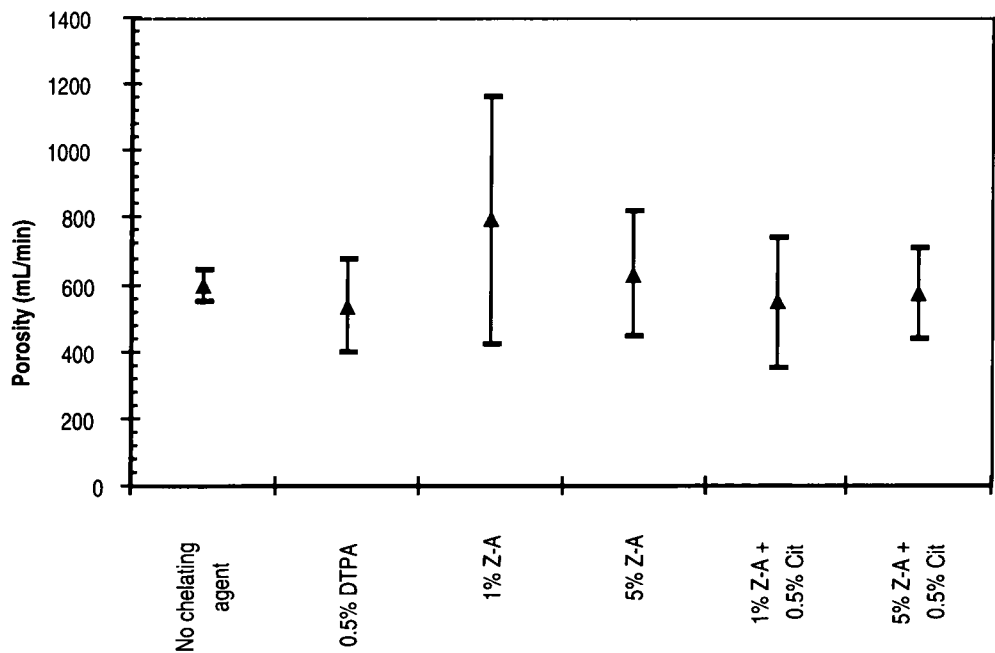


Figure 56: The effect on porosity of a bleached Pine TMP at the 95% confidence level by pretreatment with chelating agents.

TMP using chelating agents, with or without pretreatment, is not different, within the 95% confidence interval, from the case without any chelating agent.

7.5 Peroxide bleaching and optical properties

The effects of chelating systems with or without pretreatment on opacity are shown in figure 57. The samples without pretreatment of chelating agents show little difference from the case of no chelating agent present. The only exception is the case of 0.5% DTPA which has a small negative effect (1%) on opacity. The pretreated series of results is somewhat different. Only 5% addition of zeolite-A , and 5% zeolite with 0.5% citrate are equivalent to no addition of chelating agent. 0.5% DTPA, 1% zeolite-A and 1% zeolite-A with 0.5% citrate perform significantly poorer in terms of opacity when pretreated. This negative effect could be due to removal of the chelated species in the washing stage or a combined loss of chelated species and a small proportion of fines in the wash stage.

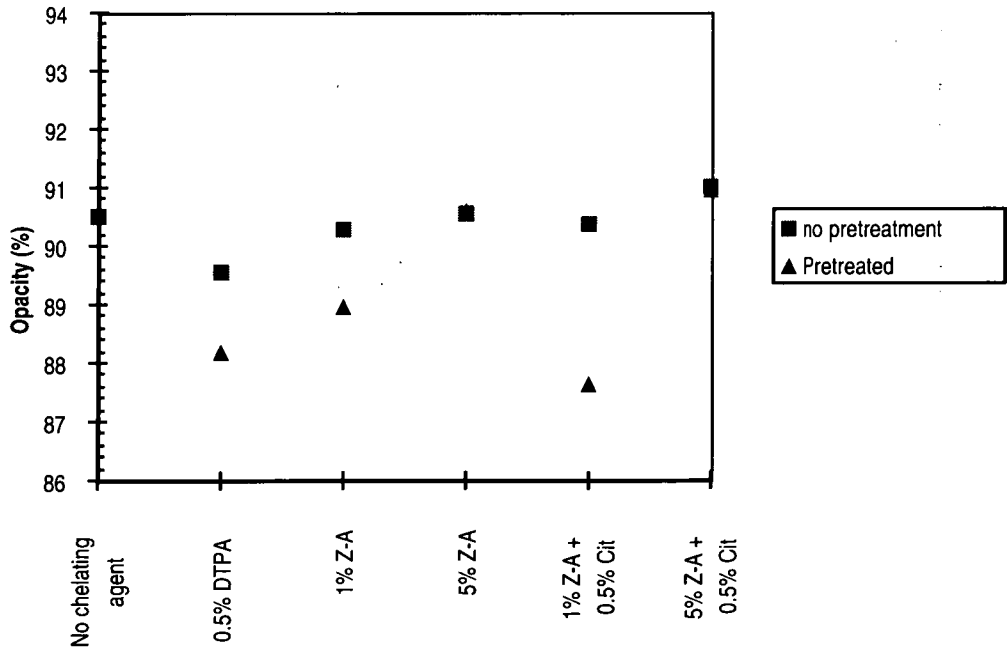


Figure 57: The effect on opacity of a bleached Pine TMP by chelating agents.

Figure 58 shows the effect of chelating agents on the light scattering co-efficient of peroxide bleached Pine TMP. The figure highlights the positive effect that systems containing 5% zeolite-A have on improving the light scattering co-efficient. The other chelating systems that do not contain 5% zeolite-A are only marginally different from the case of no chelating agent. Therefore it would seem that the best possible explanation from the performance of 5% zeolite-A containing systems could be that the higher amounts of zeolite are starting to have a filler like effect where the zeolite is starting to introduce enough additional surfaces to increase the scattering of light within the pores of the sheet matrix.

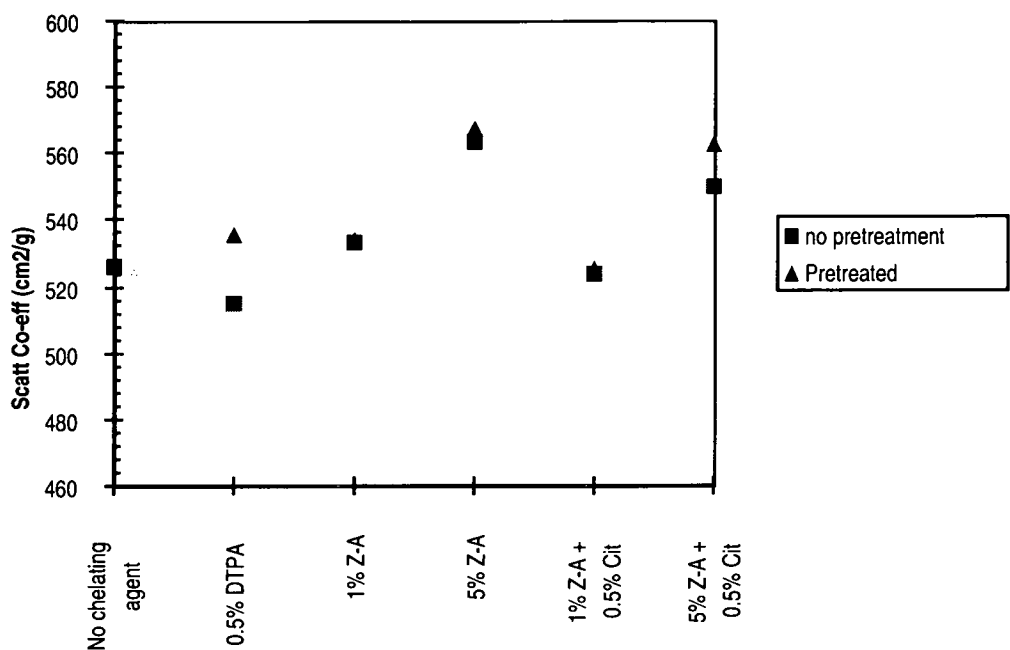


Figure 58: The light scattering co-efficient of bleached Pine TMP.

The relationships between the optical properties of paper can be used to illicit more information about the role and function of zeolites in peroxide bleaching. Opacity or inversely transmittance is a measure of the amount of light passing through a sheet of paper . 100% opacity refers to no transmitted light. The passage of light through paper is modified by two factors, the scattering of light and absorption of light. The scattering of light (scattering co-efficient) occurs due to the pores or voids in the paper, which

create surfaces where there is a change in the reflective index. The air /fibre interface bends the light from its initial path and hence reduces the transmittance of the light through paper. The number of fibre-air interfaces is dependent on fibre diameter and fibre debris (fines). Filler materials act like fines increasing the scattering due to the smaller particles sizes. The other factor which effects the opacity is the absorption of light (absorption co-efficient) by chemical constituents of paper. Lignin with its conjugated carbon double bond structure is the primary light absorbing constituent. Absorption co-efficient can also increase with scattering co-efficient as there is more opportunity for absorption as the light travels along a longer path. Fines also tend to improve absorption co-efficient as they have high light absorption. Typically anything which increases scattering or absorption also increases the opacity of a paper sheet (3). In practice printing opacity is used because of its easy determination.

$$\text{Printing Opacity} = R_o / R_{(\text{infinity})}$$

where R_o = reflectance of a single sheet backed with a black body, $R_{(\text{infinity})}$ = reflectance of an opaque pad, typically 8 sheets are used. The ratio of absorption co-efficient to scattering co-efficient can be determined from a derived Kubelka-Munk equation.

$$k / s = (1 - R_{(\text{infinity})})^2 / 2 R_{(\text{infinity})}$$

where k = absorption co-efficient, s = scattering co-efficient and both co-efficients are based on weight rather than thickness (represented by K and S). The actual values of k and s can be worked using equations in computer programs (3).

Brightness is a measure of the reflectance of light at a specific wavelength of 457 nm (blue region). It is primarily used as an indicator of the degree of bleaching of pulp as the 457 nm region is the most sensitive to bleaching over the colour spectrum(3). Therefore as brightness increases the absorption co-efficient will decrease as the bleaching agent attacks the lignin chromophores reducing the absorption of light. So unbleached pulps tend to have a higher opacity than bleached pulps.

In light of the previous discussion and the results obtained for the optical properties would suggest that zeolite-A at the higher charges increases the scattering co-efficient by creating additional scattering interfaces within the pulp matrix leading to an improvement of the opacity of the bleached Pine TMP sheet.

7.6: Conclusion

- The pulp properties such as tear index, tensile index, roughness and porosity of bleached Pine TMP are not affected by the use of chelating agents with or without pretreatment.
- Opacity of bleached Pine TMP was not significantly affected by the use of chelating agents without pretreatment, although 0.5% DTPA did show a small loss of about 1%. However when compared to the series of experiments with pretreatment only those experiments which contained 5% zeolite-A did not show a significant loss in opacity compared with the case of no chelation.
- The use of 5% zeolite-A containing chelation systems had a positive effect on the light scattering co-efficient for both the with and without pretreatment of the chelating agents. The other systems investigated in this study were not significantly different from the case of no chelating agent for both the with and without pretreatment experiment series.
- The results observed for optical properties suggest that if the higher amounts of zeolite are retained with the fibre, more surface area is present for the scattering of light.

CHAPTER 8: STRENGTH PROPERTIES OF BLEACHED EUCALYPT CCS.

The effect on strength and optical properties by chelating systems used in preparation of peroxide bleached Eucalypt CCS shall be investigated in this chapter. Strength properties such as tear and tensile index, sheet porosity and surface roughness, optical properties such as opacity and light scattering co-efficient will be measured to evaluate if there are any detrimental effects in using various chelation systems in the bleaching process. The chelating agents will be applied in two different methods (as stated in method 4), with or without pretreatment. It is more likely that in a real world situation that a pretreatment stage would occur, e.g. the pulp is more likely to be washed before bleaching in a “thickening” stage in medium to high consistency peroxide bleaching, and after the bleach plant before use in a paper mill to remove anionic trash and other materials that may retard retention aid systems. The results quoted in this chapter give error bars around the mean at the 95% confidence level.

8.1: Peroxide bleaching and tear index

Figures 59 and 60 show the effects of chelating systems on tear index of bleached Eucalypt CCS without and with pretreatment respectively. These figures show that at the 95% confidence level there is no significant effect on tear index by any of the chelating systems over the case of no chelation, whether they have been applied with or without pretreatment.

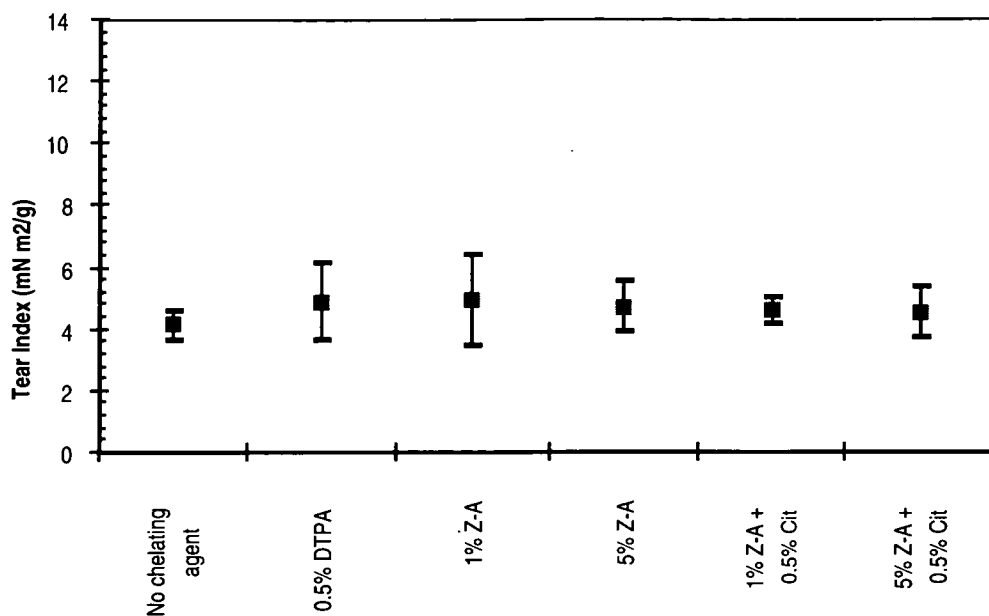


Figure 59 : The effect on the tear index of a peroxide bleached Eucalypt CCS pulp at the 95% confidence level by various chelating agents.

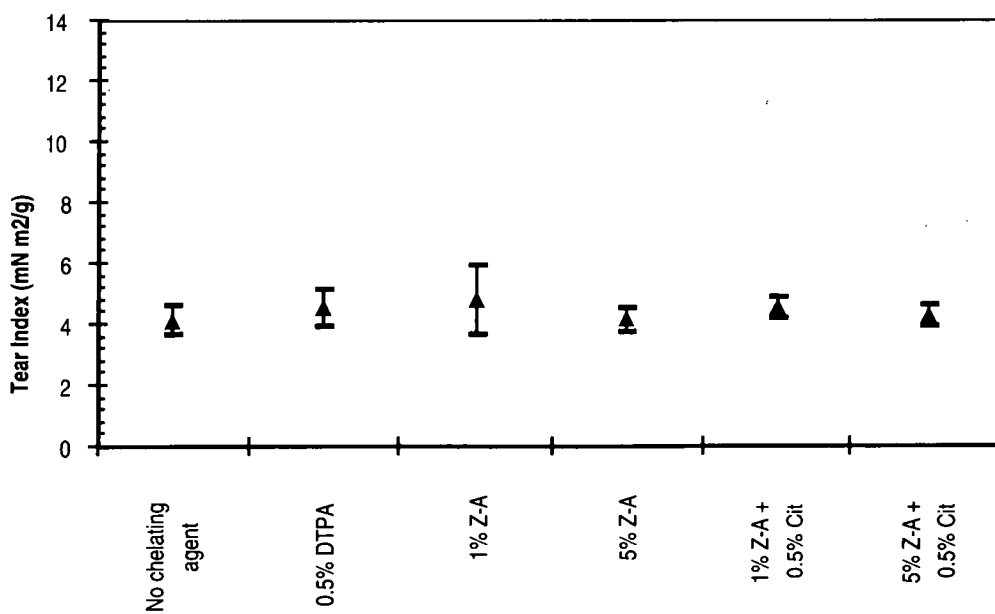


Figure 60: The effect on tear index for peroxide bleached CCS pulp by pretreatment with various chelating agents at the 95% confidence level.

8.2: Peroxide bleaching and tensile index.

The effect on tensile index of bleached Eucalypt CCS pulp by various chelating agents without and with pretreatment is shown in figures 61 and 62 respectively. The use of the various chelating systems without pretreatment (figure 61) has no effect over the control case with no chelation on tensile index for bleached Eucalypt CCS at the 95% confidence level.

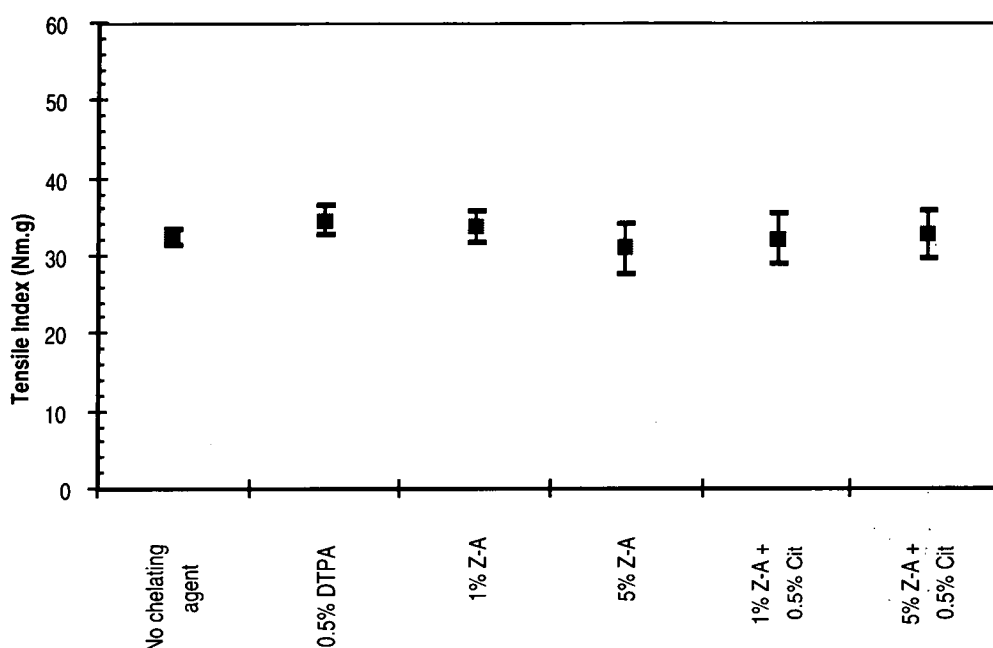


Figure 61: The effect on the tensile index of peroxide bleached Eucalypt CCS pulp at 95% confidence level by various chelating agents.

The pretreatment with the chelating systems (figure 62) on bleached Eucalypt CCS pulp with the exception of the case of 5% zeolite-A does have a small positive effect on tensile index at the 95% confidence level. However there is no appreciable difference at 95% confidence level between 0.5% DTPA, 1% zeolite-A, 1% zeolite-A with 0.5% citrate, and 5% zeolite-A with 0.5% citrate. In light of these results a possible explanation could be that the extra 30 minutes mixing in the pretreatment stage could slightly increase the flexibility or remove some kinks in some fibres. The fibres can

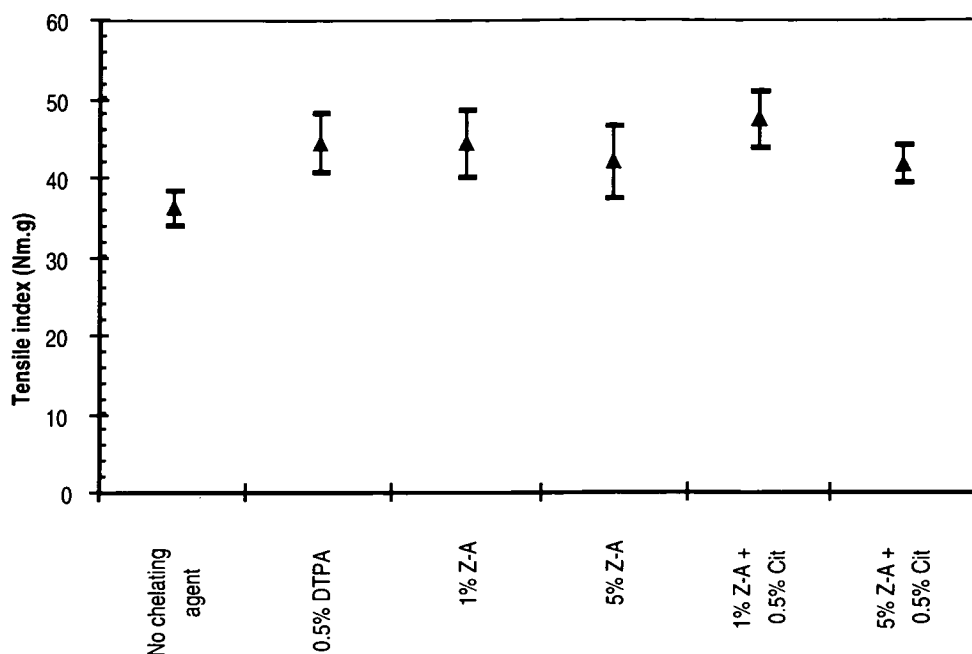


Figure 62: The effect on the tensile index of peroxide bleached Eucalypt CCS pulp with 95% confidence intervals by pretreatment with various chelating agents.

then pack together better leading to more fibre-fibre contact and consequently improving fibre bonding. The increase in fibre bonding leads to a direct increase in tensile index, which is a function of the resistance of fibres to being pulled out of the sheet matrix (3).

8.3: Peroxide bleaching and roughness

Surface roughness is not affected by the use of the various chelating systems with or without pretreatment as shown in figures 63 and 64 respectively for bleached Eucalypt CCS pulp. The addition of the chelating agents has lead to an increase in the amount of error (based on 95% confidence intervals) in roughness measurements and so it is unlikely that there is any significant difference between samples.

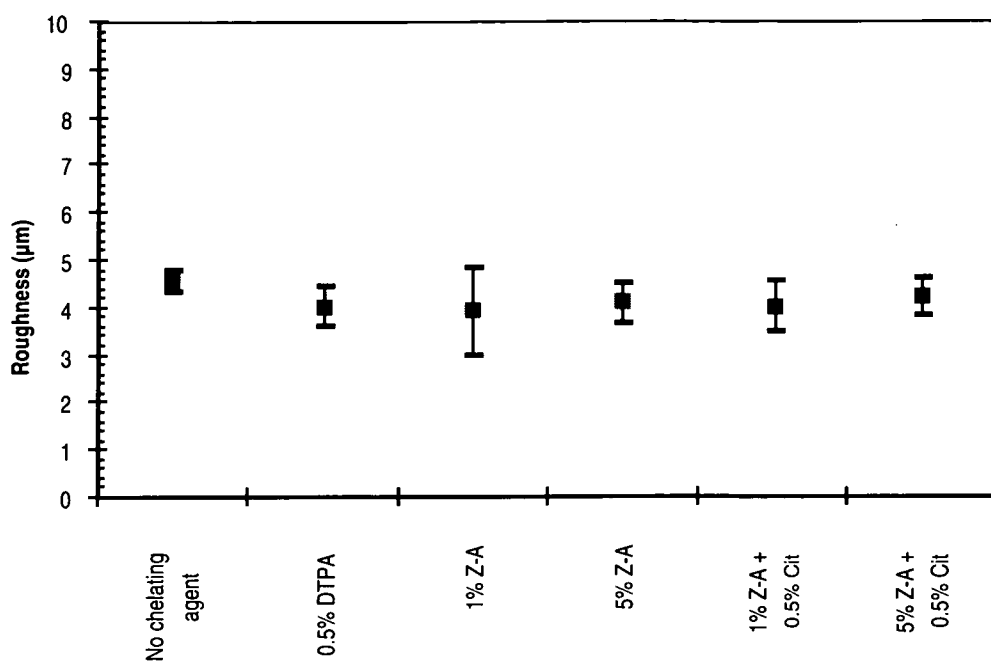


Figure 63: The effect on roughness of peroxide bleached Eucalypt pulps at the 95% confidence level with various chelating agents.

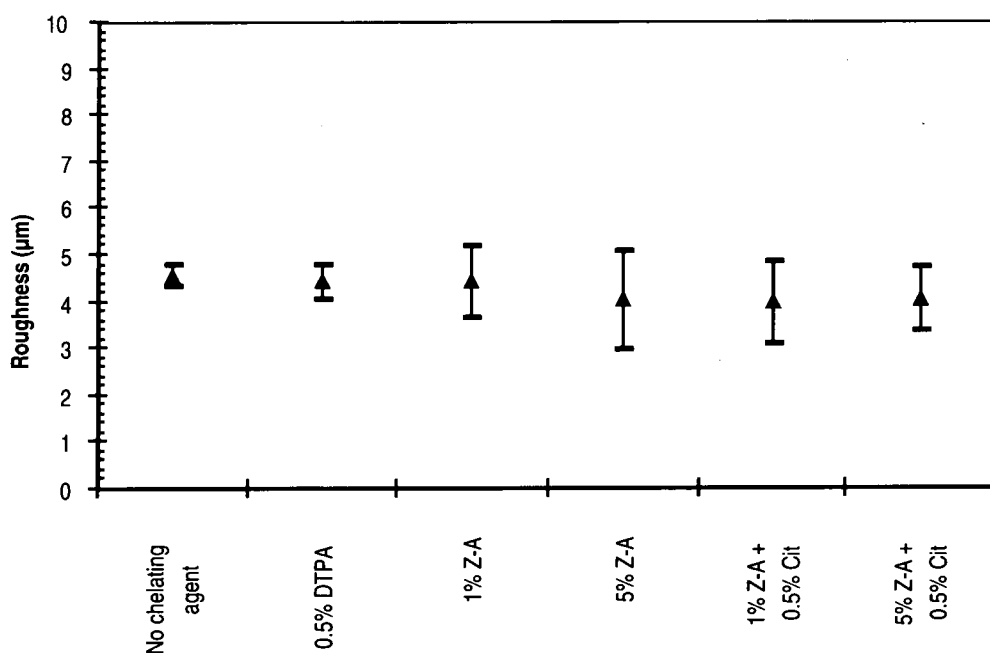


Figure 64: The effect on roughness for peroxide bleached Eucalypt CCS pulps at the 95% confidence level by pretreatment with various chelating systems.

8.4:Peroxide bleaching and sheet porosity

Figures 65 and 66 show the effect of chelation systems without or with pretreatment on sheet porosity of bleached Eucalypt CCS respectively. In both cases, addition of chelating agents significantly reduced sheet porosity in the order 1000 mL/min. There was however no significant difference between the five chelating systems employed in this study in terms of porosity results for bleached Eucalypt CCS pulp. The porosity of the unchelated bleaching system for Eucalypt CCS seems to be unusually high as the ANM Boyer mill usually runs in the range of 200 to 300 ml/min. However despite this anomaly, the low porosity of the chelated systems does compare favourably with

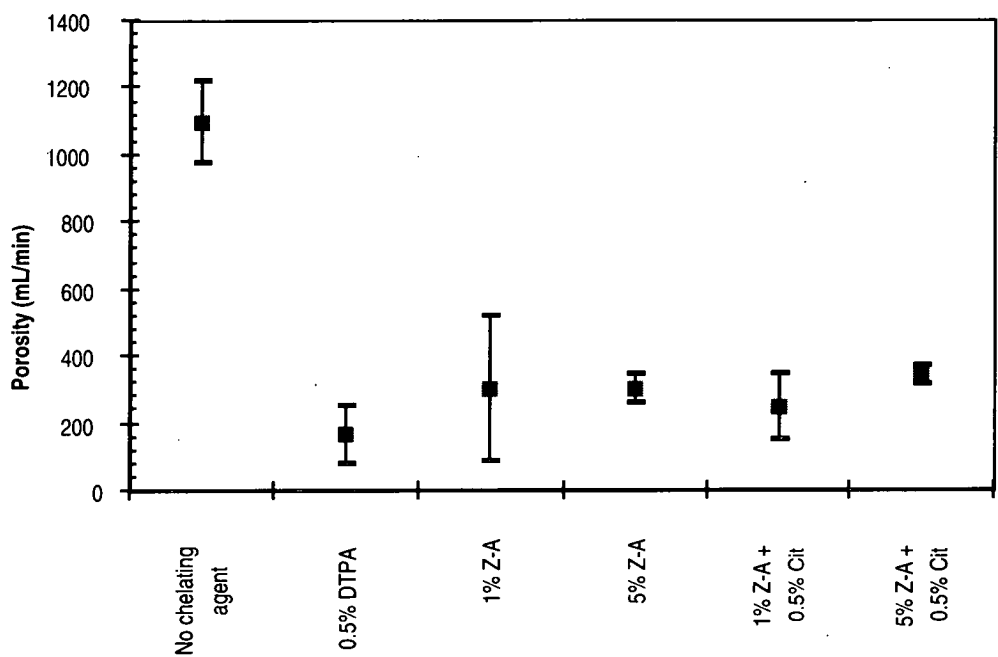


Figure 65: The effect on porosity of peroxide bleached Eucalypt CCS pulps with 95% confidence intervals by various chelating agents.

the tensile index. Tensile index is a measure of fibre bonding, so low porosity or low volume of cavities or pores corresponds to closer fibres and hence better bonding. Typically filler like materials reduce porosity by filling up pores or cavities(3). However the “filler” explanation would not account for the results with DTPA (water

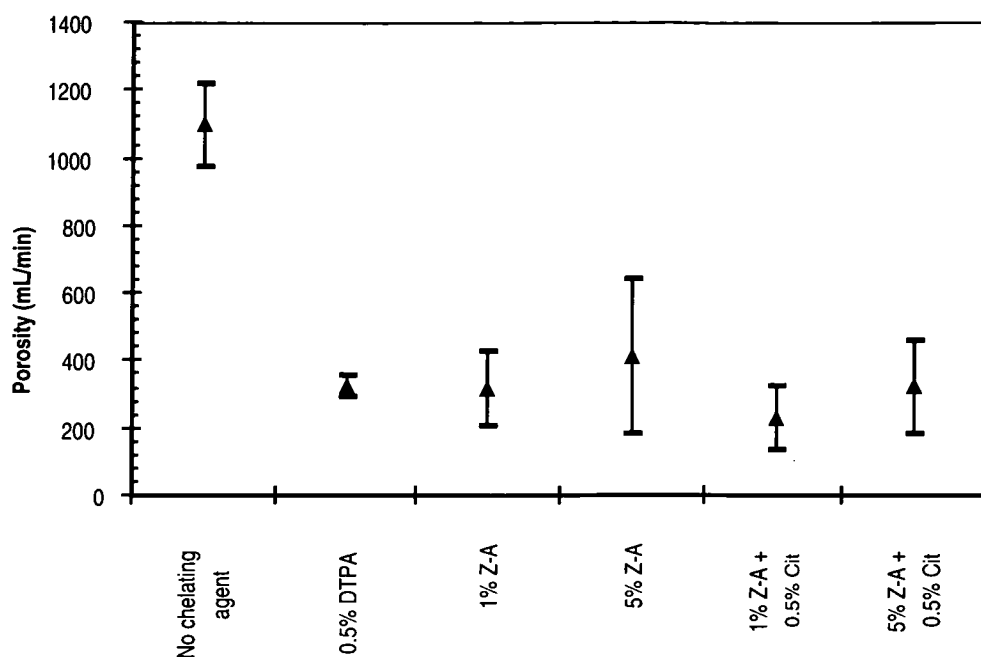


Figure 66: The effect on porosity with 95% confidence intervals for peroxide bleached Eucalypt CCS pulps by pretreatment with various chelating systems.

soluble), and therefore it seems likely that the porosity for the case without any chelating agent is misleading high.

8.5 Peroxide bleaching and optical properties

Figure 67 illustrates the effect on opacity of handsheet produced from bleached Eucalypt CCS pulp by using chelating agents with and without pretreatment. In both cases addition of a chelating system has improved the opacity of the resulting bleached pulp. The highest gains in opacity occurred for those systems containing 5% zeolite-A. This result is similar to those obtained with Pine TMP and it would appear likely that the mechanism of the increases in opacity are due to filler like effects of high amounts of zeolite-A present.

The effects on light scattering co-efficient of bleached Eucalypt CCS pulp containing various chelating agents with and without pretreatment are highlighted in figure 68.

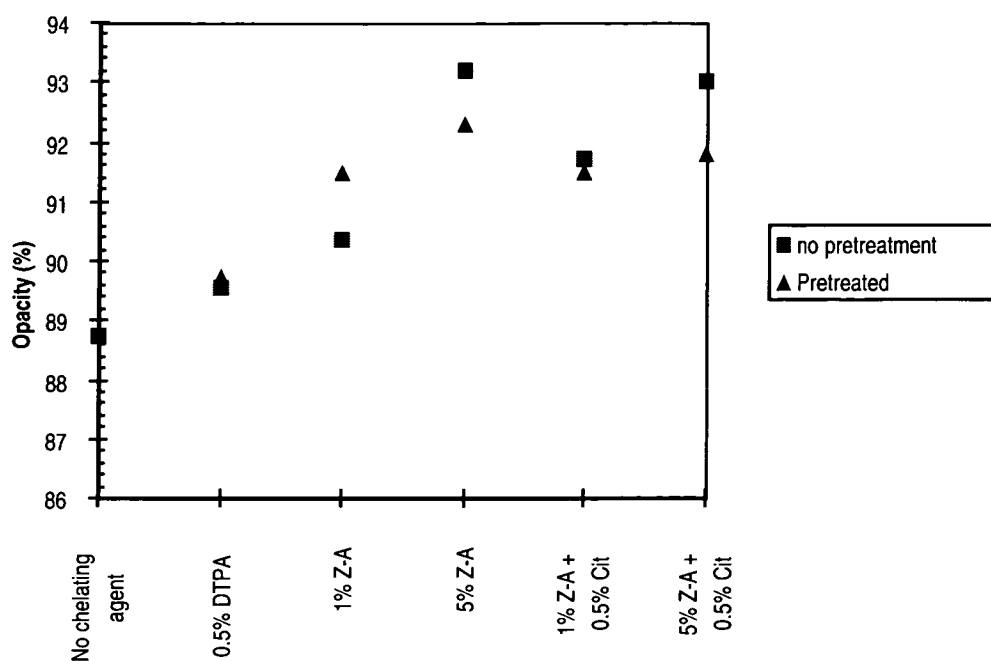


Figure 67: The effect on opacity of peroxide bleached Eucalypt pulps by various chelating systems.

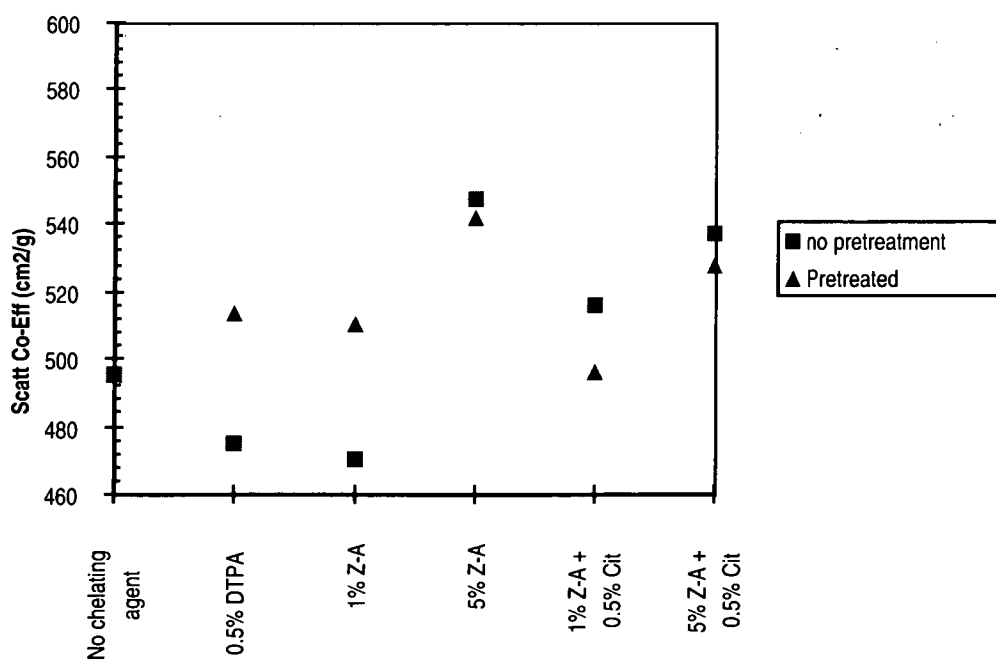


Figure 68: The effect on light scattering co-efficient of peroxide bleached Eucalypt CCS pulps by various chelating agents.

The figure 68 shows that chelating systems containing 5% zeolite-A perform substantially better than those that do not, in raising the light scattering co-efficient. There results follow along with those of opacity which is not suprising as light scattering co-efficient forms part of the Kubelka-Munk equation for opacity. This would tend to support the hypothesis postulated already that the higher amount of zeolite-A is having a small filler like effect on the optical properties of pulp handsheets.

8.6 Conclusion

- Tear index is not affected by the use of the various chelating systems with or with pretreatment in the preparation of peroxide bleached Eucalypt CCS.
- Tensile index of Eucalypt CCS is not appreciably affected by the chelating agents when present in the system. However a slight beneficial increase occurs using a pretreatment regime, particularly with no or low zeolite chelating systems. It is likely that the extra 30 minutes mixing has a small effect on fibre flexibility leading improve fibre bonding.
- Roughness of Eucalypt CCS handsheets was not affected by the use of the various chelating system with or without pretreatment.
- The chelating systems had a lower porosity than the system containing no chelating agent. However there was no significant difference between the chelating systems with or without pretreatment.
- The systems containing the highest charge of zeolite-A with or without pretreatment show superior performance in terms of opacity and light scattering coefficient over the other systems and the case of no chelating agent. This effect is most likely linked to zeolite acting as a “filler” by increasing the refractive surface area of the paper sheet.

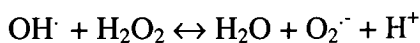
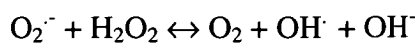
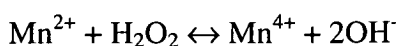
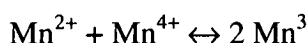
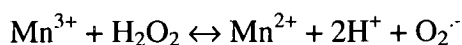
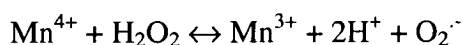
References: (Part 2)

- (1) Bassett, J., Denney, R.C., Jeffrey, G.H. and Mendham J., **Vogel's textbook of quantitative inorganic analysis**- 4TH edition: Longman (1978)
- (2) Ginting, Y., PhD Thesis, University of Tasmania, 1997
- (3) Casey, J.P., **Pulp and Paper; Chemistry and Chemical Technology** - 3RD edition , Volume 3: Wiley-Interscience (1981)
- (4) Breck, D.W., **Zeolite Molecular Sieves: structure, chemistry and uses:** Wiley and Sons (1974)

CONCLUSION:

This study has focused on investigating the use of Zeolite and sodium citrate as a replacement for DTPA in hydrogen peroxide bleaching under manganese induced peroxide decomposition conditions. Manganese is one of several metal ions that rapidly decompose peroxide and reduce bleaching response of peroxide due to catalytic decomposition reactions.

The mechanism of manganese decomposition is slightly different from other metal ions. manganese under alkaline conditions oxidizes from its Mn^{2+} state to higher oxidation states such as Mn^{3+} , Mn^{4+} , Mn^{7+} and can form many different Mn-O complexes such as MnO_2 , Mn_3O_4 or Mn-O-Mn species. It is under alkaline conditions and thus at the higher oxidation states that manganese decomposes hydrogen peroxide. The reaction mechanism is believed to be based on the Mn^{4+}/Mn^{3+} couple.



The effect of iron, copper and manganese on peroxide decomposition were studied under acid (~pH=4), slightly basic (~pH=8.5-9.0) and alkaline (~pH=11.0) pH's before peroxide addition. Manganese, under alkaline conditions, was the only metal ion of those tested to show any significant peroxide decomposition over the reaction period of 60 minutes.

Mechanism of zeolite/ citrate action:

It seems most likely that the zeolite, based on the literature and results obtained in this study, is acting primarily as chelating agent with the main reactions involving cation exchange of transition metal ions into the zeolite cage structure. Therefore the cation exchange capacity of the zeolite is important in prevention of manganese induced peroxide decomposition. Zeolite-A proved to be the most effective in reducing manganese induced peroxide decomposition of the three commercial zeolite types (A, X, Y) evaluated in this study at both 20°C and 70°C. One of the reasons why zeolite-A performs better than types X, and Y is that zeolite-A has a greater cation exchange capacity. The greater cation exchange capacity is due to a lower Si/Al ratio, or greater aluminium content that introduces negative charges into the zeolite structure. The negative charge is countered with sodium ions during zeolite formation. These sodium ions may later be exchanged with other ions leading to the zeolite becoming a cation exchange material. The Si/Al ratio plays a prime role in the exchange behaviour, for example zeolites X and Y, with Si/Al ratio of 1.25 and 2.5 respectively, have the same pore size and cage structure yet zeolite-X has 86 more exchangeable sodium ions per unit cell and consequently was found to inhibit manganese induced peroxide decomposition better than zeolite-Y. Zeolite-A with a Si/Al ratio of 1 has the most exchangeable sodium ions per unit cell of the three zeolites and consequently performed better than both zeolites X and Y which had larger Si/Al ratios. The Si/Al ratio also plays a role in the exchange site location. Zeolite-A primarily exchanges Mn^{2+} ions into the β -cages of the zeolite (site I). This site is the most preferred site for exchange as the manganese ions are protected from alkali and peroxide attack by ionic and covalent bonds with oxygen atoms of AlO_4^- tetrahedra in the β -cages. Zeolite-X does have some site I locations, but these are filled with water when the zeolite is hydrated. Therefore exchange occurs on the surface sites. Site II is located on the oxygen atoms of the β -cages that face out into the internal pore. The other surface site, site III, is located on the rings that join the β -cages. Both of these sites provide exchanged manganese with

significantly less protection from attack by alkali and peroxide than the site I location. The large pore size of zeolite-X and Y allows water to form an liquid phase inside the zeolite structure, which affects the exchange site chemistry with the hydrolysis of sodium counterions. The chemistry changes from ionic and covalent bonds through AlO_4^- to weakened dipole moments through $\text{AlO}_4\text{-H}$. This arrangement is much less preferred for ion exchange. Mn^{2+} ions are fully hydrated when exchanged into zeolites X and Y. Zeolite-Y does not significantly prevent manganese induced peroxide decomposition because of the small number of cation exchange sites. Consequently the majority of hydrated manganese ions are located in the liquid phase inside zeolite-Y. The hydrated manganese ions are then easily converted to the active decomposition species by alkali and peroxide. Zeolite-A produced a greater reduction in the manganese induced peroxide decomposition than the other zeolite types due to the increased number and location of the exchange sites. Consequently the brightness and residual peroxide values for peroxide bleached Pine TMP with zeolite-A were the highest of the 3 zeolite types used.

The beneficial effect of zeolite in preventing peroxide decomposition is however dependent on the order of chemical addition. If Mn^{2+} ions are oxidised when the pH is raised before addition of zeolite, the active decomposition species of an Mn-O type of arrangement cannot penetrate the small pores of the zeolite. Thus the active decomposition species are not deactivated by complexation and are able to interact with peroxide causing rapid decomposition. None of the three zeolites evaluated were able to prevent decomposition if the manganese containing solution was alkaline before addition of zeolite. Sodium citrate was also found to have no effect on peroxide decomposition if the manganese containing solution was alkaline before addition of citrate. DTPA on the other hand was able to prevent peroxide decomposition despite the order of chemical addition, because of its strong complexing ability with manganese.

Zeolite and citrate containing systems do improve brightness and residual peroxide concentrations for bleached Pine TMP, with brightness levels slightly less than those achieved with DTPA though residual peroxide concentrations were significantly lower. They had no effect in bleaching of Eucalypt CCS. The poor performance of zeolite and citrate with Eucalypt CCS is due to the pulp being alkaline before addition of the chelating agents. It was found in decomposition studies that zeolite and citrate could not exchange manganese once it was converted to higher oxidation states that are partially insoluble. Therefore zeolite and citrate must be added prior to the addition of alkali to complex metal ions in order to be effective in mill situations. CCS pulps could possibly be acidified before zeolite addition to increase the effectiveness of the zeolite, but it would seem a waste of chemicals particularly if the CCS pulp is to be bleached with peroxide. There would also be a cost penalty due to the addition of extra acid and then alkali which would be required for bleaching.

In the absence of pulp (decomposition study), the interaction between manganese, zeolite and peroxide is complex and the kinetics are important. Increasing the zeolite-A charge above 1% zeolite-A increased the rate of decomposition at both 20°C and 70°C. At the higher temperature zeolite-A in the absence of manganese provided a significant proportion of the decomposition, such that zeolite-peroxide interactions become the dominant decomposition reaction.

In the presence of pulp at 70°C, higher levels of zeolite were required to bring about brightness improvements. The highest brightness for peroxide bleached Pine TMP with zeolite-A alone under conditions of this experiment occurred at a zeolite charge of 10%, although the trend was still increasing at a reduced rate. The higher amount of zeolites required for bleaching as compared to decomposition studies is most likely due to the zeolites having to compete with fibres for metal ions.

Sodium citrate was found to prevent peroxide decomposition at 20°C at charge levels above 0.5%. At 70°C, only higher charges (3%) of citrate showed large reductions in peroxide decomposition. However the main benefit of citrate addition occurred with zeolite-A, providing a synergistic effect over that of zeolite alone in the inhibition of peroxide decomposition at both temperatures. The combined system worked best when small amounts of citrate (0.2%) were added with zeolite-A. Further additions of citrate with zeolite-A increased the rate of decomposition. Therefore, either more manganese is being transferred to solutions and undergoes oxidation, or manganese ions spend more time transferring between the solids allowing for more oxidation due to more competition and transfer between citrate molecules. In peroxide bleaching studies of Pine TMP, a charge of 0.5% citrate with 5% zeolite-A provided the optimum brightness. Further addition of citrate had no significant effect on brightness but did increase residual peroxide values. The beneficial effects of adding small amount of citrate to zeolite systems suggests that the most appropriate mechanism to explain these observation is that the citrate is acting as a transfer agent for transition metals between fibres and zeolite, the “Carrier Effect”(diagram 2). This is similar to the mechanism proposed for zeolite and citrate in chelating calcium ions in detergent applications. The optimum brightness for the combined system of zeolite and citrate occurred at 7.5% zeolite-A and 0.5% citrate. Furthermore the addition of 0.5% sodium citrate with zeolite-A reduced the dose for equivalent brightness from 10% with zeolite-A alone to 5% zeolite with citrate. Thus resulting in a saving in the order of 50% of the zeolite charge for bleaching of Pine TMP.

Opacity and light scattering coefficients were not affected by systems containing no or low amounts of zeolite for both Pine TMP and Eucalypt CCS bleached pulps. However systems containing 5% zeolite maintained opacity and increased light scattering coefficient for Pine TMP with or without pretreatment. The higher zeolite charge with Eucalypt CCS produced beneficial increases in opacity and light scattering coefficient

with or without pretreatment. This improvement in optical properties at the higher zeolite concentrations is likely due to increased surface area for light scattering as the zeolite behaves like a filler. In unbleached pulps, the filler effect is obvious with 1% - 2% brightness gains achieved with addition of zeolite-A. The brightness improvement occurs because zeolite is brighter than the pulp fibres.

Studies of handsheets made from peroxide bleached pulp for both Pine TMP and Eucalypt CCS with and without the various chelating agents showed that there was no significant effect on properties such as tear index, tensile index, roughness and porosity.

Future Work:

Studies could be initiated into the use of MgO as an alkali source, as Mg and Mn are known to accelerate peroxide decomposition(1). Currently in some peroxide bleaching processes MgO is already being used as an alkali source because it is cheaper than sodium hydroxide. So it would be also important to study its effect when using a zeolite/citrate chelation system.

The use of ESCA or other surface techniques to determine the location of manganese ions on the surface or in the pores of the zeolite could be studied to provide more information about the mechanism of interaction between manganese, zeolite and citrate.

References : (Conclusion)

- (1) Brown, D.M., **Effects of metal catalysed peroxide decomposition on the bleaching of mechanical pulp**: PhD Thesis, University of Tasmania (1993)

APPENDIX:

Design, Construction and Use of a Pneumatic Laboratory scale Pulp Press.

Daniel Finnegan *, Peter Dove[#]

*M.Sc Student, Department of Chemistry, University of Tasmania

[#] Engineering Staff, Chemistry Department, University of Tasmania

INTRODUCTION:

It is general knowledge that the pulp consistency at which bleaching is undertaken is a major factor in bleach response along with chemical concentration, initial wood brightness, temperature and many other variables depending on the exact bleaching situation.

It has been shown in a number of situations by increasing the pulp consistency, the final brightness of pulp will increase with relation to consistency as the chemicals have improved contact with the fibres. Therefore there has been a move by many pulp mills to move the bleaching operations from low consistency to medium consistency (10-15 %). Some mills have gone even further to high consistency bleaching (25-35%) using refiner bleaching or screw press dewatering stages.

The response from the equipment supplier companies to the demand from many mills for machine scale and pilot plant scale dewatering equipment has been such that there are many manufacturers and designs on the market. However there has been a poor response from laboratory scale equipment manufacturers to the requirement for laboratories to conduct research into bleaching at these higher consistencies which preclude simple laboratory vacuum dewatering processes.

In our case, pulp which hasn't had any chemical pre-treatments or bleaching chemicals after pulp production, has been utilised for research into hydrogen

peroxide bleaching. Pine TMP and Eucalypt CCS pulp is obtained from Australian Newsprint Mills, Boyer. However the sampling locations in the plant are such that the consistency for Pine TMP is around 7% and 10-15% for the Eucalypt CCS. The research is going to be concentrated on peroxide bleaching at 15 % consistency or higher, and as such a laboratory scale pulp dewatering press is required. The research will also include evaluation the strength properties of the handsheet produced from medium to high consistency bleaching. In an effort to produce standard handsheets, the Australian/New Zealand Standard AS/NZS 1301.214s:1993 section 6 requires that a "press must be capable of exerting an even pressure of 410 + or - 10 kPa over the area of a test sheet within 30 s of initial application and holding this pressure for 5 min". Consequently there has been a need in our laboratory for a dewatering and a handsheet press.

DESIGN AND CONSTRUCTION:

The design of the pulp press has included a number of factors. The major factors are safety, functionality, ease of use, and ease of construction. The materials used were stainless steel and polyvinylchloride(PVC) as these materials are resistant to corrosion and rust which are readily prevalent in this type of application.

Frame:

The frame is made out of 50 mm square steel tubing. The top and bottom plates have a 540 mm long pieces of steel tubing across the front and back. The front and back are 316 mm apart (internal measurements), separated by an X shape using square steel tubing. The top plate is held 500 mm above the bottom plate by 19 mm diameter steel tubing. A 550 mm, 12.7 mm diameter stainless steel threaded rod bolts to the top and bottom plate through the inside of the 19 mm tubing. This arrangement is repeated 4 times and is located 15 mm in from the edge of the steel frame.(See pages A8, A9, A12).

Air Bag:

An air bag sits on the bottom of the frame and it provides the motive force in the press, raising up the bottom internal section and the pulp containing box into the top section. The air bag was sourced from "Power Team", model no. IJ128. It is 381*381 mm with a collapsible height of 22.2 mm. The air capacity is 2.7 cu ft (manufacturers readings) with a maximum rated pressure of 116 psi, that can delivery a maximum lift of 12 tonnes at a maximum lift height of 152.4 mm (see pages A8, A9).

Press Block Section:

The press block section consists of two polyvinylchloride (PVC) plates of the dimensions 450 mm x 450mm x 45 mm. These two plates sit on a 300 mm diameter, 12.7 mm thick steel plate on top of the airbag (see pages A8, A9).

The lower of the two polyvinylchloride(PVC) plates does not have any modifications. The upper of the two plates has been extensively milled to create a drainage area and a deeper rebate in which the pulp containing box sits. The rebate for the pulp box is located 14 mm in from the outer edge of the upper PVC plate. The rebate is 25 mm wide and 12 mm deep. 10 mm in from the bottom of the rebate is a further rebate of 6mm by 6.5mm for an o-ring seal (See page A11).

The drainage area is formed by milling channels of dimensions 9 mm wide by 5 mm deep into the upper plate. The first channel on edge side is located 40 mm in from the inside edge of the pulp box rebate. The other channels have been milled in such a way that the distance between channels is 30 mm. This arrangement forms a drainage area with 8 by 8 channels (See page A10). The water is removed from the drainage channels via two drainage holes. The two holes are located on the left and right sides of the upper plate. The first hole is located 158 mm back from the front left side and the second is located 165 mm back towards the front from the rear right hand side. The drainage holes are 6.35 mm diameter, 50 mm in from the edge of the

plate and the exit the plate 25 mm from the top. The outlet connects into 10 mm hose tubing for connection to a variety of vacuum sources. (See pages A10, A11).

The two PVC plates are joined together by 4 semi-circle pieces of polyvinylchloride (PVC). The semi-circles have a diameter of 84 mm and a height of 90 mm. The plates are bolted to the semi-circles by 6 mm hex bolts. Each plate has two bolts per semi-circle. The semi-circles also connect the two PVC plates to the frame via the 19 mm steel tubing. The semi-circle has a 22.2 mm hole drilled through to locate the 19 mm tube. When the air bag inflates, the plates slide up tubing via the semi-circles. (see pages A8-A11).

Pulp Box section:

The box is made out of PVC with the dimensions of 191mm high by 420 mm wide and 10 mm thick. This arrangement is such that the internal measurements are 400 mm by 400 mm. The bottom of the box has a rebate of 25 mm in from the outer edge and 12 mm thick. On top of the rebate sits a 400 by 400 mm piece of wet end forming fabric. The fabric is secured to the box by 15 by 10 mm inserts that run the length of the inside of the box, with 4 nylon screws per side. (see pages A10, A12)

Top Press block:

The top press block consists of a PVC plate of dimensions 397 mm by 397mm by 45 mm and a box like structure made out of 1 mm plate stainless steel. The height of the box above the polyvinylchloride (PVC) plate is 135 mm. The top section is bolted to the upper frame by 6 mm stainless steel bolts (see pages A8, A9). When the airbag is inflated the box rises up the outside of the top section. Depending on the quantity of pulp in the box, some PVC inserts (397 by 397 by 20 mm) may be needed to ensure that the airbag doesn't reach the top of its lift before delivering its maximum pressure load.

Air Control Manifold:

The manifold has 4 inlets. The inlet from the air bag regulator and the outlet to the emergency relief valve have been bored out to 12.7 mm diameter. The outlet to the air bag has been decreased to 1.59 mm diameter with a nylon plug insert. These modifications have been made so that the airbag will dump air through the emergency relief valve even if the airbag regulator is in the fully on position. Thus ensuring that the safety of the operation of the press if articles of clothing, fingers etc are caught in the press, while still delivering the required pressure in general operation (see page A8).

RESULTS:

The following results of press operation include studying the effect pressure, vacuum source for water removal, and pulp type. There are two vacuum sources used in this experiment, namely a Water Aspirator (refer to as WA in the following graphs) and a wet/dry vacuum (refer to as VC in following graphs). The vacuum cleaner is a Makita Industrial vacuum cleaner, model 403 Q87302 , 1050 W.

The pulps used in this experiment are a Pine TMP with a corrected CSF of 82, and a Eucalypt CCS with a corrected CSF of 139. In this experiment the following conditions were applied. A charge of approximately 500 g.o.d of pulp was added to 10 L of water. The pulp slurry was then mixed using an industrial dough mixer with a metal whisk attachment @101 rpm for 10 minutes. The temperature was adjusted to 25 degrees Centigrade before mixing for a further 5 minutes. Once the pulp was added to the press, suction was applied for 10 minutes at each pressure reading, then a sample of the pulp was removed for consistency evaluation. Graphs 1 and 2 show the effect of the vacuum source on the dewatering of Pine TMP and Eucalypt CCS.

Conclusions:

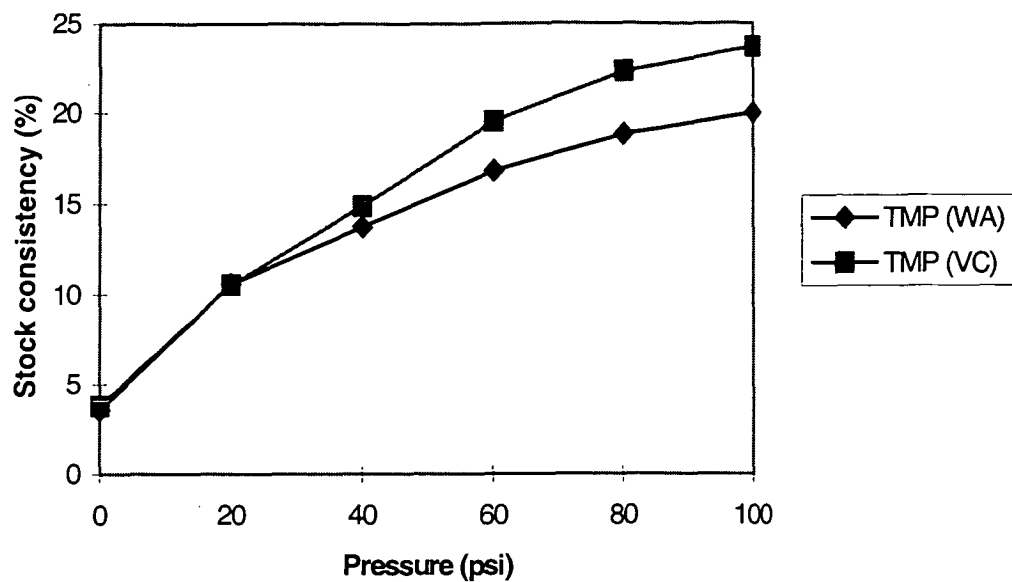
It is believed that these experimental data validate the concept of the press design because the press successfully dewatered the wood pulp, thus allowing bleaching or

other unit operations research. This has enabled the researcher to conduct experiments under similar conditions to those in the pulp mill. These results show that the final stock concentration is dependent on vacuum source, and applied pressure. The most important factor of this process is pulp freeness which measures the water drainage capability of the pulp, with higher freeness being preferred for pulp dewatering. It should be noted that the press requires a reasonably initial flat pulp level or surface to prevent misalignment of the press block and box sections when they are raised under the higher pressures by the air bag. In some cases depending upon the level of the pulp in the press, additional polyvinylchloride (PVC) inserts may have to be added inside the pulp box to reduce the lift distance to within the maximum lift height of the airbag so that the maximum pressure may be applied.

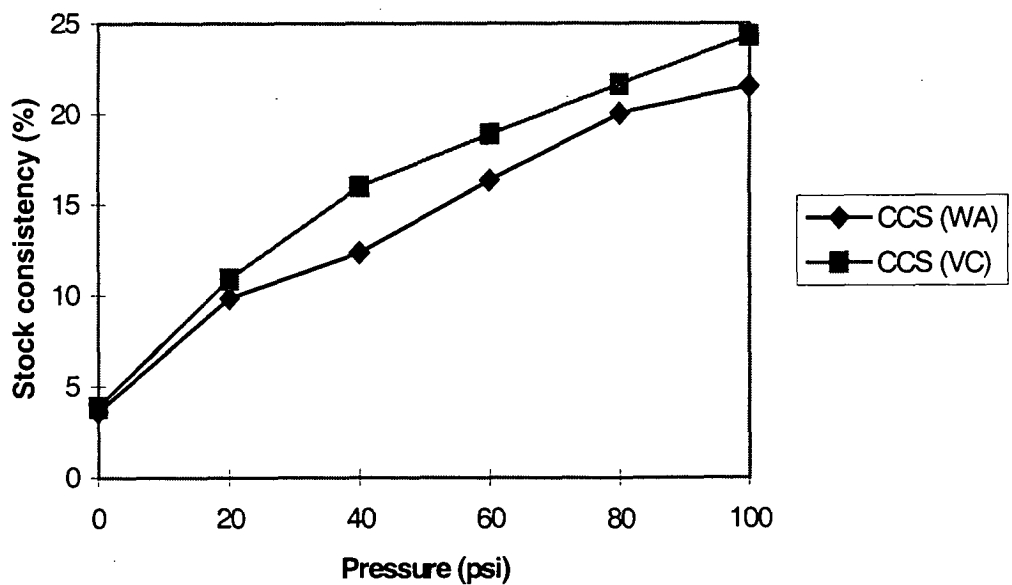
Futhermore when the pulp box is removed from the press block section and it is replaced with a PVC insert, the pulp press can then meet the press requirements in (section 6) AS/NZS 1301.214s:1993 for British handsheet production. The press in this configuration can also be used for production of A4 handsheets often used in printability tests.

Acknowledgements:

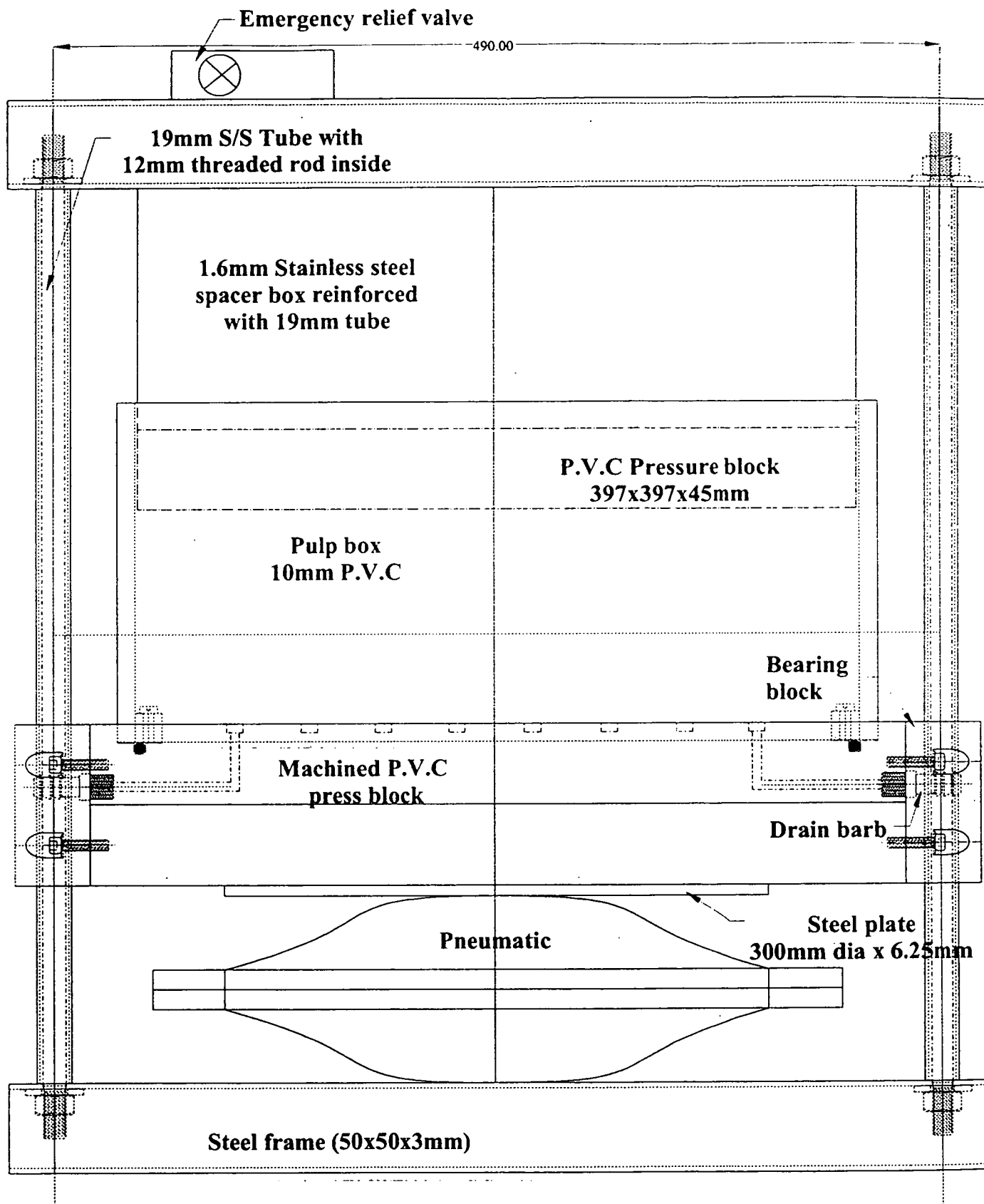
We would like to thank Mike Brandon for the creation of the engineering diagrams of the pulp press.



Graph 1: Dewatering of Pine TMP in a pulp press using two vacuum sources.

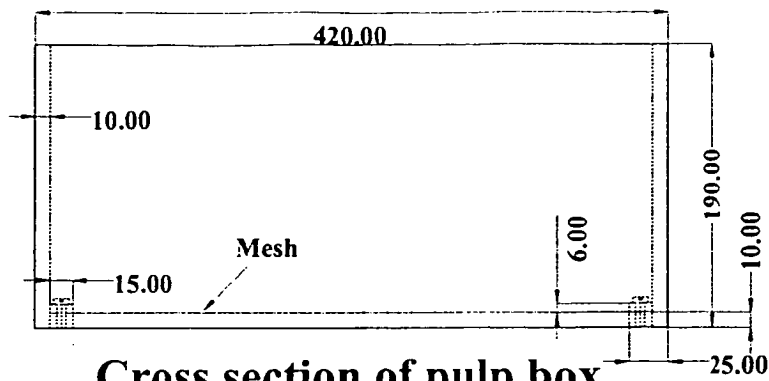


Graph 2: Dewatering of Eucalypt CCS with a pulp press using two vacuum sources.

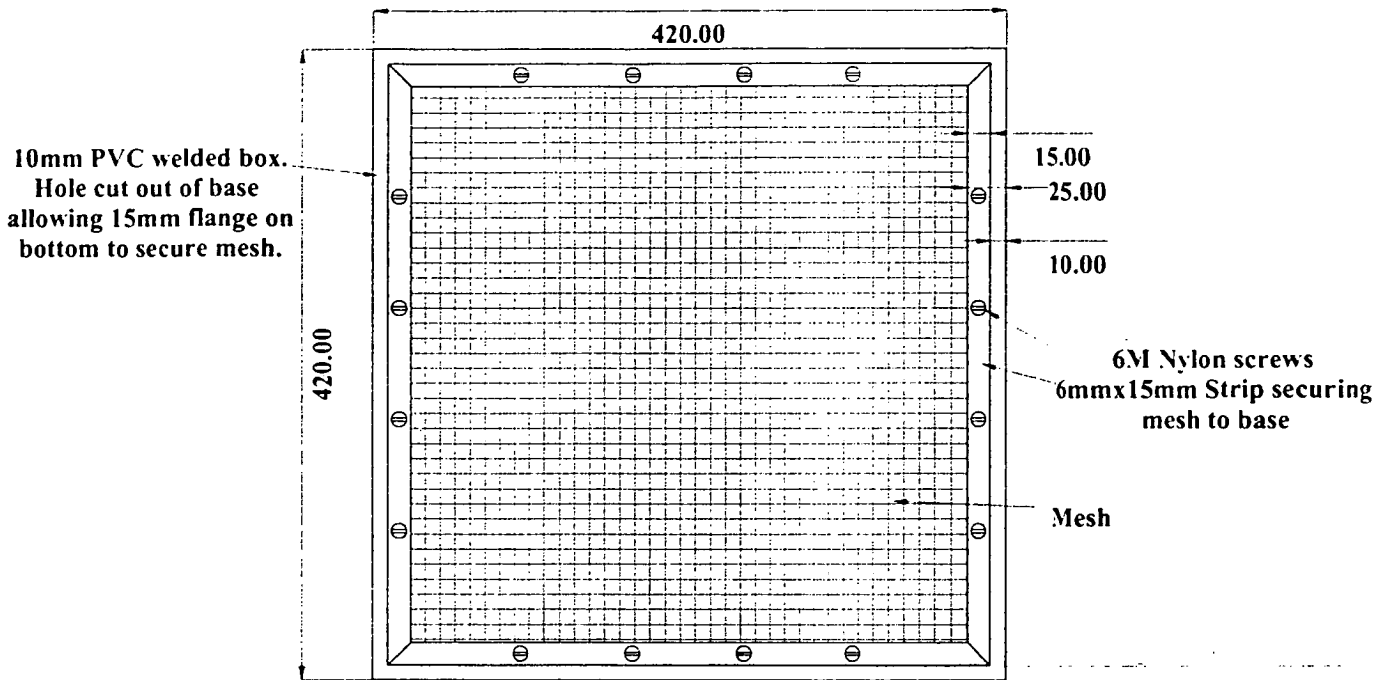


FRONT VIEW OF PULP PRESS

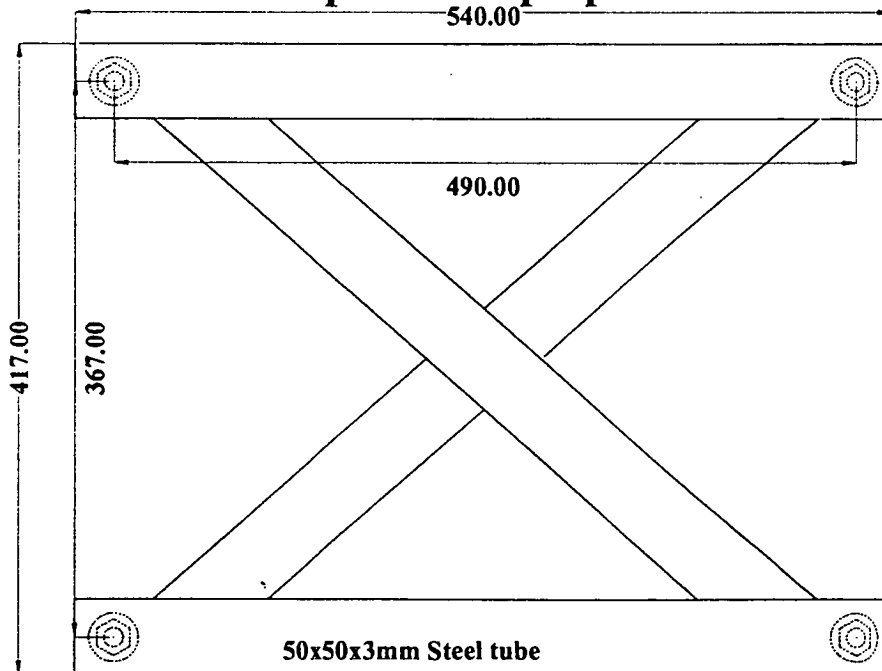
Title			Date	
Pulp Press Front View			13/11/97	
Designer	Cat No		DWG No	Rev
P Dove			PD 3	2
Units	Scale	Author		
mm	1:3	M J Brandon		



Cross section of pulp box

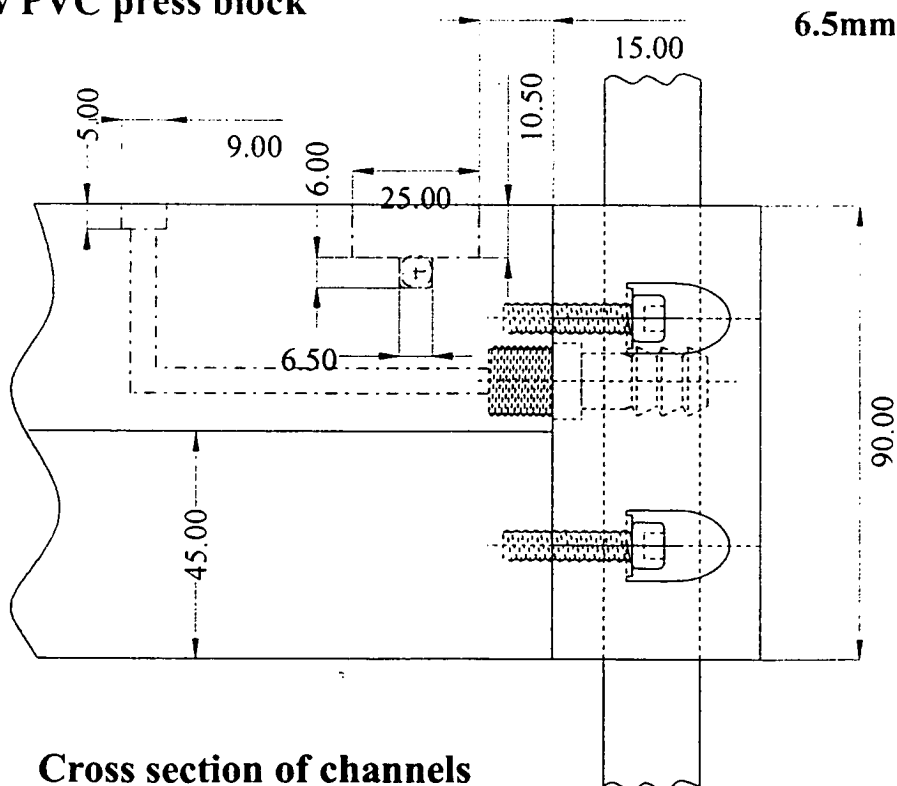
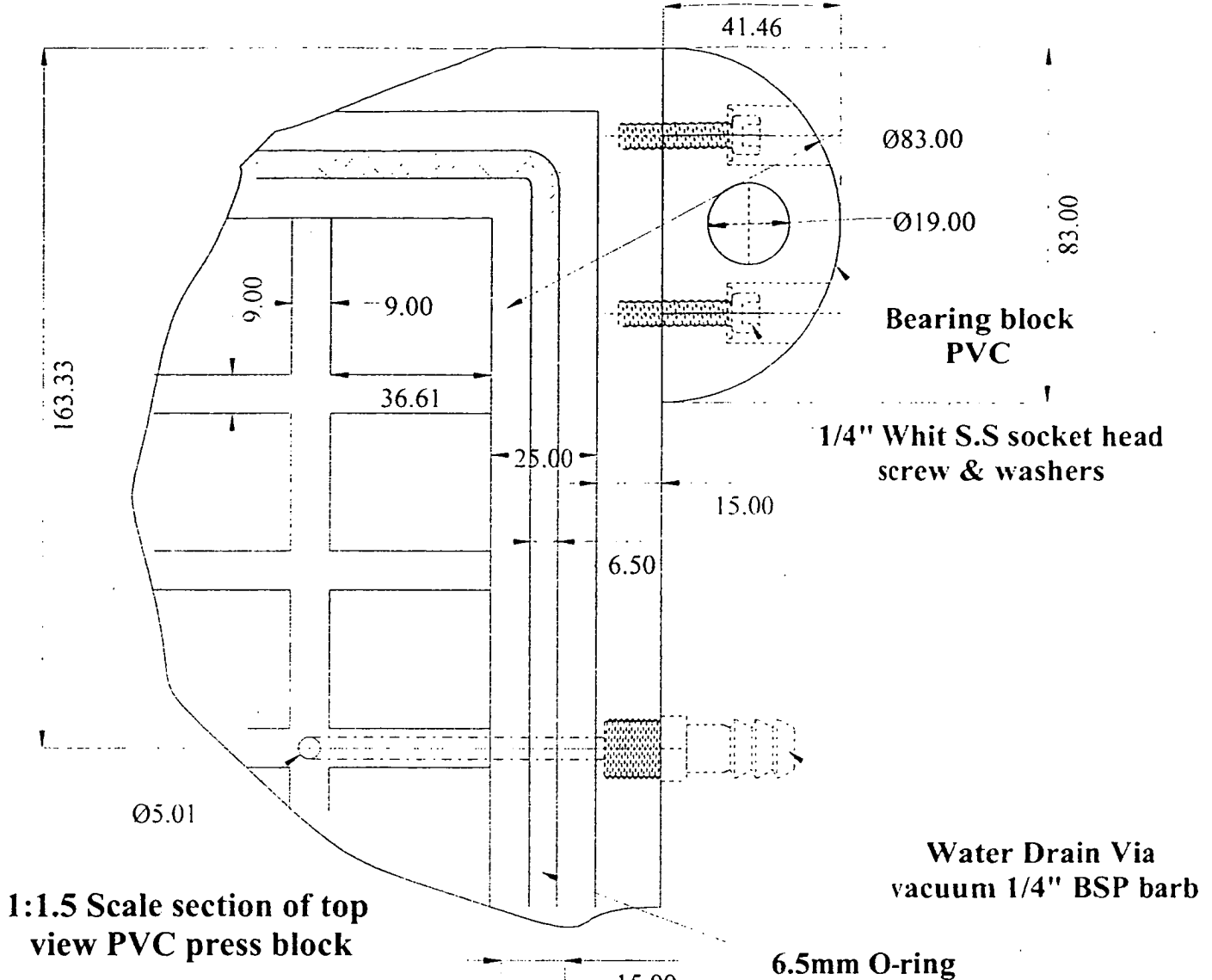


Top view of pulp box

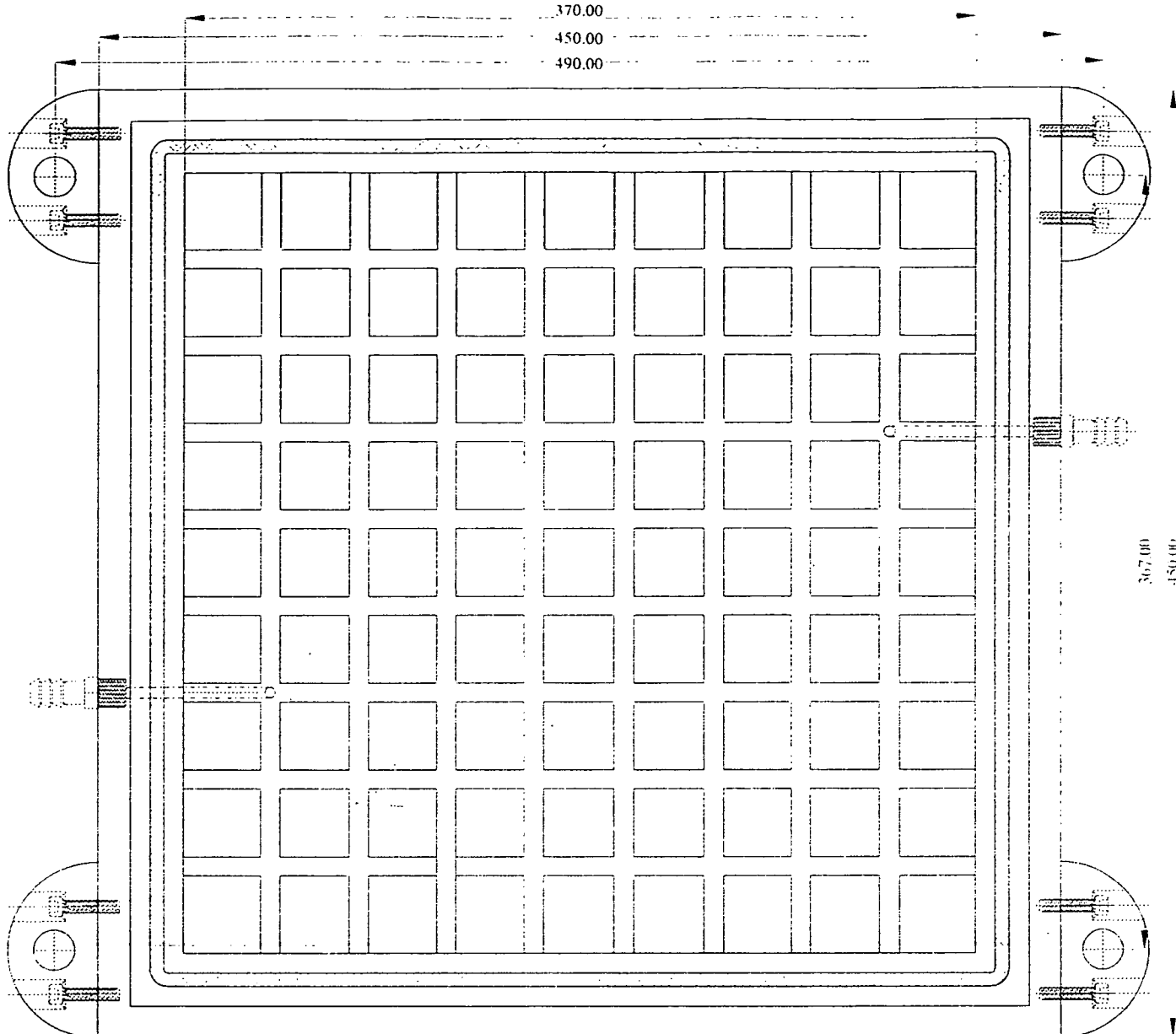


Top view of steel frame

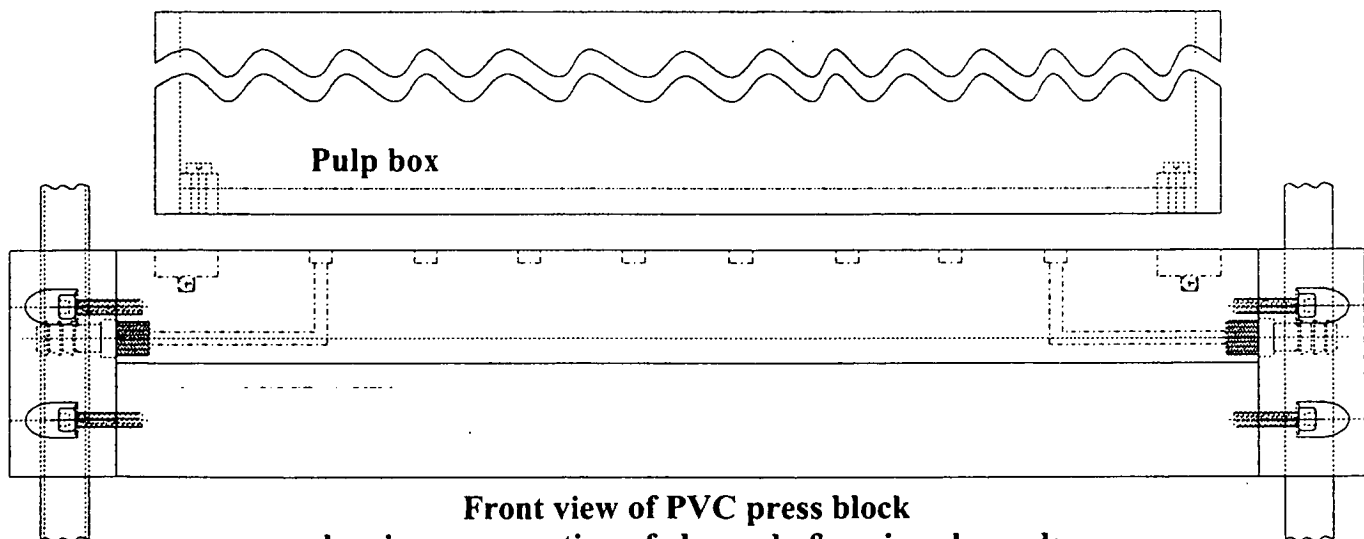
Title Pulp box & top view steel frame			Date	17/11/97
Designer	P Dove	Cat No	DWG No	PD7
Units	mm	Scale	1:5	Author
				M J Brandon



Title			Date	
PVC press block close up			14/11/97	
Designer	Cat No	DWG No	Rev	
P Dove		PD6	2	
Units	Scale	Author		
mm	1:1.5	MJBrandon		

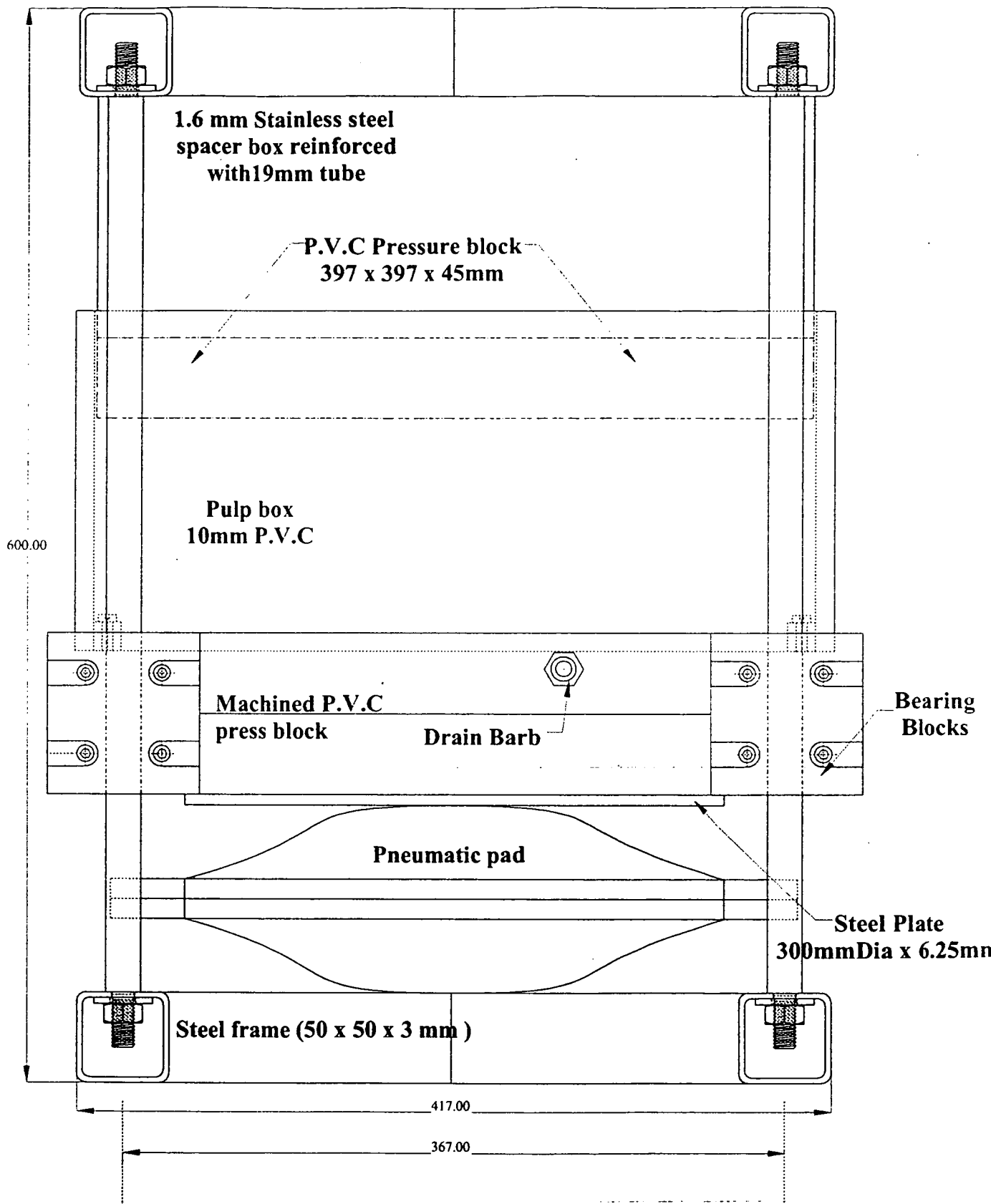


**Top view of machined PVC press block
showing drain channels and o-ring channel**



**Front view of PVC press block
showing cross section of channels & o-ring channels**

Title			Date	
PVC press block top & side view			13/11/97	
Designer	Cat No		DWG No	Rev
P Dove			PD 5	2
Units	Scale	Author		
mm	1:3	M J Brandon		



· SIDE VIEW OF PULP PRESS

Title			Date		
Pulp Press Side View			12/11/97		
Designer	P Dove	Cat No	DWG No	PD 2	Rev
Units	mm	Scale	1:3	Author	M J Brandon
					2